

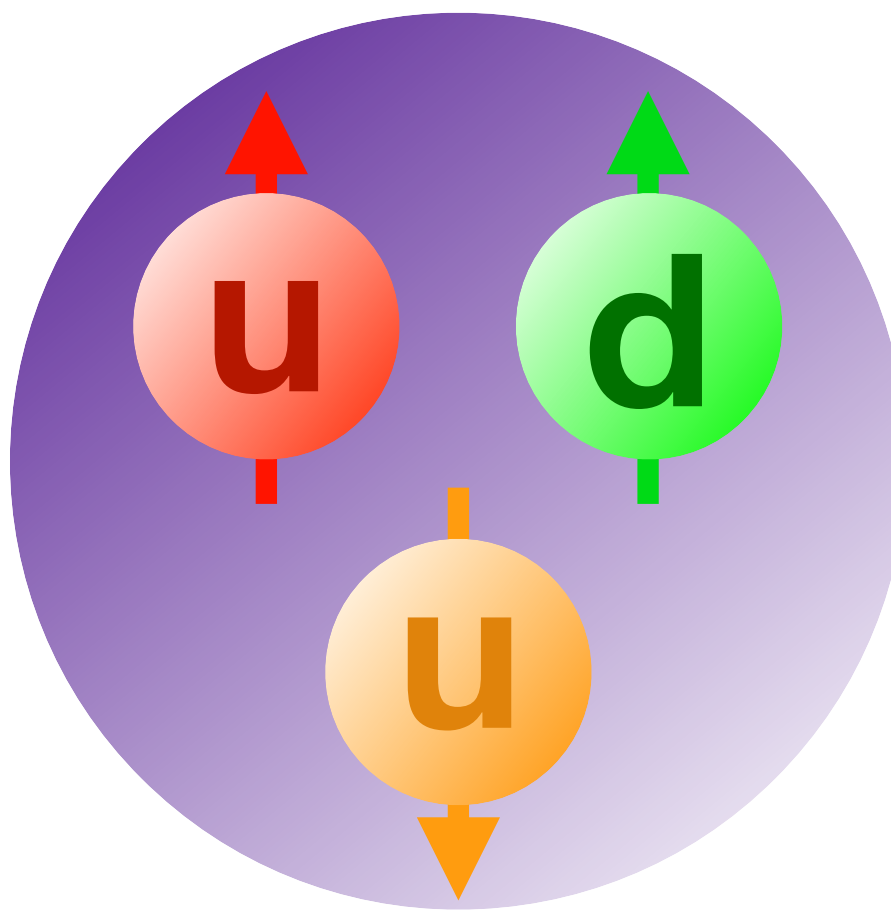
Recent and future experiments exploring N- Δ transition form factors at Jefferson Lab

CD24, Ruhr University Bochum, Germany, August 26 2024

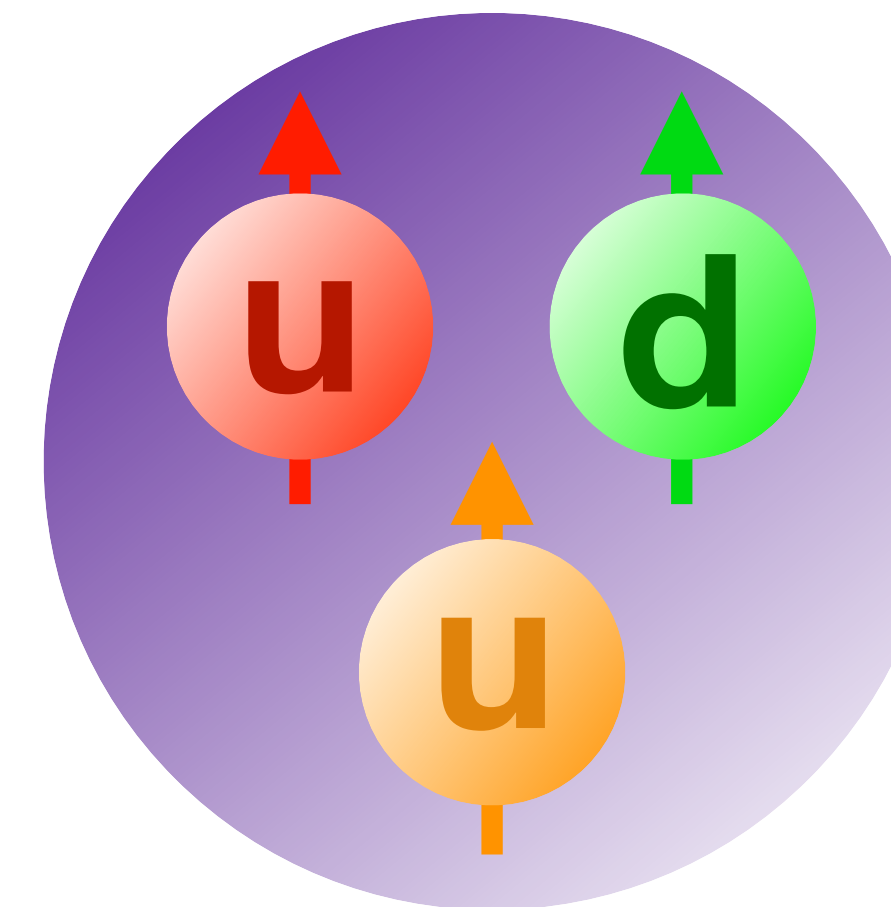
Michael Paolone, New Mexico State University

The N- Δ transition

Proton (938 MeV)



Delta (1232 MeV)

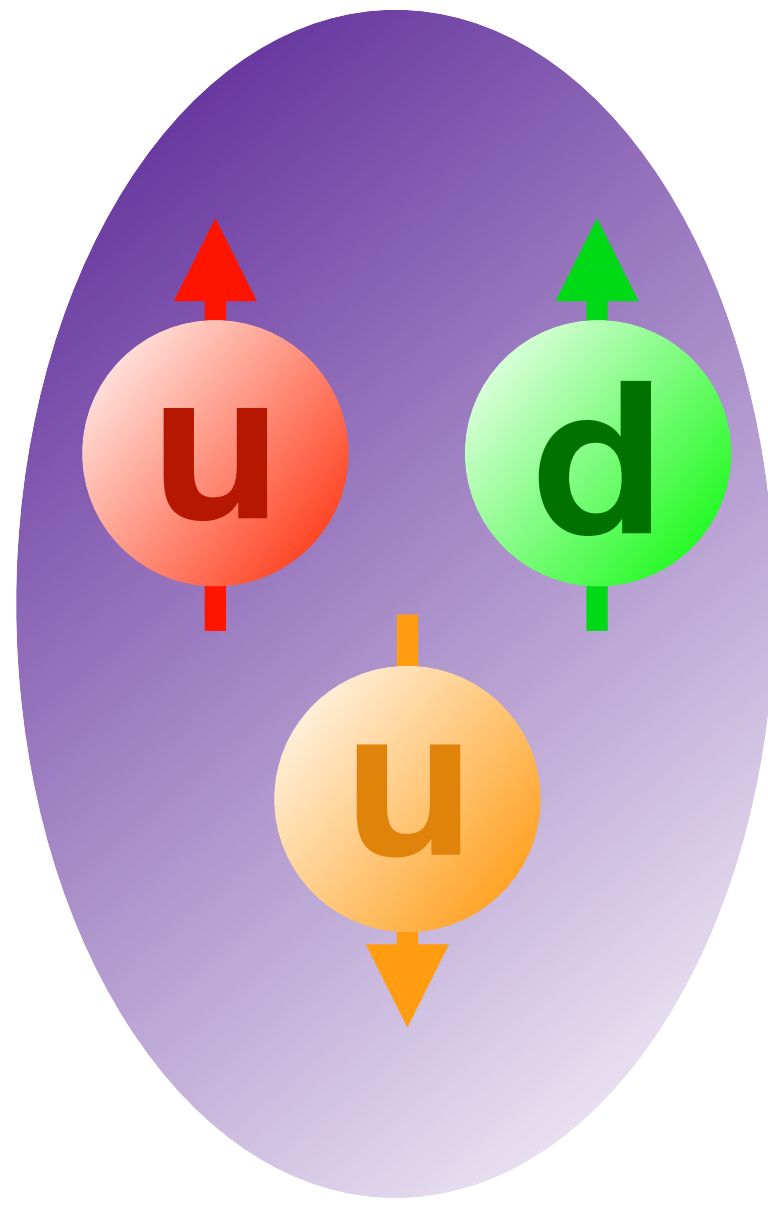


$\gamma^*, M1$

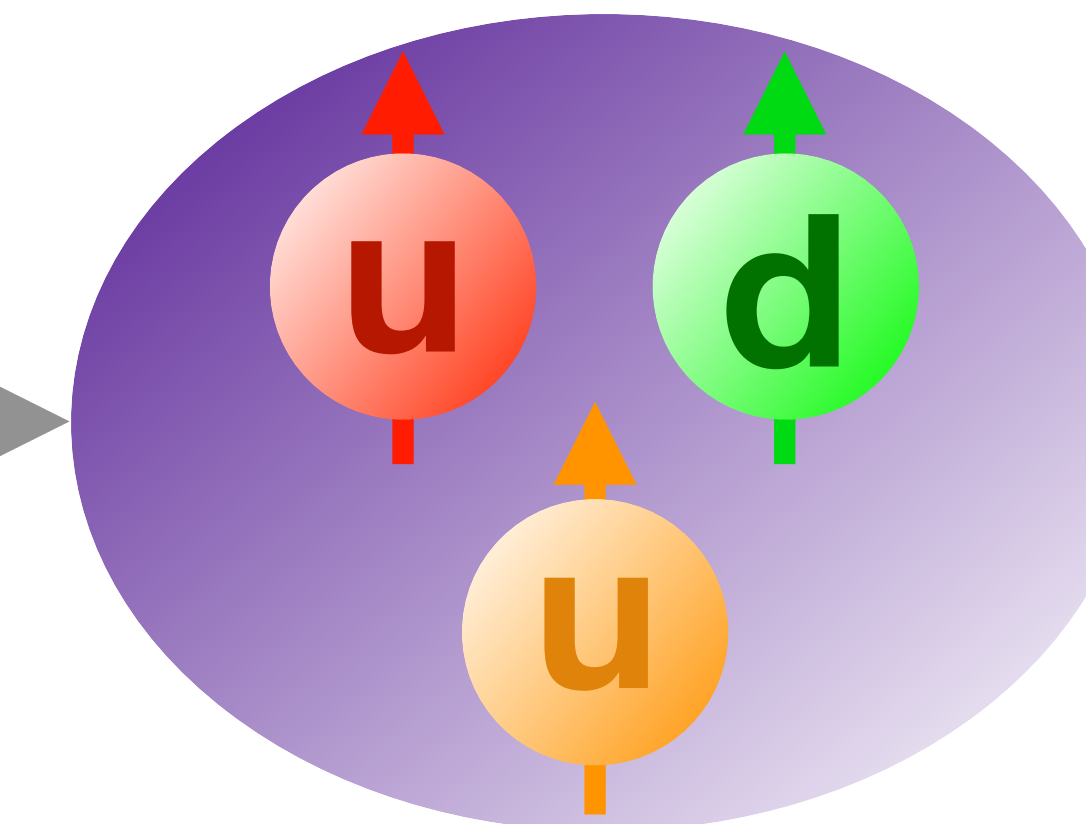
The dominant transition from proton to delta involves a dipole (M1) transition
(spherical S-wave proton WF \rightarrow spherical S-wave Delta WF)

The N- Δ transition

Proton (938 MeV)



Delta (1232 MeV)

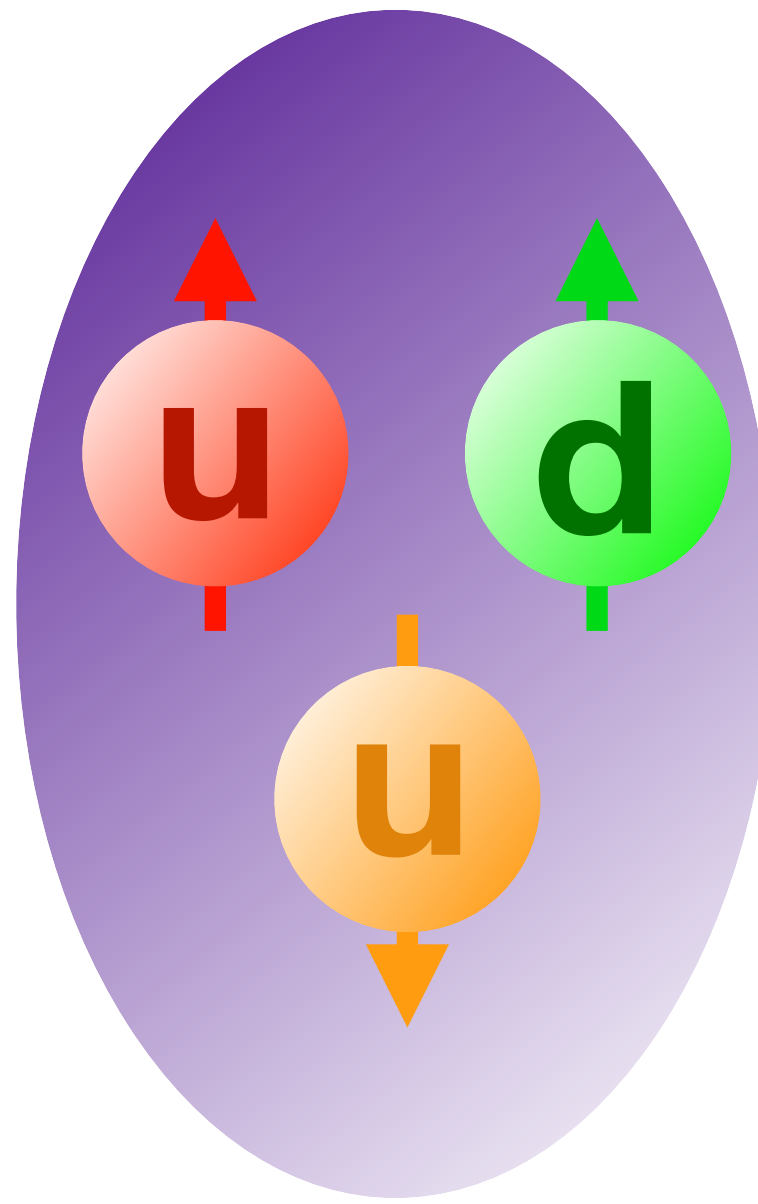


$\gamma^*, E2, C2$

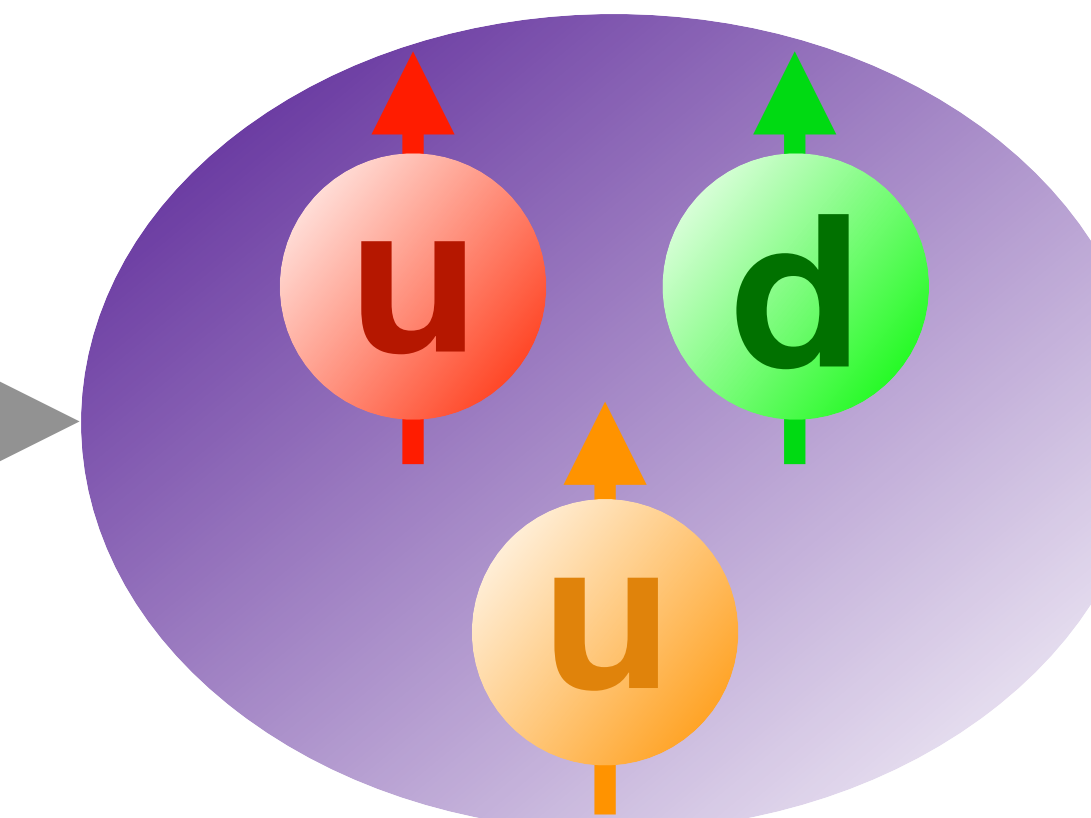
There also exists a quadrupole (E2 or C2) transition from proton to delta.
(The quadrupole amplitudes are associated with the existence of non-spherical components in the proton and Delta WF)

The N- Δ transition

Proton (938 MeV)



Delta (1232 MeV)



$\gamma^*, E2, C2$

There also exists a quadrupole (E2 or C2) transition from proton to delta.
(The quadrupole amplitudes are associated with the existence of non-spherical components in the proton and Delta WF)

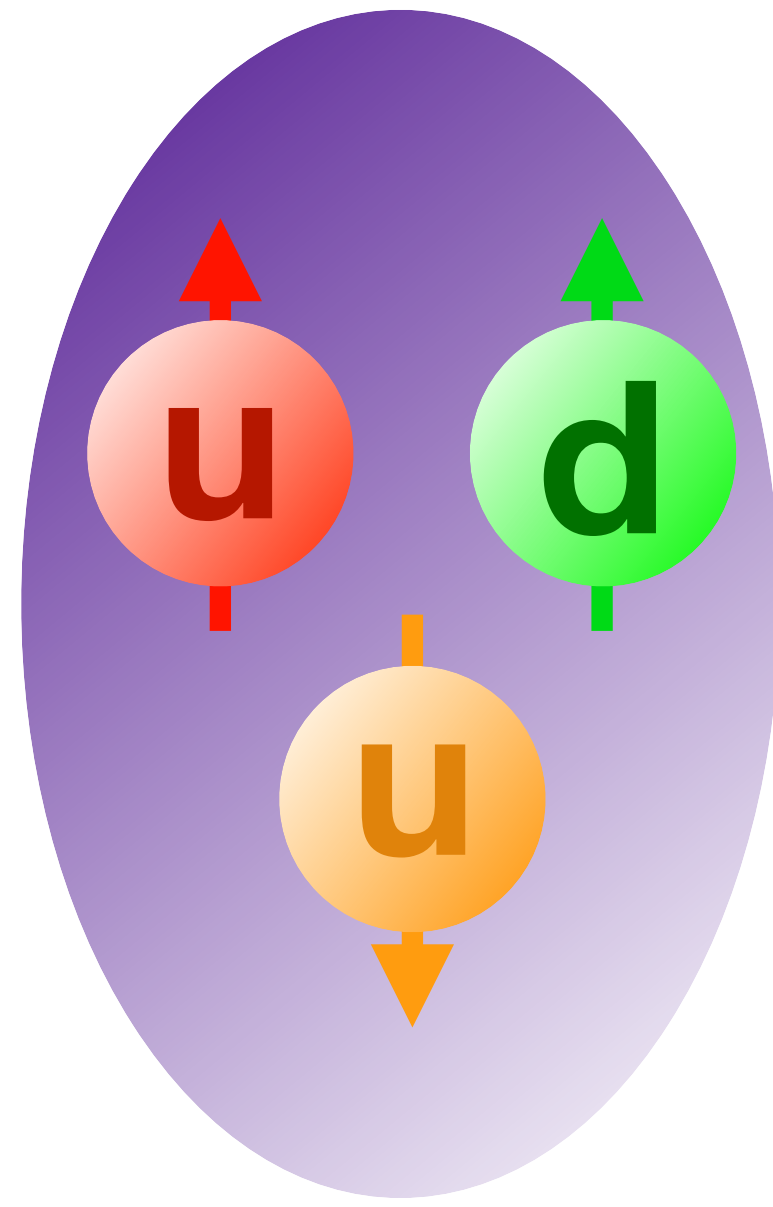
The quadrupole to dipole ratio (**E2/M1** or **C2/M1**) is non-zero... Why?

Electric-Quadrupole to Magnetic-Dipole Ratio = **EMR** = **E2/M1**

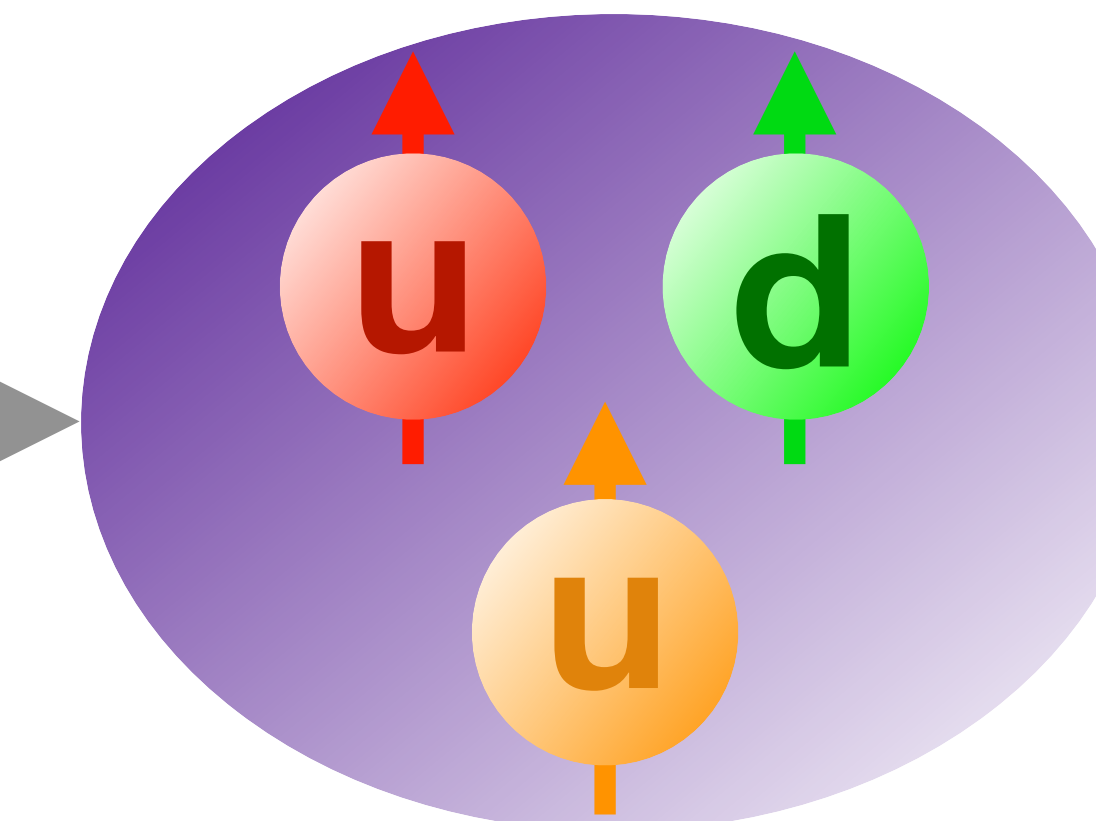
Coulomb-Quadrupole to Magnetic-Dipole Ratio = **CMR** = **C2/M1**

The N- Δ transition

Proton (938 MeV)



Delta (1232 MeV)



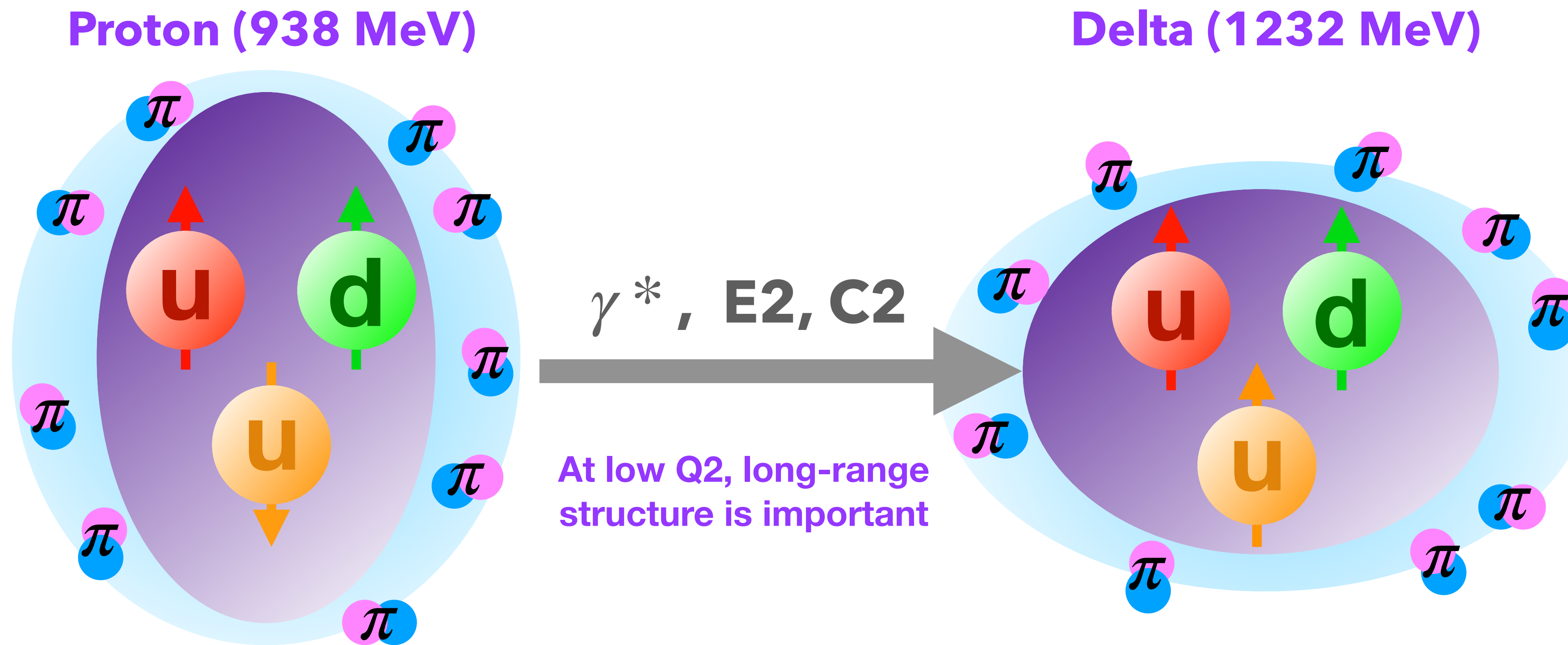
$\gamma^*, E2, C2$

There also exists a quadrupole (E2 or C2) transition from proton to delta.
(The quadrupole amplitudes are associated with the existence of non-spherical components in the proton and Delta WF)

The quadrupole to dipole ratio (**E2/M1** or **C2/M1**) is non-zero... **Why?**

Non-central (tensor) interactions between quarks can account for some of the spherical deviation, but not all...

The $N\Delta$ transition



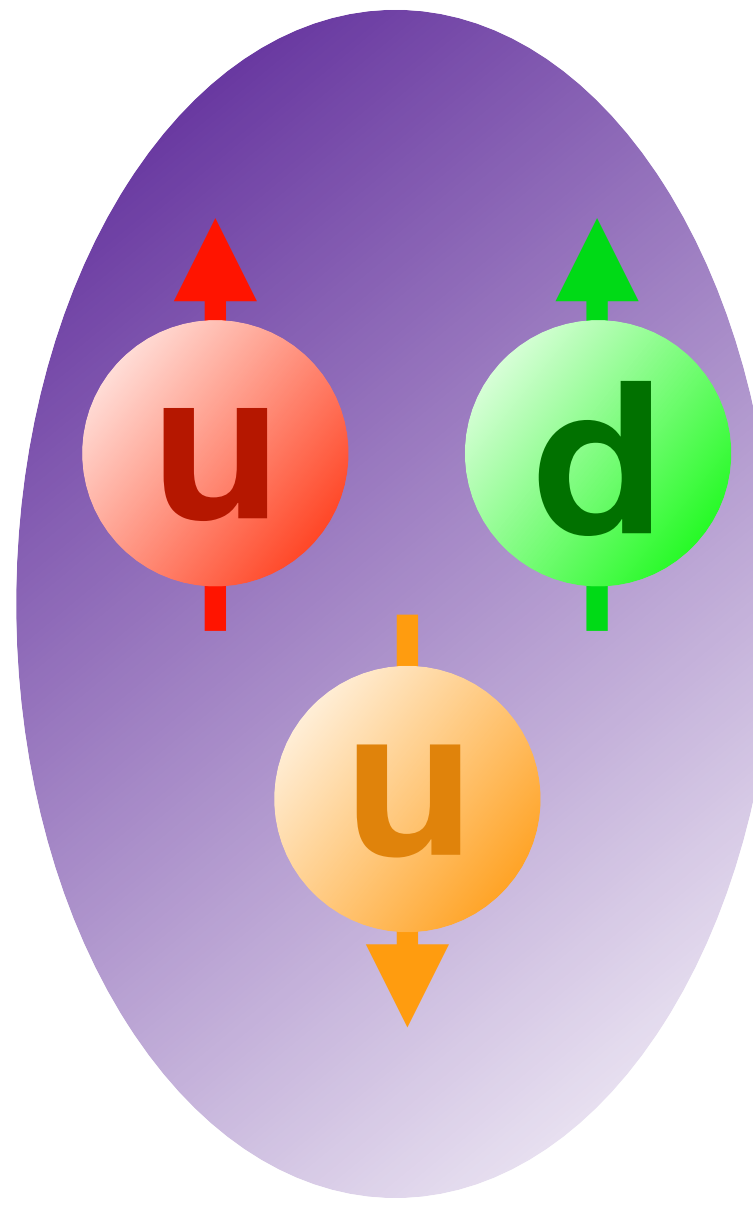
There also exists a quadrupole (E2 or C2) transition from proton to delta.
(The quadrupole amplitudes are associated with the existence of non-spherical components in the proton and Delta WF)

The quadrupole to dipole ratio (E2/M1 or C2/M1) is non-zero... Why?

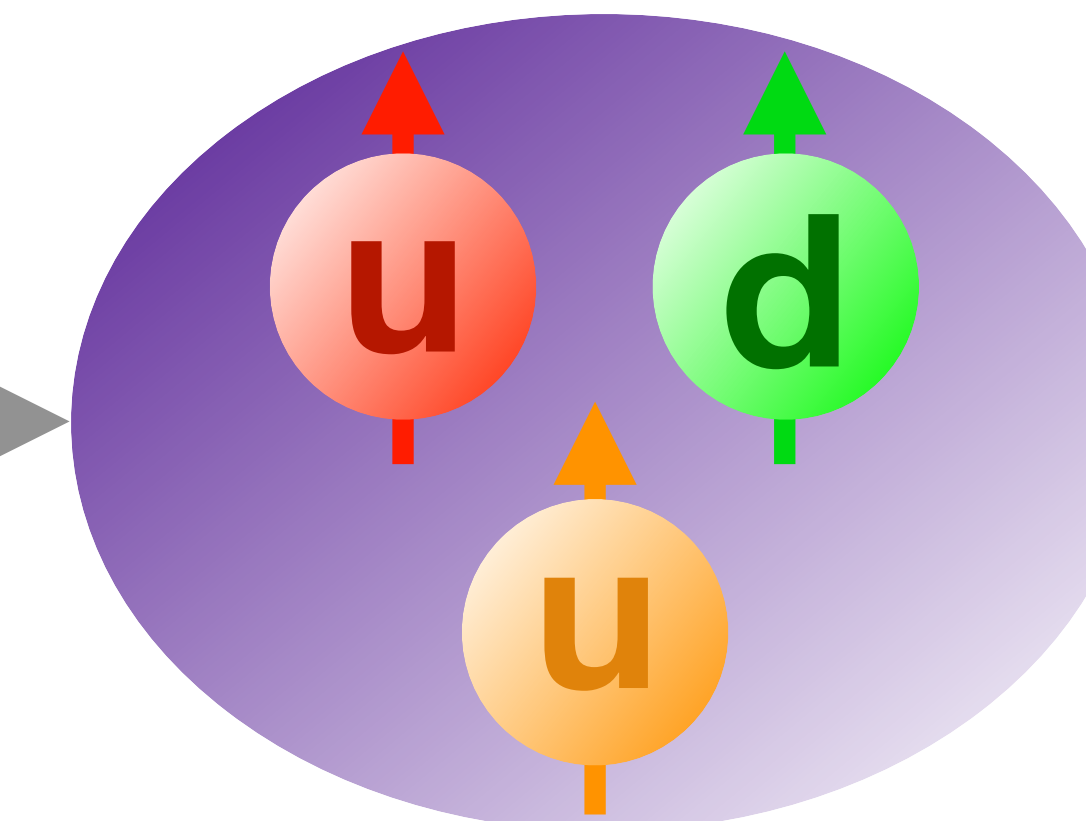
At low Q₂, the dynamics of a meson cloud are important to describe the structure of the nucleon.

The $N-\Delta$ transition

Proton (938 MeV)



Delta (1232 MeV)



$\gamma^*, E2, C2$

Large Q_2 , pQCD predicts
EMR $\rightarrow +1$, CMR \rightarrow constant

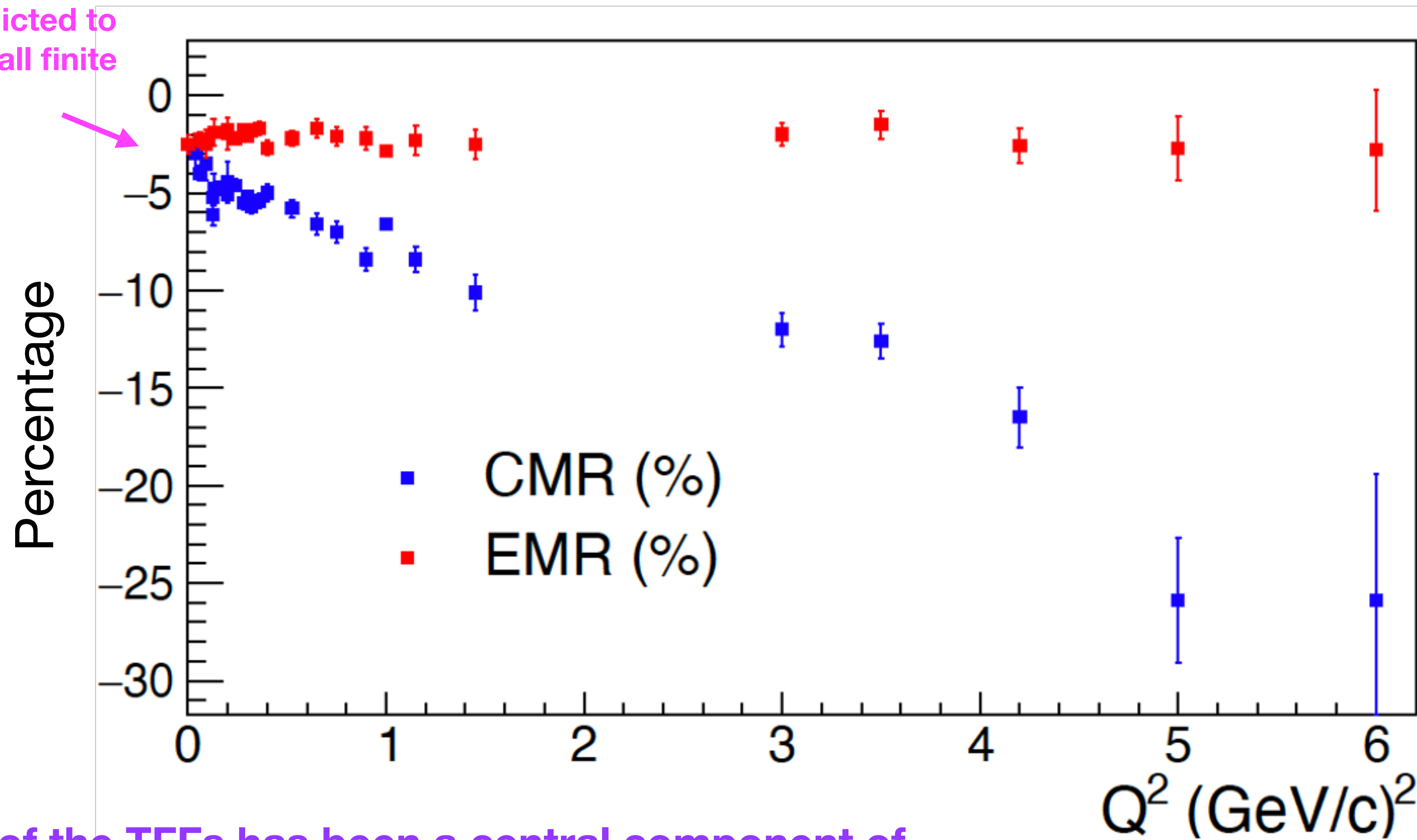
There also exists a quadrupole (E2 or C2) transition from proton to delta.
(The quadrupole amplitudes are associated with the existence of non-spherical components in the proton and Delta WF)

The quadrupole to dipole ratio (E2/M1 or C2/M1) is non-zero... Why?

At high Q_2 , perturbative calculations should become more reliable and helicity conserving amplitudes are expected to dominate.

World data and status of TFFs

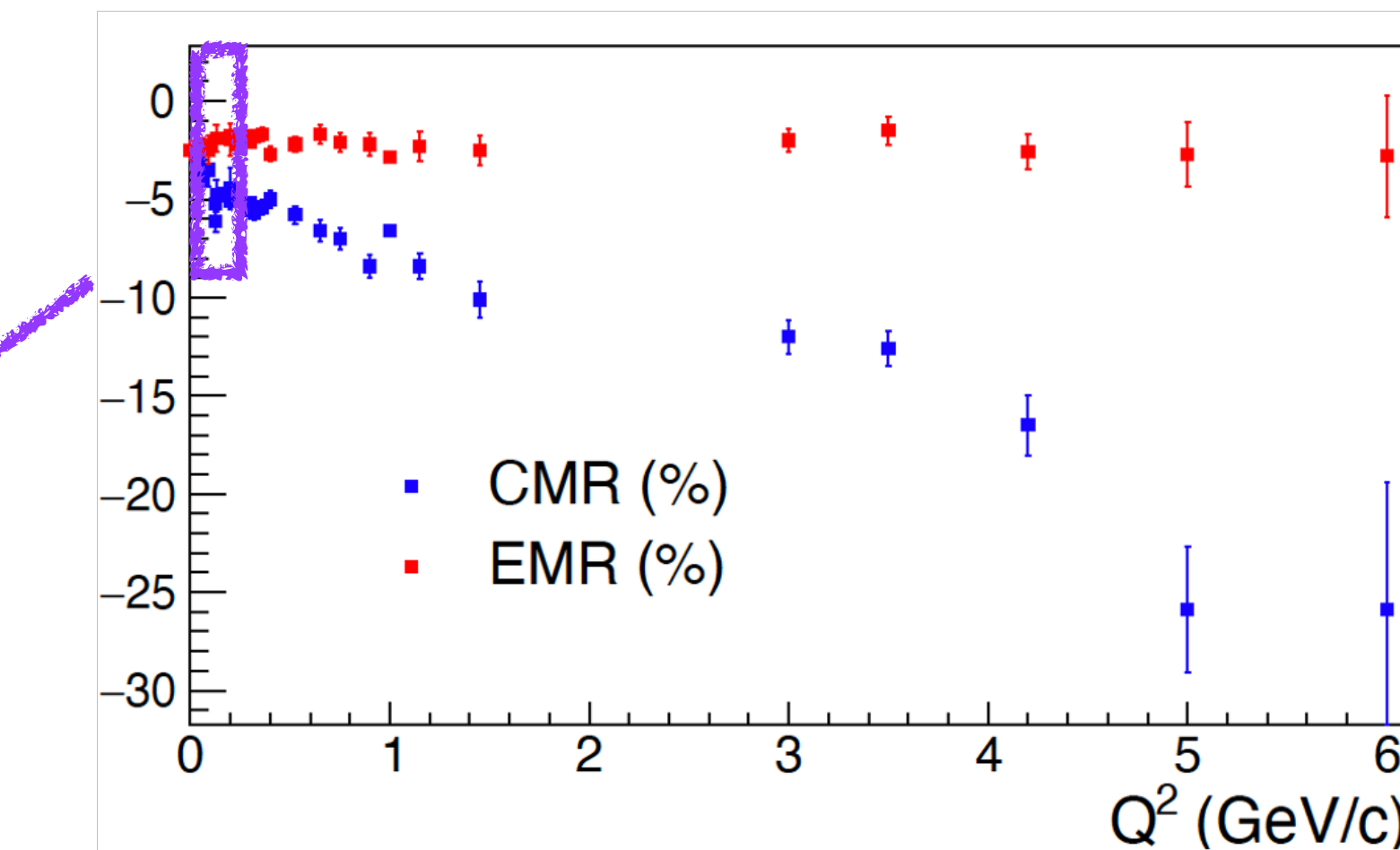
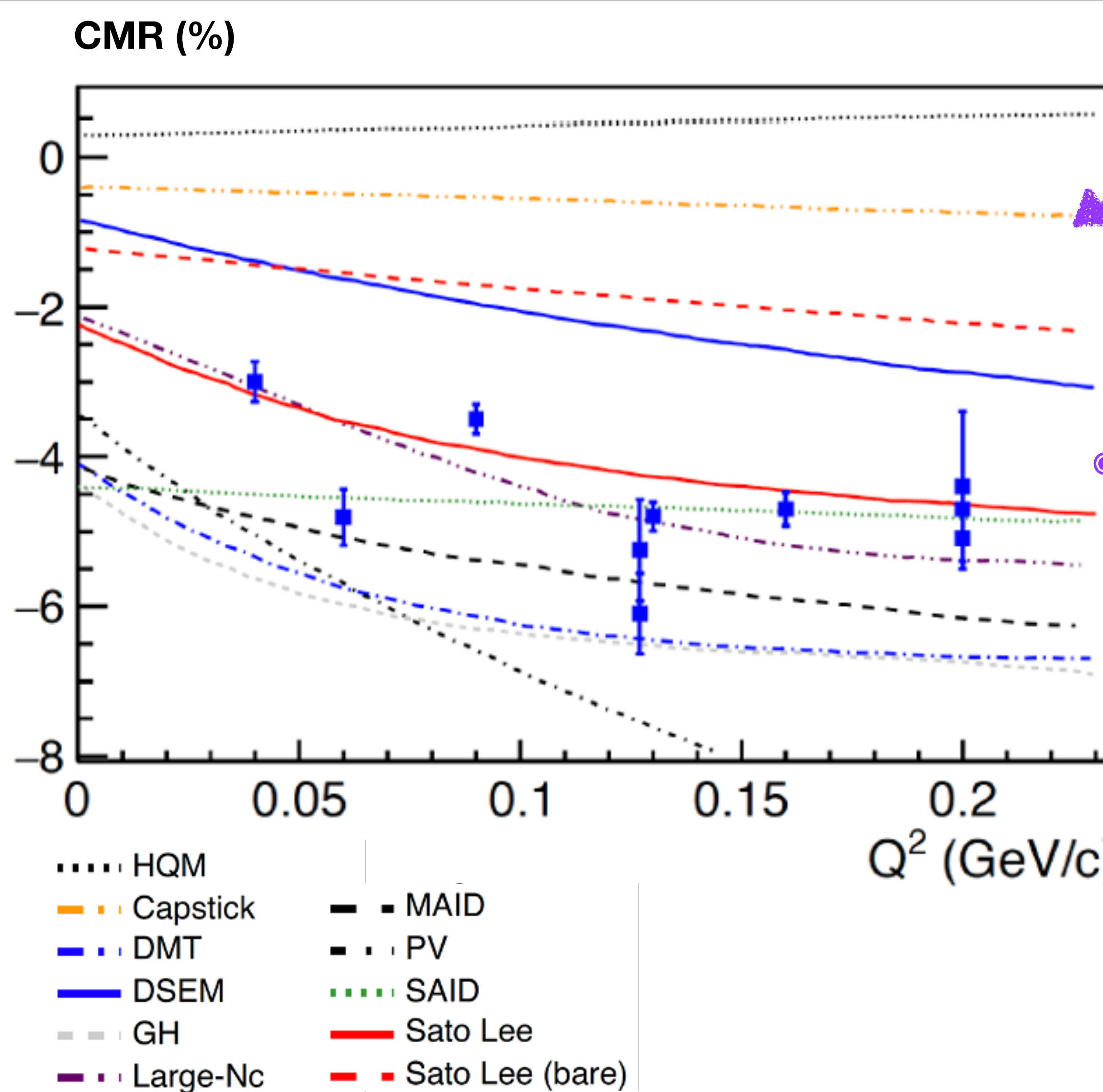
CMR & EMR predicted to converge at a small finite value as $Q^2 \rightarrow 0$



Extraction of the TFFs has been a central component of
Jlab's experimental program:
(Most of these measurements are from JLab Halls A, B, and C)

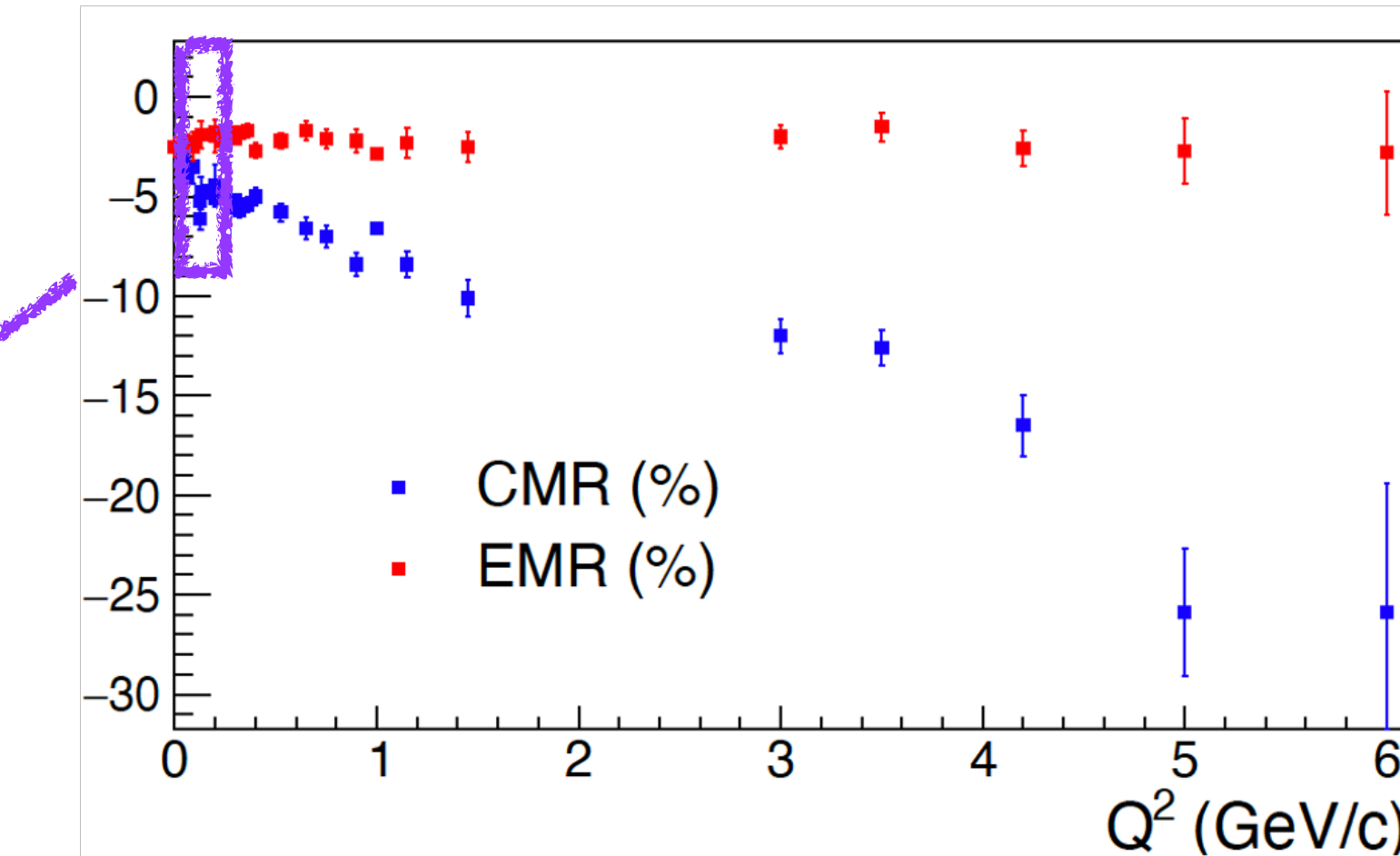
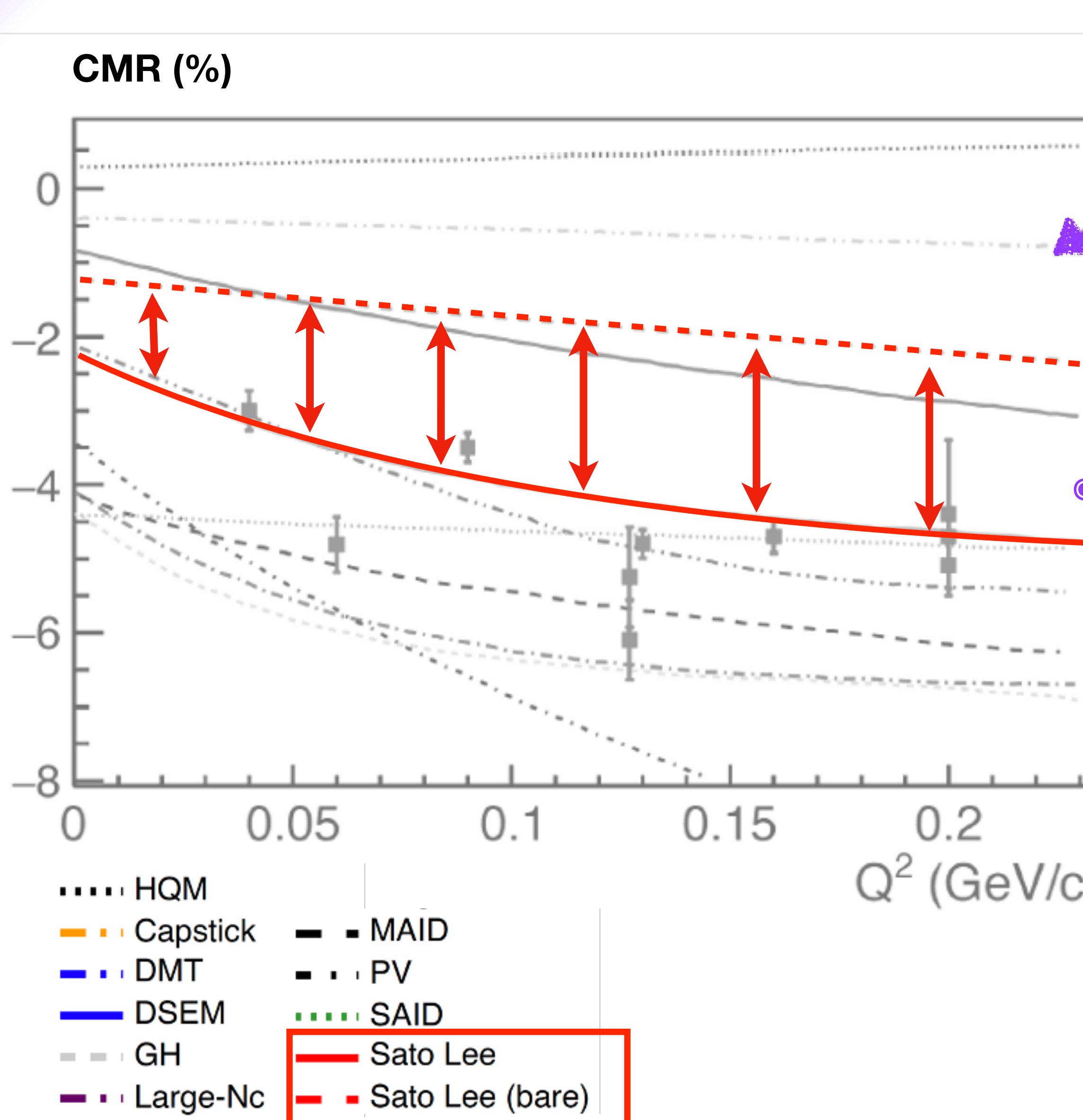
At large Q^2 , no direct indication of
EMR $\rightarrow 100\%$ and CMR \rightarrow constant
(predicted in pQCD regime)

Low Q^2 $N\text{-}\Delta$ transition form factors



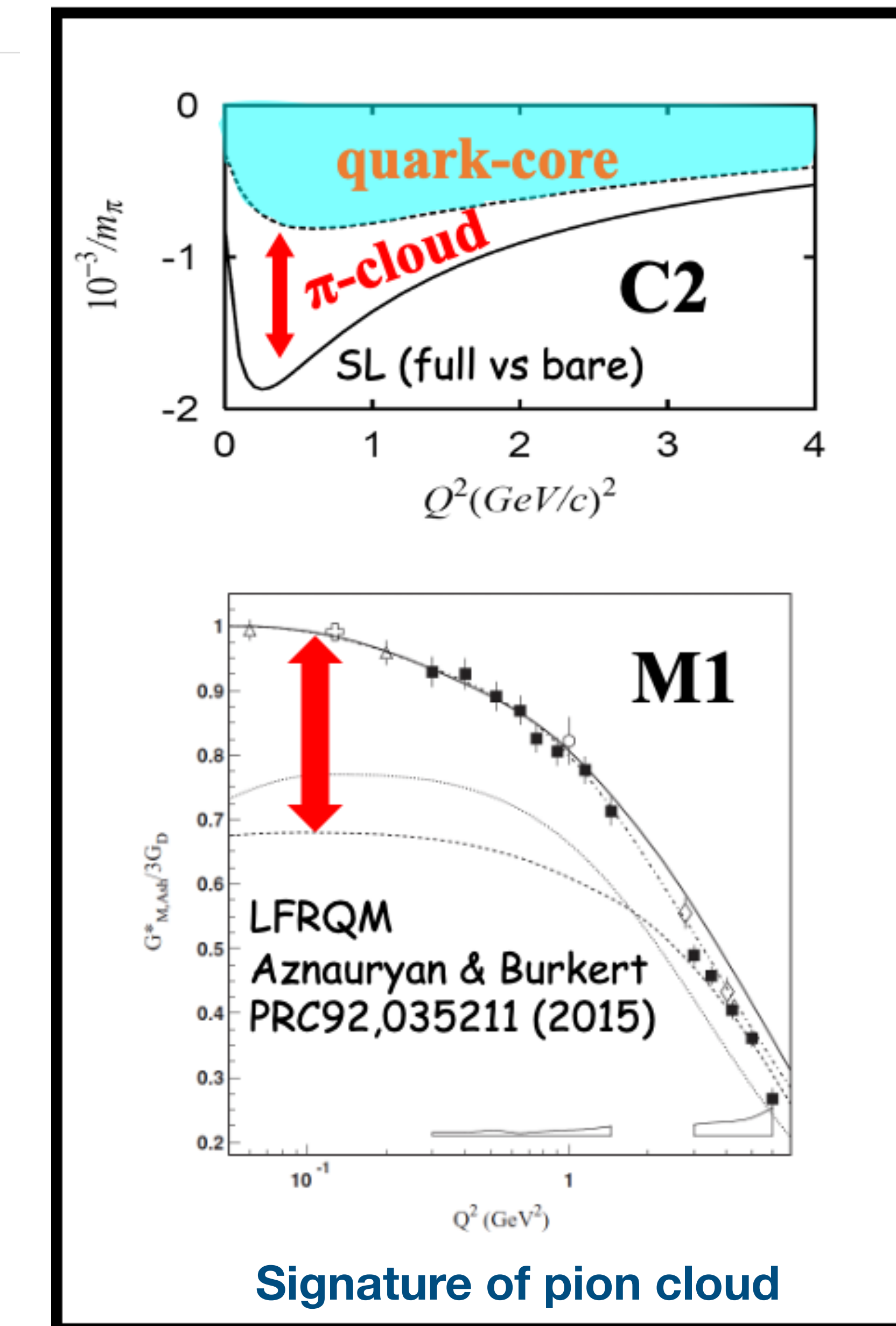
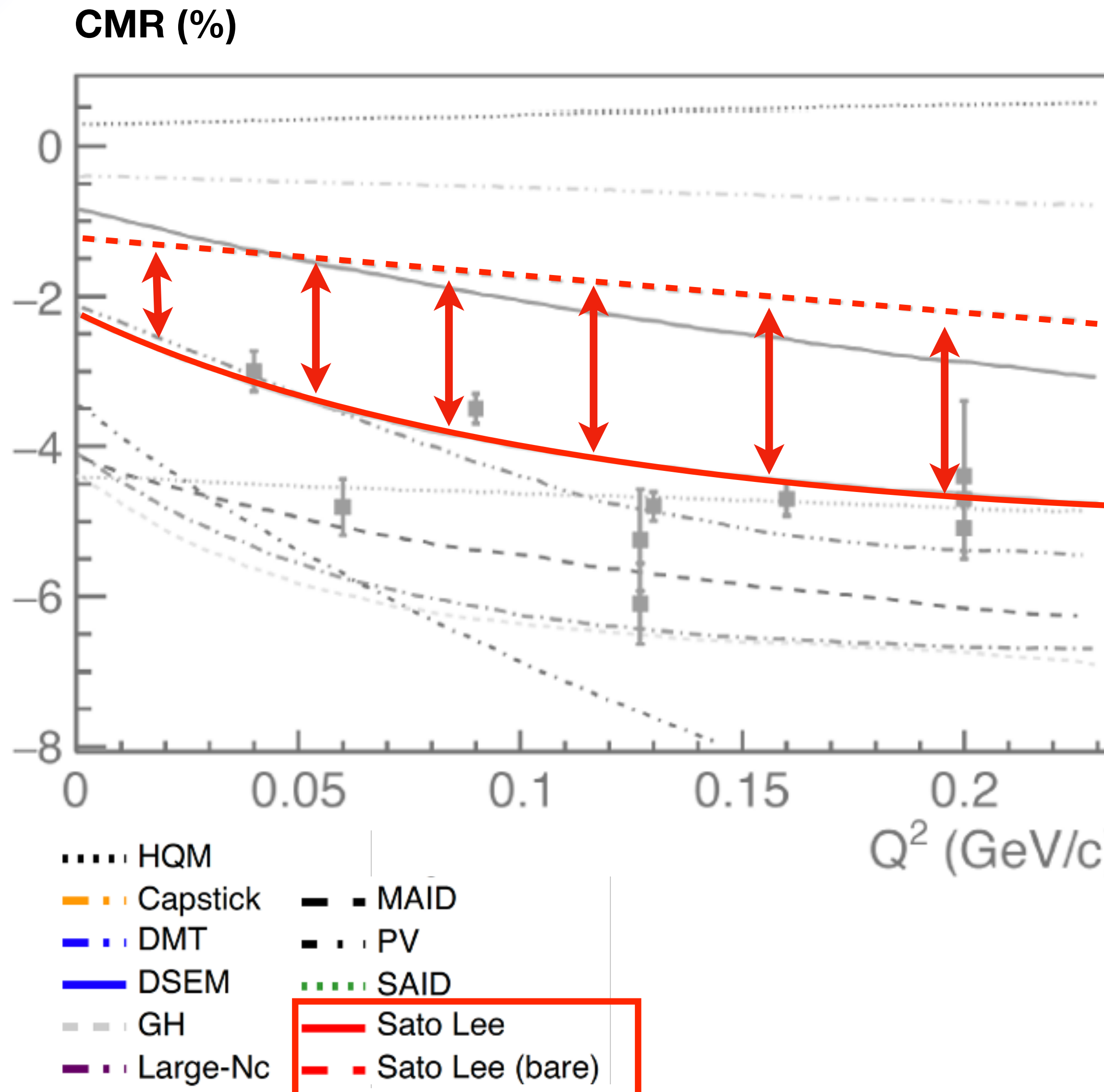
- Low Q^2 landscape is an important region to measure:
 - Mesonic cloud effects are predicted to be:
 - dominant in explaining the magnitude of the TFFs
 - changing most rapidly over all Q^2
 - Provides an excellent test bed for ChEFT and LQCD calculations
 - Relates the excitation mechanism to spatial information of the proton and the Delta.
 - Tests the predicted convergence of EMR and CMR as $Q^2 \rightarrow 0$.
 - Sparsely measured region.

Low Q^2 $N\text{-}\Delta$ transition form factors

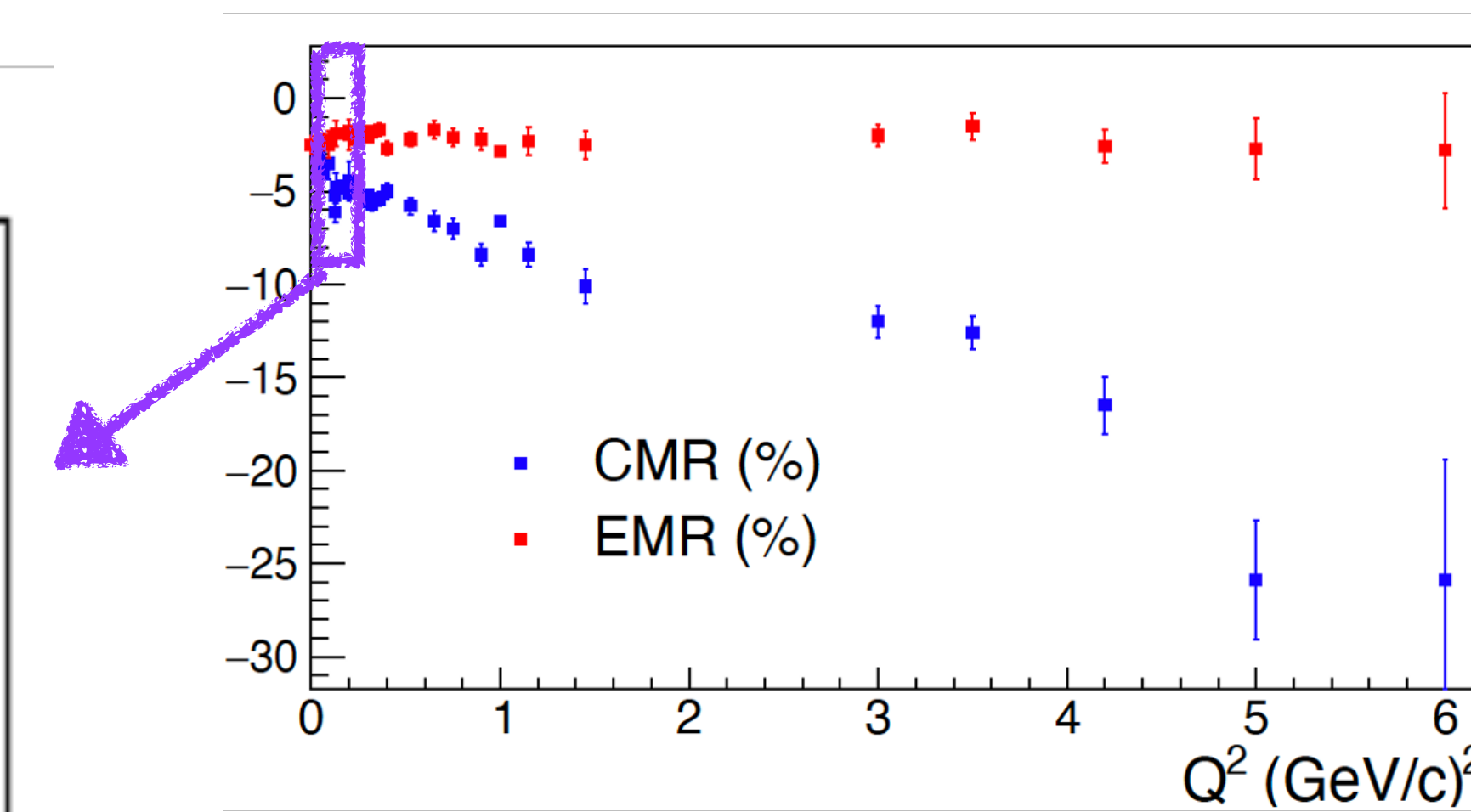
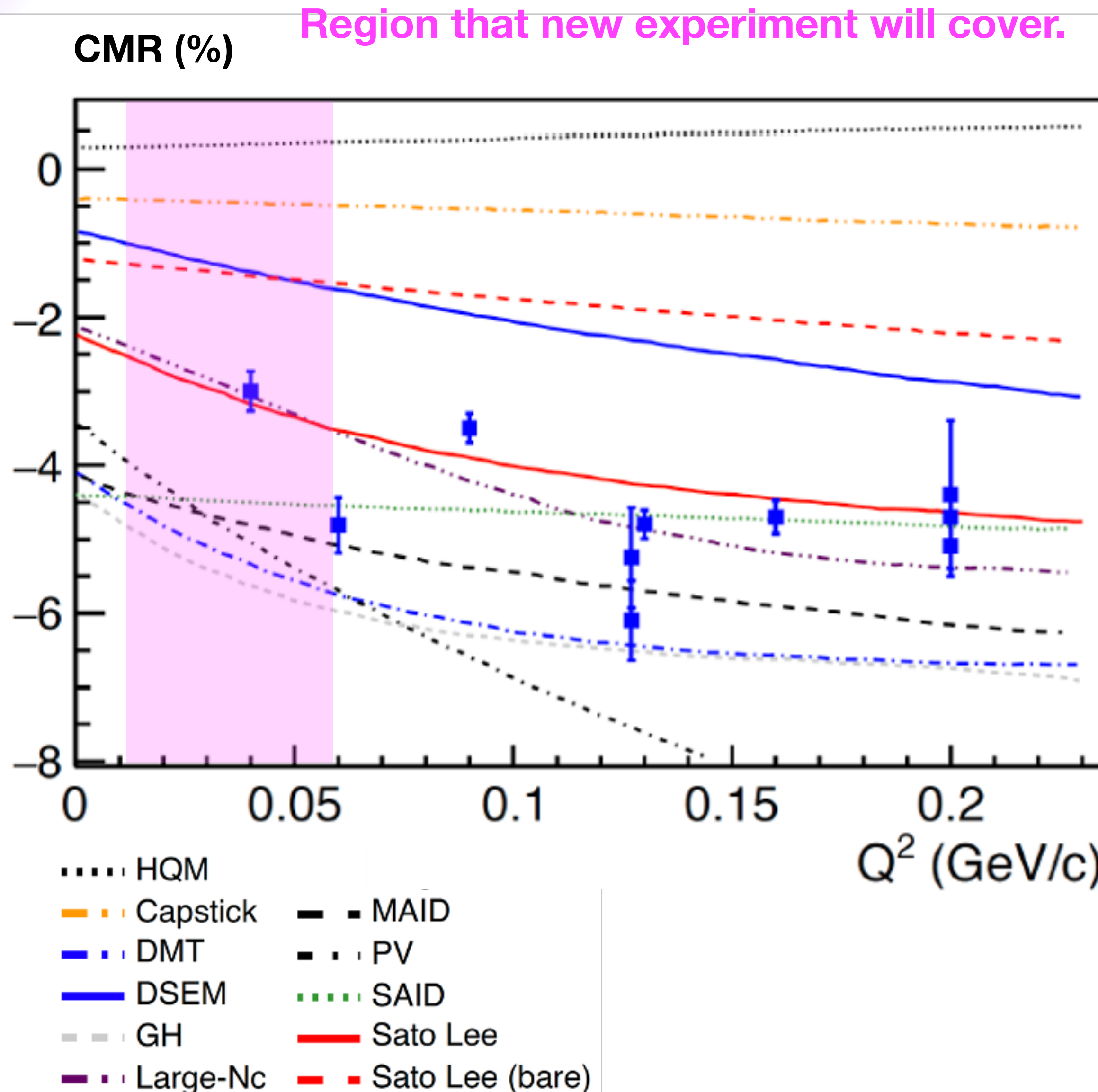


- Low Q^2 landscape is an important region to measure:
 - Mesonic cloud effects are predicted to be:
 - dominant in explaining the magnitude of the TFFs
 - changing most rapidly over all Q^2
 - Provides an excellent test bed for ChEFT and LQCD calculations
 - Relates the excitation mechanism to spatial information of the proton and the Delta.
 - Tests the predicted convergence of EMR and CMR as $Q^2 \rightarrow 0$.
 - Sparsely measured region.

Low Q^2 $N\Delta$ transition form factors

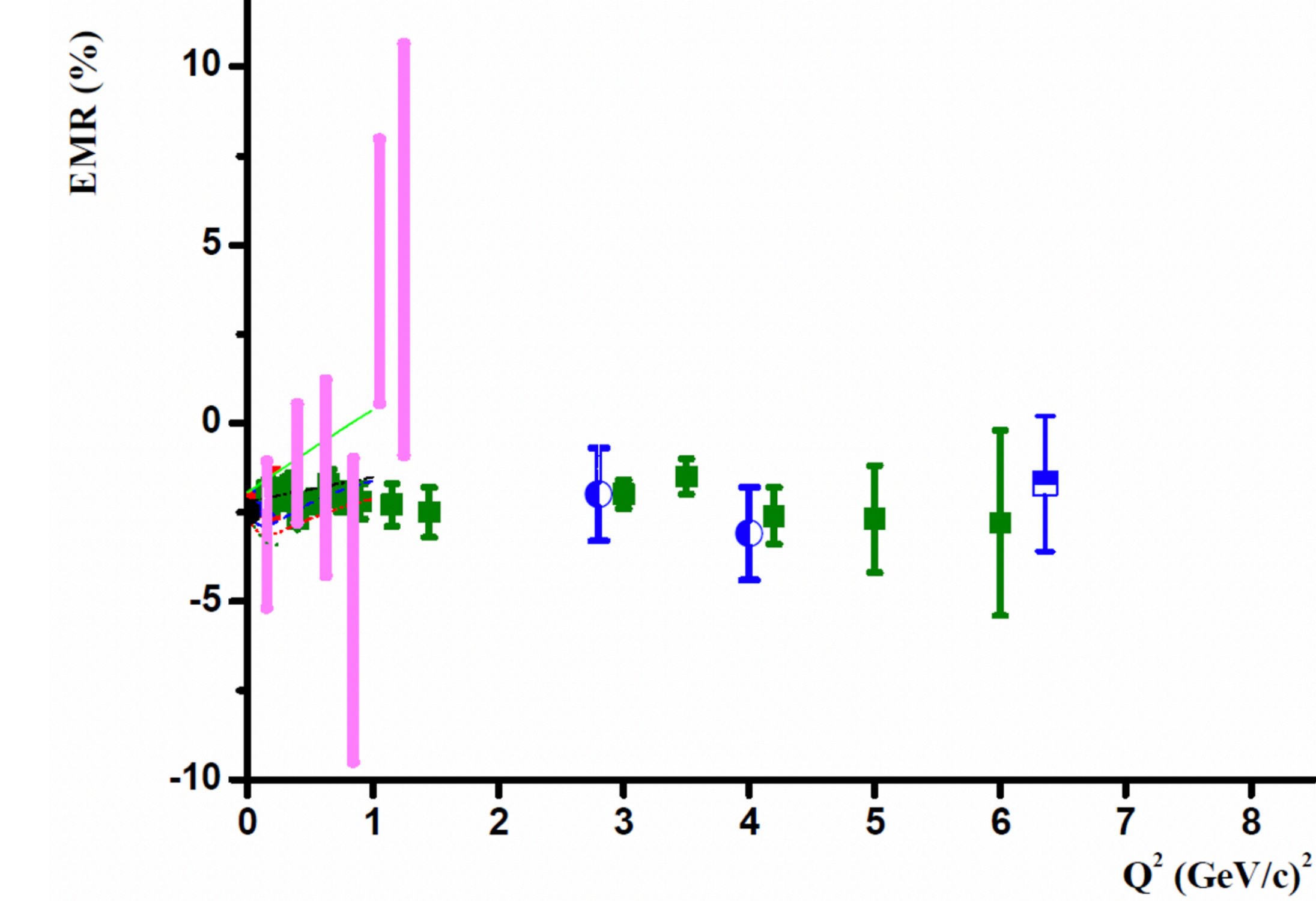
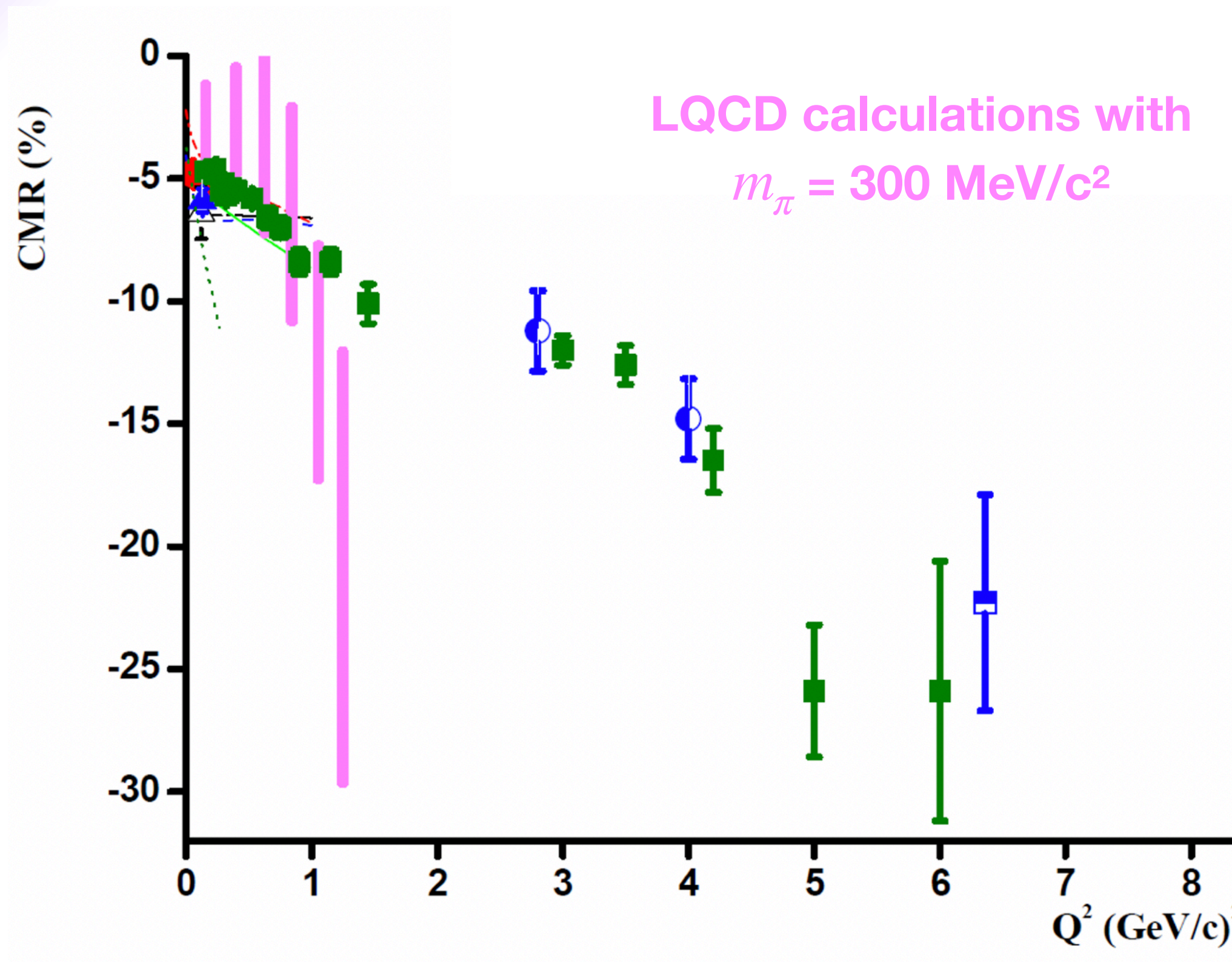


Low Q^2 $N\Delta$ transition form factors



- Low Q^2 landscape is an important region to measure:
 - Mesonic cloud effects are predicted to be:
 - dominant in explaining the magnitude of the TFFs
 - changing most rapidly over all Q^2
 - Provides an excellent test bed for ChEFT and LQCD calculations
 - Relates the excitation mechanism to spatial information of the proton and the Delta.
 - Tests the predicted convergence of EMR and CMR as $Q^2 \rightarrow 0$.
 - Sparsely measured region.

Lattice Calculations



- Updated LQCD calculations are in progress → new calculations will have a physical pion mass and uncertainties comparable to experiment.
 - Extended Twisted mass collaboration results expected within 2 years.
 - Efforts are partly motivated to understand baryon structure for neutrino scattering.
- Low Q^2 data will provide a precision benchmark for LQCD calculations.

What can we say about the geometry (shape) of the nucleon?

...an issue since the 80's

- What is the "shape" of the nucleon?

- Is it spherically symmetric or deformed?
 - If deformed, what is the origin of the deformation?
 - Exactly how are shape and structure related?

- How can one explore shape?

- Quadrupole moment of the ground state is identically 0 for a spin 1/2 system.
 - Pure proton scattering without spin excitation can't give you any information.
 - The only isolated spin-excitation resonance of the proton is the $\Delta^+(1232)$.

- A more comprehensive review can be found at:

- C. Alexandrou, C. Papanicolas, M. Vanderhaeghen,
 - "*The shape of hadrons*", Rev. Mod. Phys. 84, 1231 (2012)
- A. Bernstein, C. Papanicolas
 - "*Overview: The shape of hadrons*", AIP Conf. Proc. 904, 1 (2007)

Imaging the Δ and the $N\Delta$ transition

Empirical transverse charge transition densities

Eur. Phys. J. Special Topics 198, 141 (2011)

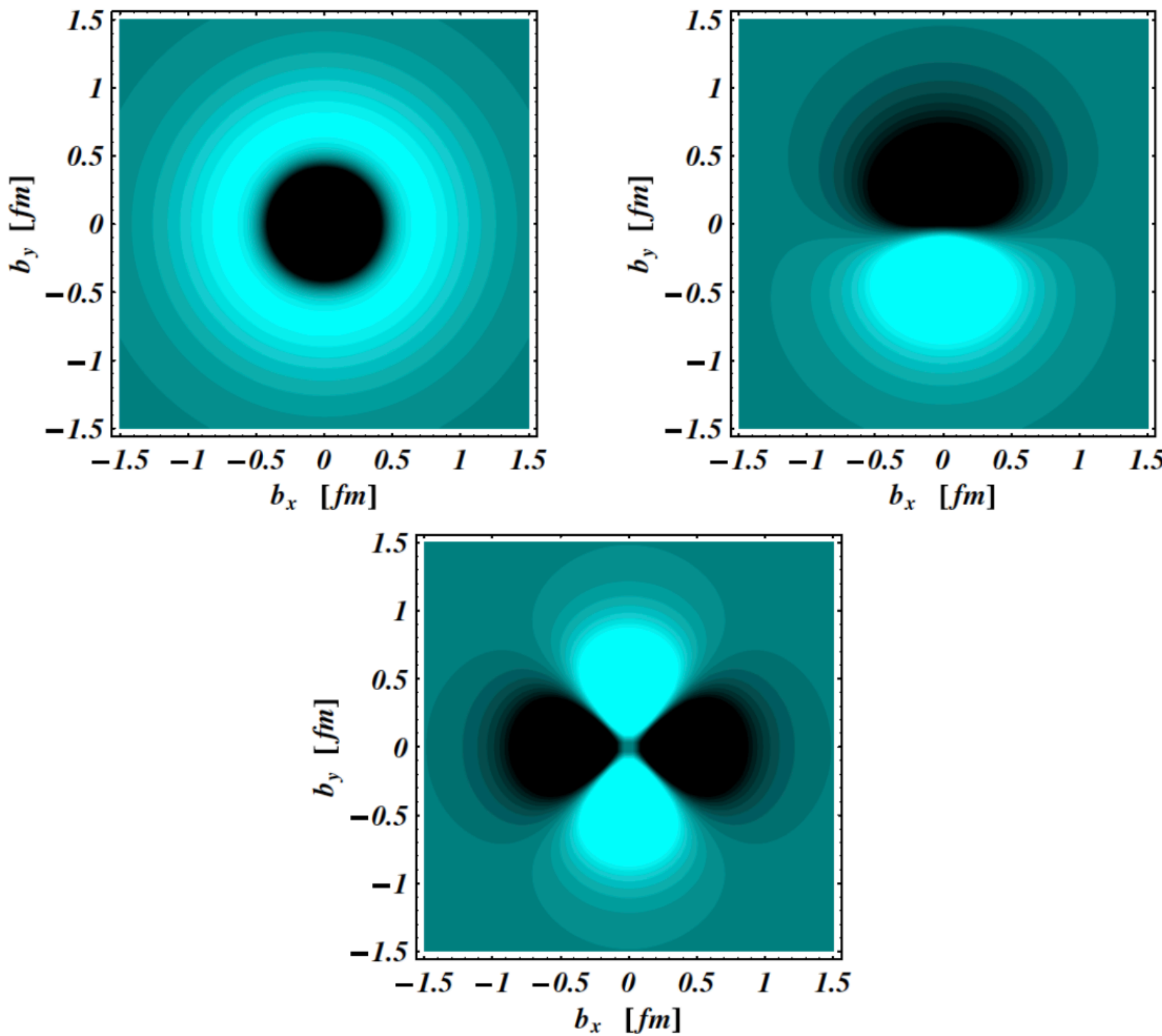


Fig. 18. Quark transverse charge density corresponding to the $p \rightarrow \Delta(1232)P_{33}$ e.m. transition. Upper left panel: p and Δ are in a light-front helicity $+1/2$ state ($\rho_0^{pP_{33}}$). Upper right panel: p and Δ are polarized along the x -axis ($\rho_T^{pP_{33}}$) as in Fig. 14. The lower panel shows the quadrupole pattern, whose contribution to the polarized transition density is very small due to the weak $E2/C2$ admixtures in the $N\Delta$ transition and practically invisible in the upper right panel. The light (dark) regions correspond to positive (negative) densities. For the $p \rightarrow P_{33}(1232)$ e.m. transition FFs, we use the MAID2007 parametrization.

Probing hadron wave functions
in Lattice QCD

Phys. Rev. D. 66, 094503 (2002)

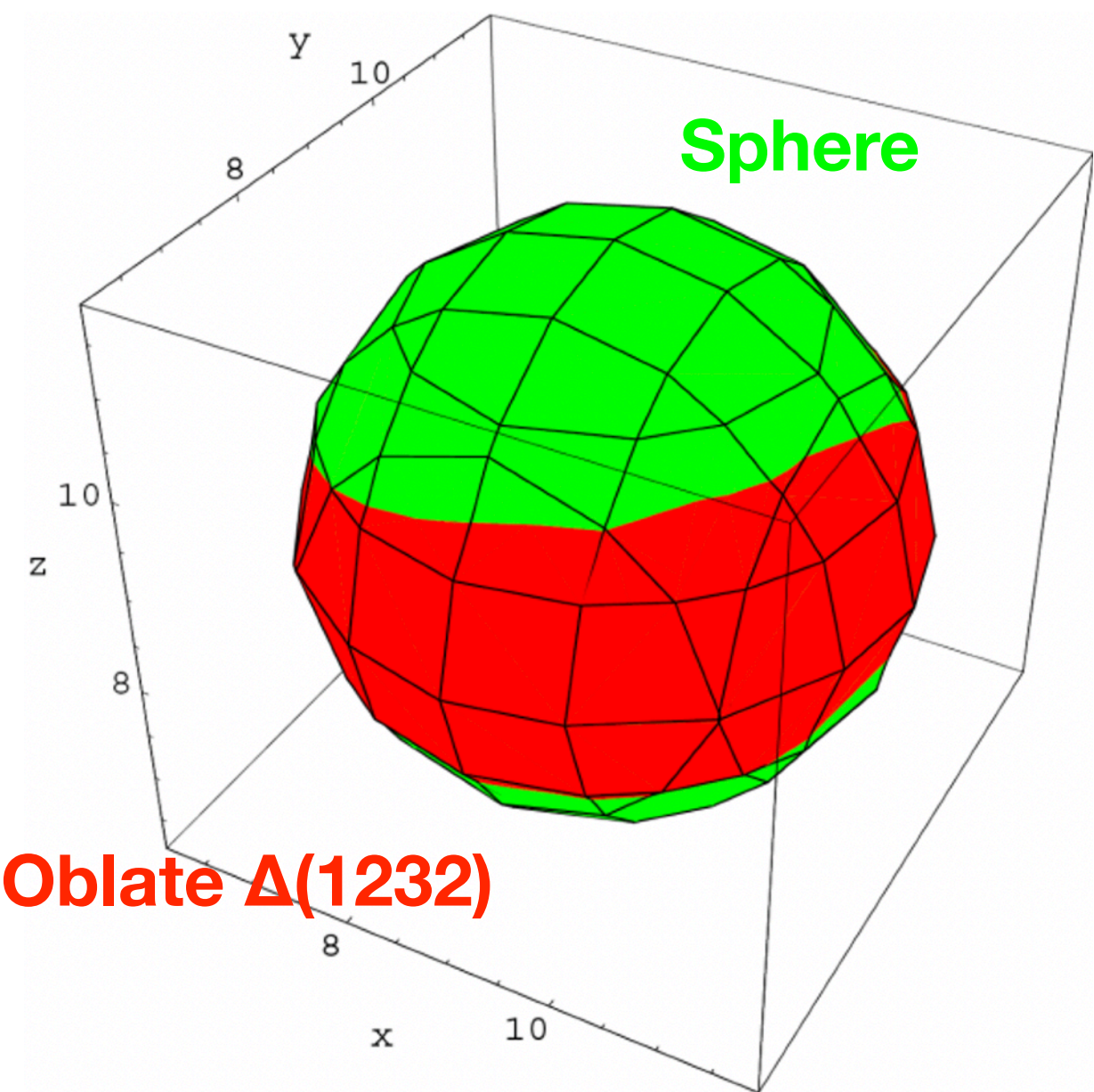


FIG. 18. Three-dimensional contour plot of the correlator (black): upper for the rho state with 0 spin projection (cigar shape) and lower for the Δ^+ state with $+3/2$ (slightly oblate) spin projection for two dynamical quarks at $\kappa = 0.156$. Values of the correlator (0.5 for the rho, 0.8 for the Δ^+) were chosen to show large distances but avoid finite-size effects. We have included for comparison the contour of a sphere (grey).

Latice QCD: Quark transverse
charge density in $\Delta^+(1232)$

Phys. Rev. D. 79, 014507 (2009)

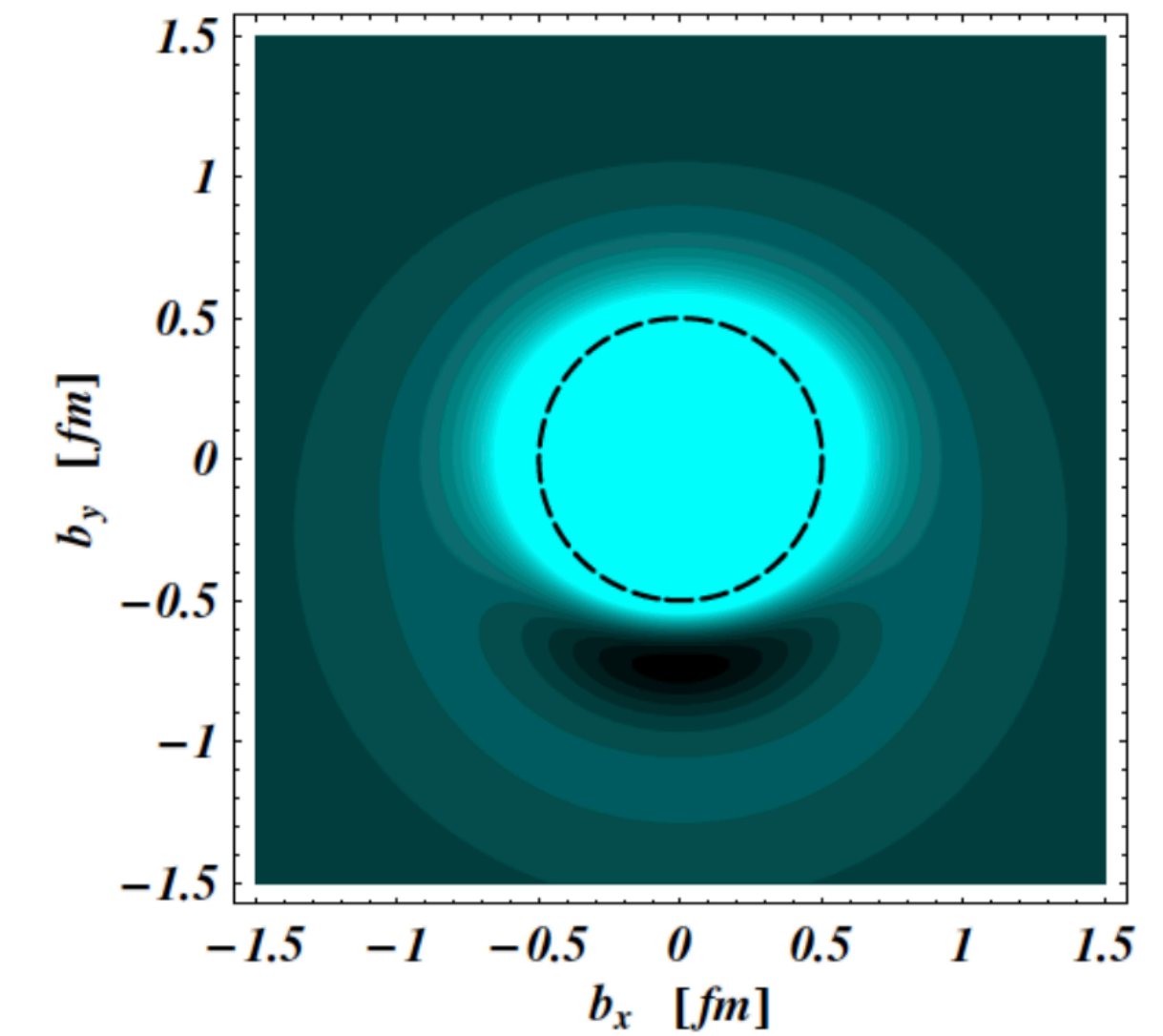
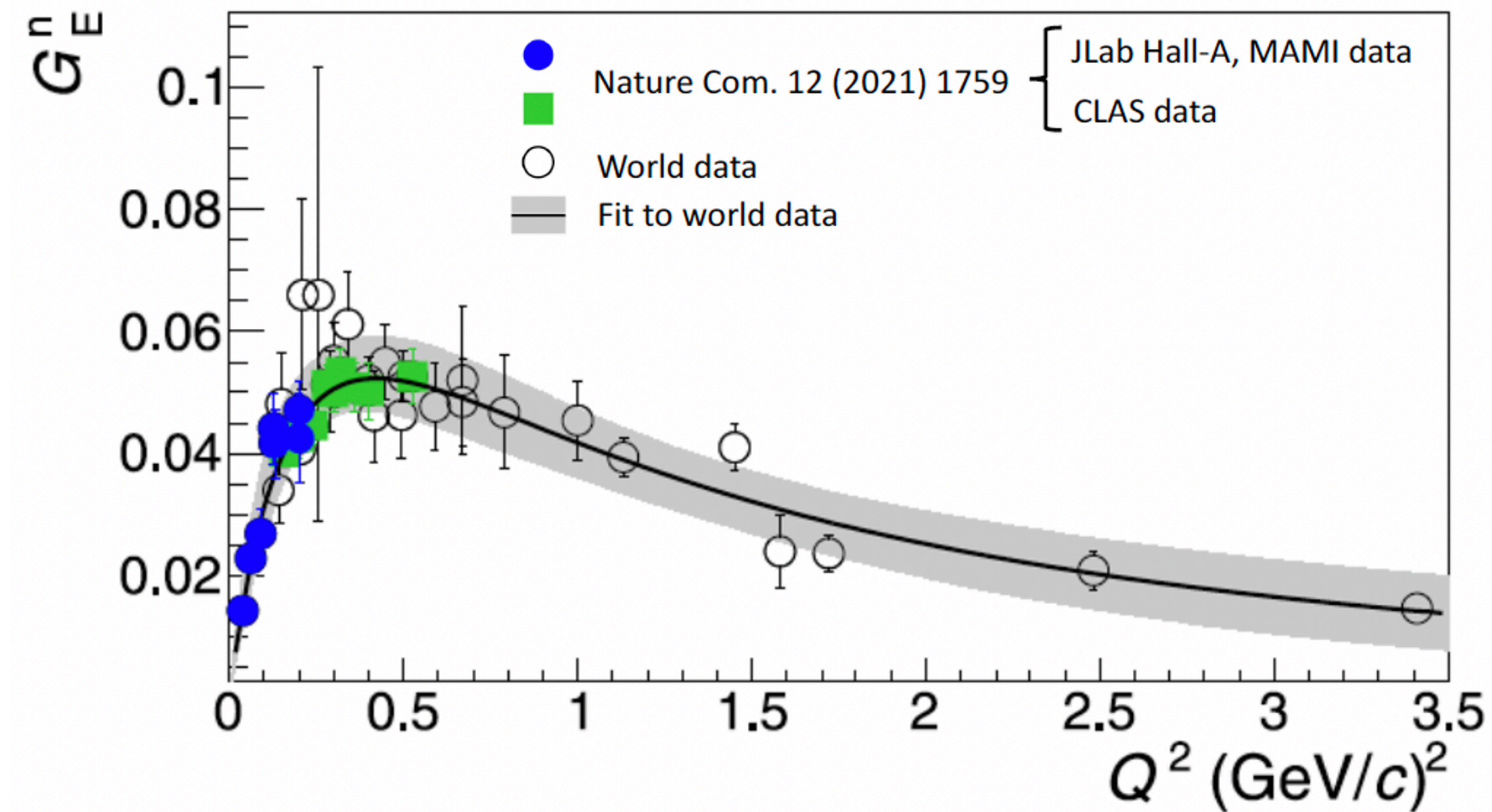


FIG. 10: Lattice QCD results for the quark transverse charge density $\rho_T^{\Delta_{3/2}}$ in a $\Delta^+(1232)$ which is polarized along the positive x -axis. The light (dark) regions correspond to the largest (smallest) values of the density. In order to see the deformation more clearly, a circle of radius 0.5 fm is drawn for comparison. The density is obtained from quenched lattice QCD results at $m_\pi = 410$ MeV for the Δ e.m. FFs [48].

Connections to the neutron structure

- There are long-known relations between the TFFs and the neutron FFs.
 - Pascalutsa, V. & Vanderhaeghen, M. : Phys. Rev. D 76 (2007) [Large-Nc]
 - Grabmayr, P. & Buchmann, A. J. : Phys. Rev. Lett. 86 (2001) [CQM + 2-body currents]
- G_E^n extraction from TFFs show strong agreement with world data.
 - Allows access to low- Q^2 region where direct measurement of G_E^n is difficult.
 - The relations receive theoretical corrections that can be analyzed and confronted with experimental data e.g. they can be analyzed in a theoretical framework that combines ChPT with the $1/N_c$ expansion.



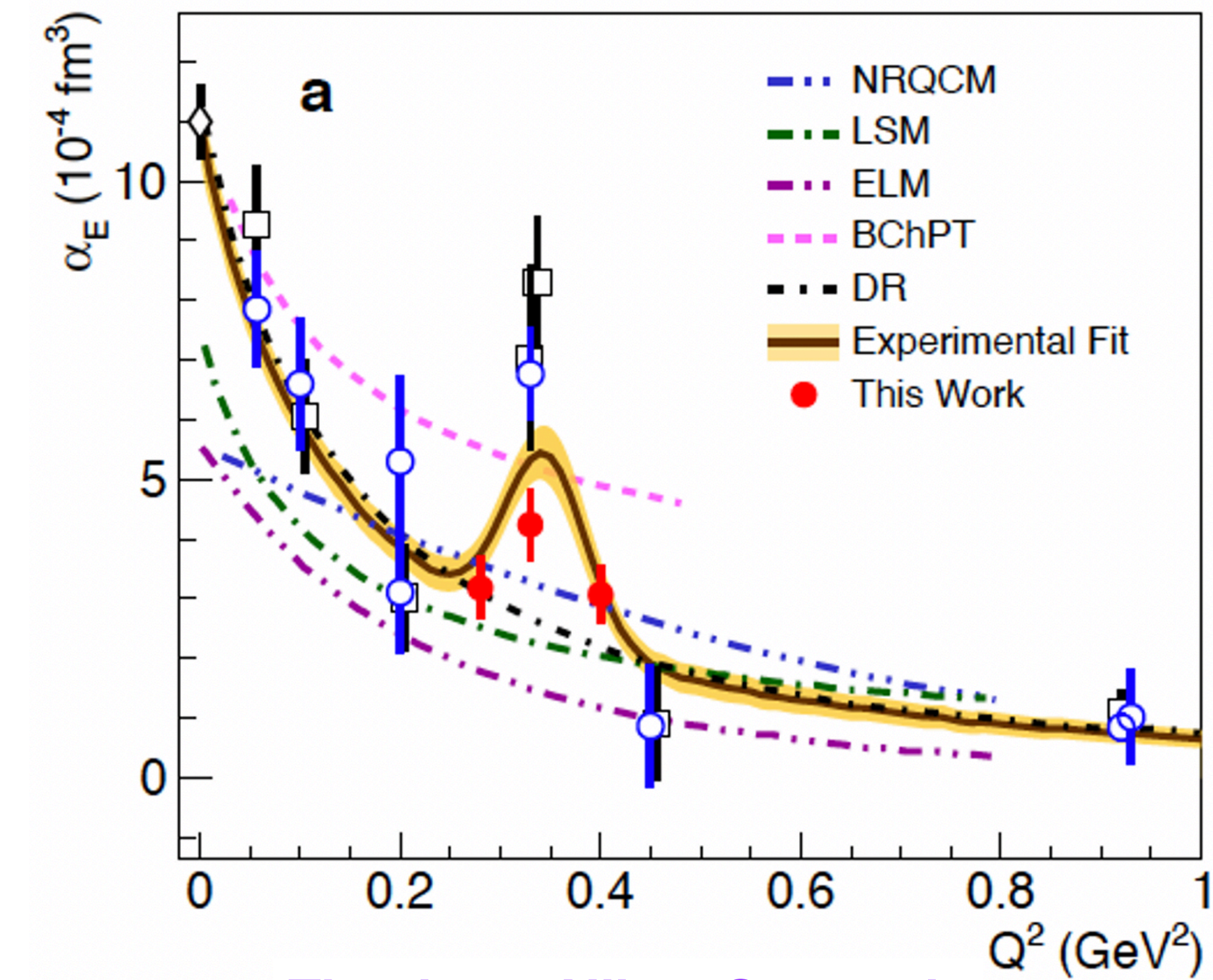
Impact on other domains of nuclear physics

- Generalized polarizabilities (GPs) of the proton:

- The TFFs enter as an input in the VCS cross section over the Δ resonance region - their precise knowledge is necessary for the precise extraction of the GPs from the measured cross sections
- Physics of interest:
 - Electric polarizability puzzle
 - Interplay of paramagnetism & diamagnetism in the proton
 - Extraction of the polarizability radii and imaging of the induced polarization density.

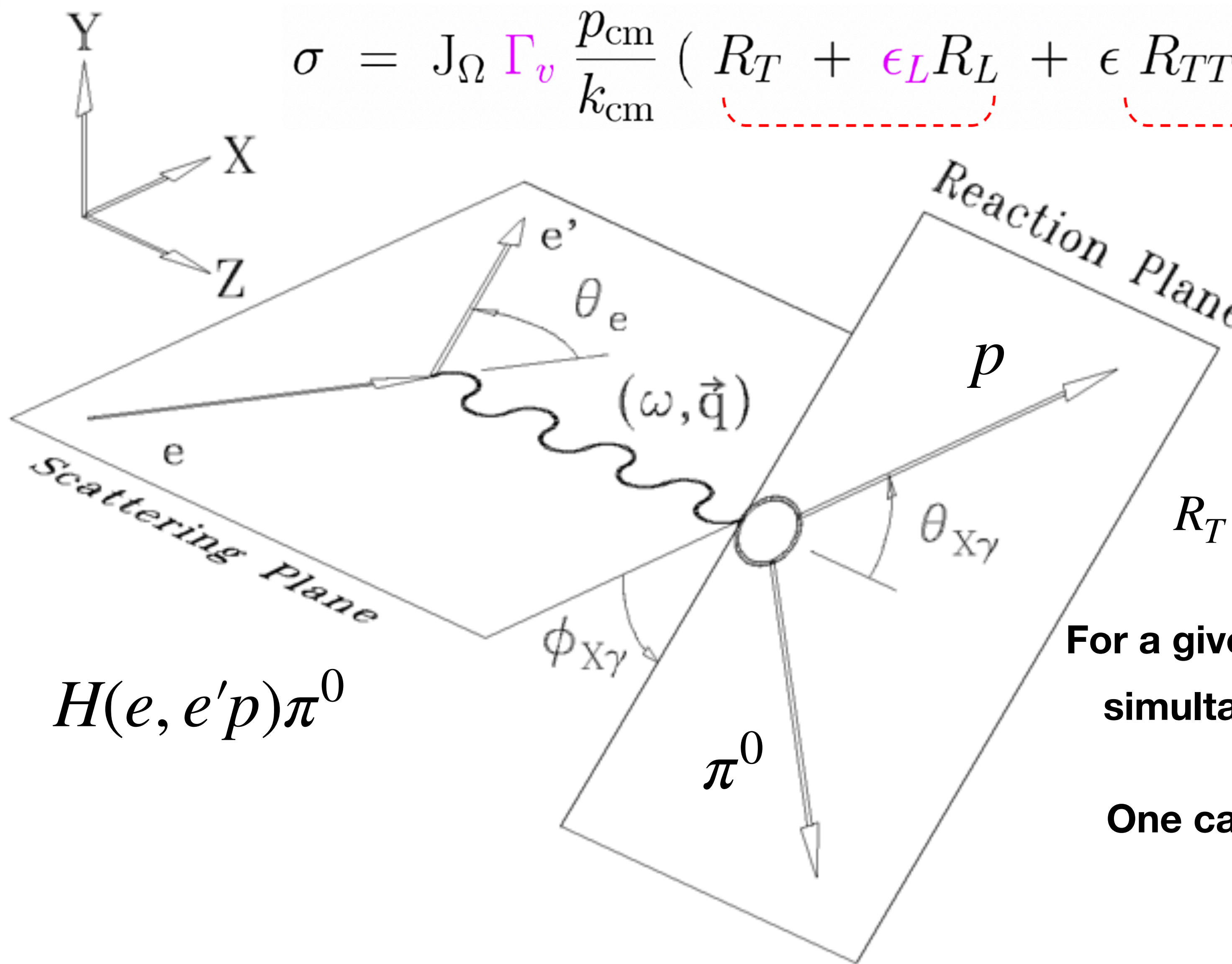
- Neutrino oscillation studies and neutrino-nucleus scattering

- Dominant source of systematic error: uncertainties in neutrino-nucleus reaction cross sections in the nucleon-resonance region.



Thanks to Nikos Sparveris
for his talk on Wednesday!

Experimental Methodology



Experimental Methodology

$$R_{TT} = 3 \sin^2 \theta (E2 M1 + M1^2 + \dots \Sigma_{\text{background}})$$

$$R_{LT} = -6 \cos \theta \sin \theta (C2 M1 + \dots \Sigma_{\text{background}})$$

$$R_T + R_L = M1^2 + \dots \Sigma_{\text{background}}$$

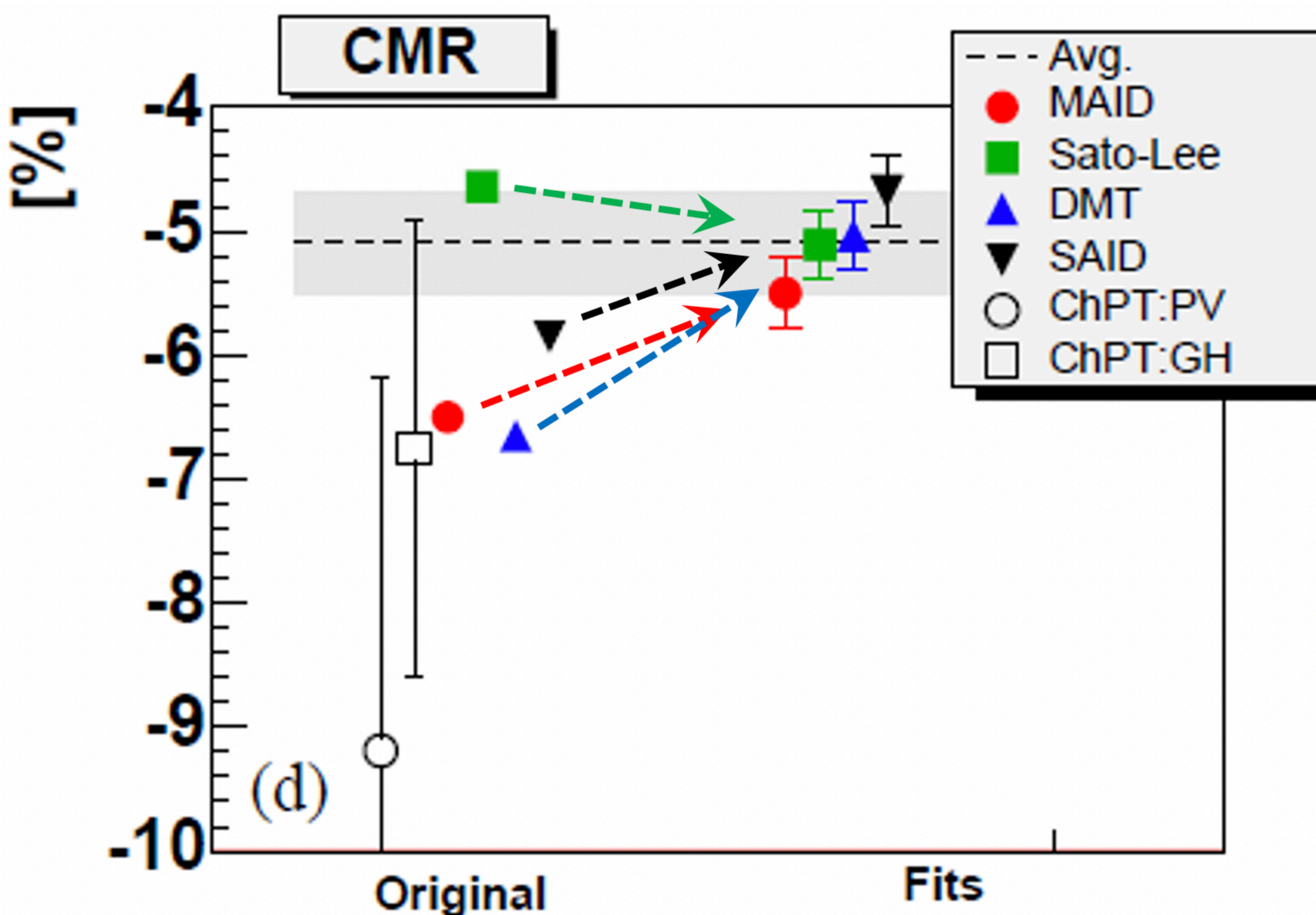
$R_{TT} \rightarrow$ sensitive to the EMR

$R_{LT} \rightarrow$ sensitive to the CMR

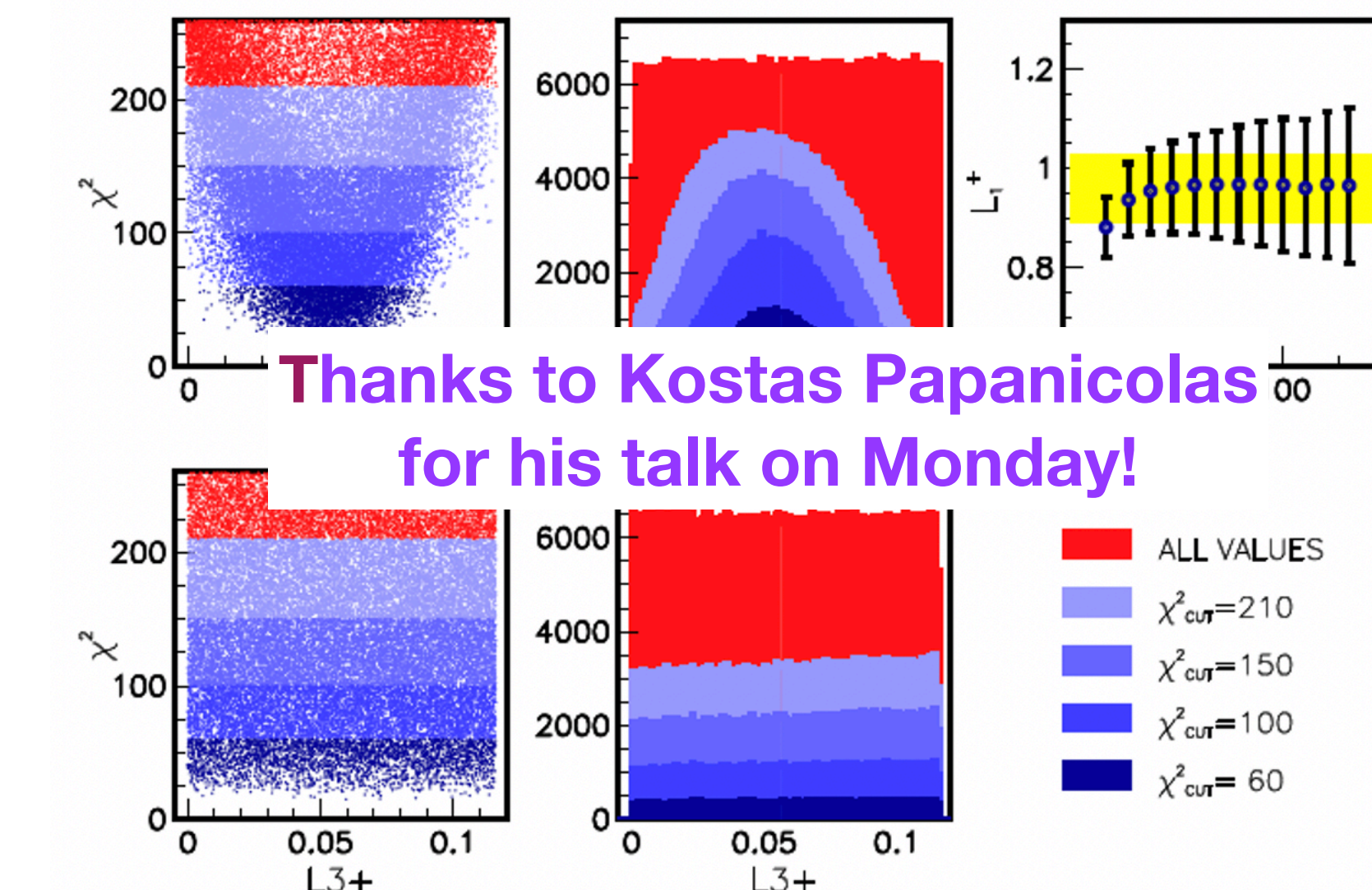
$R_T + R_L \rightarrow$ sensitive to $M1$

Fit parameterized models to data

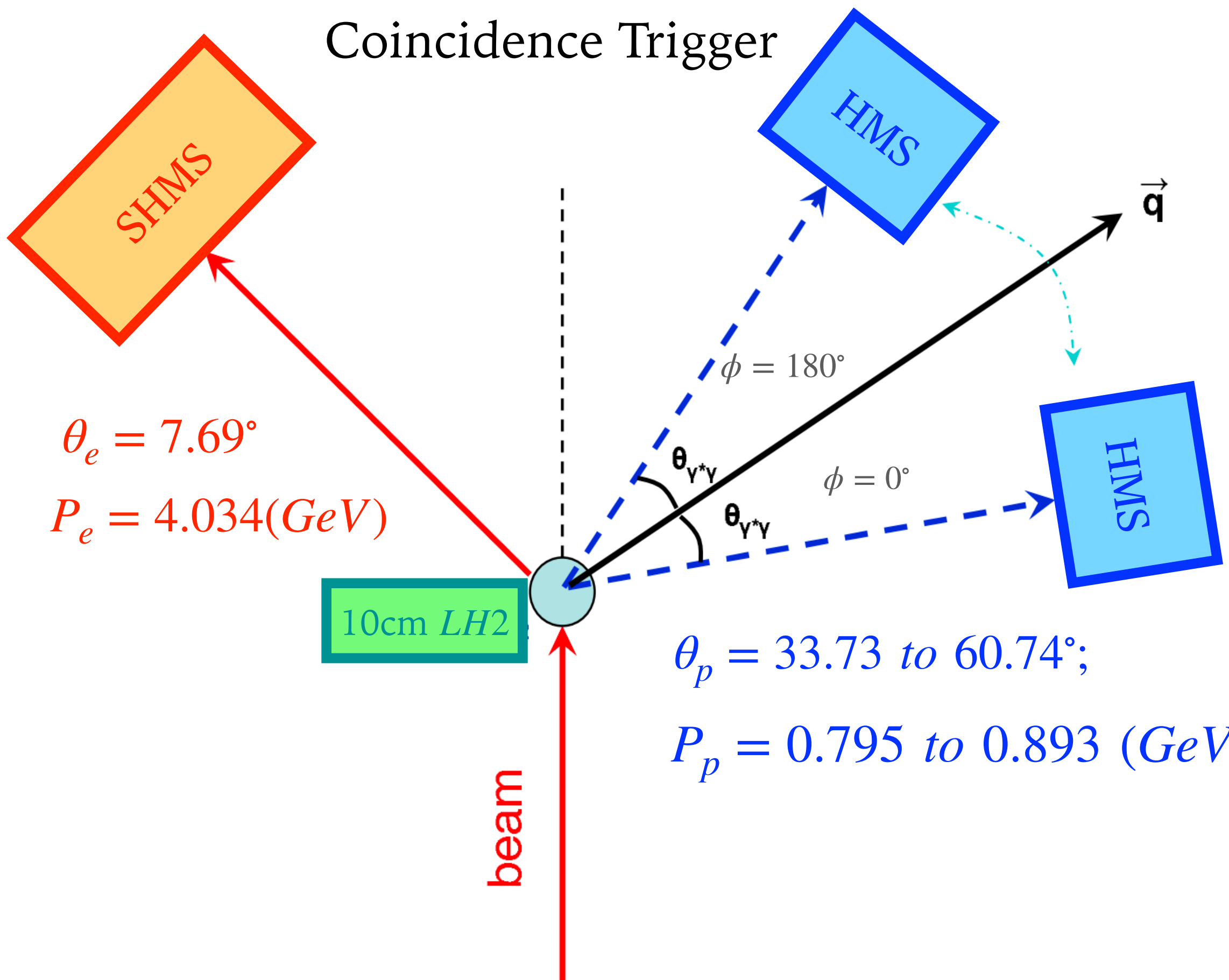
and/or



Use model independent statistical methods to identify and determine with maximal precision parameters that are sensitive to the data:
AMIAS (Eur. Phys. J. A 56 (2020) 10, 270)



JLab E12-15-001 Experiment

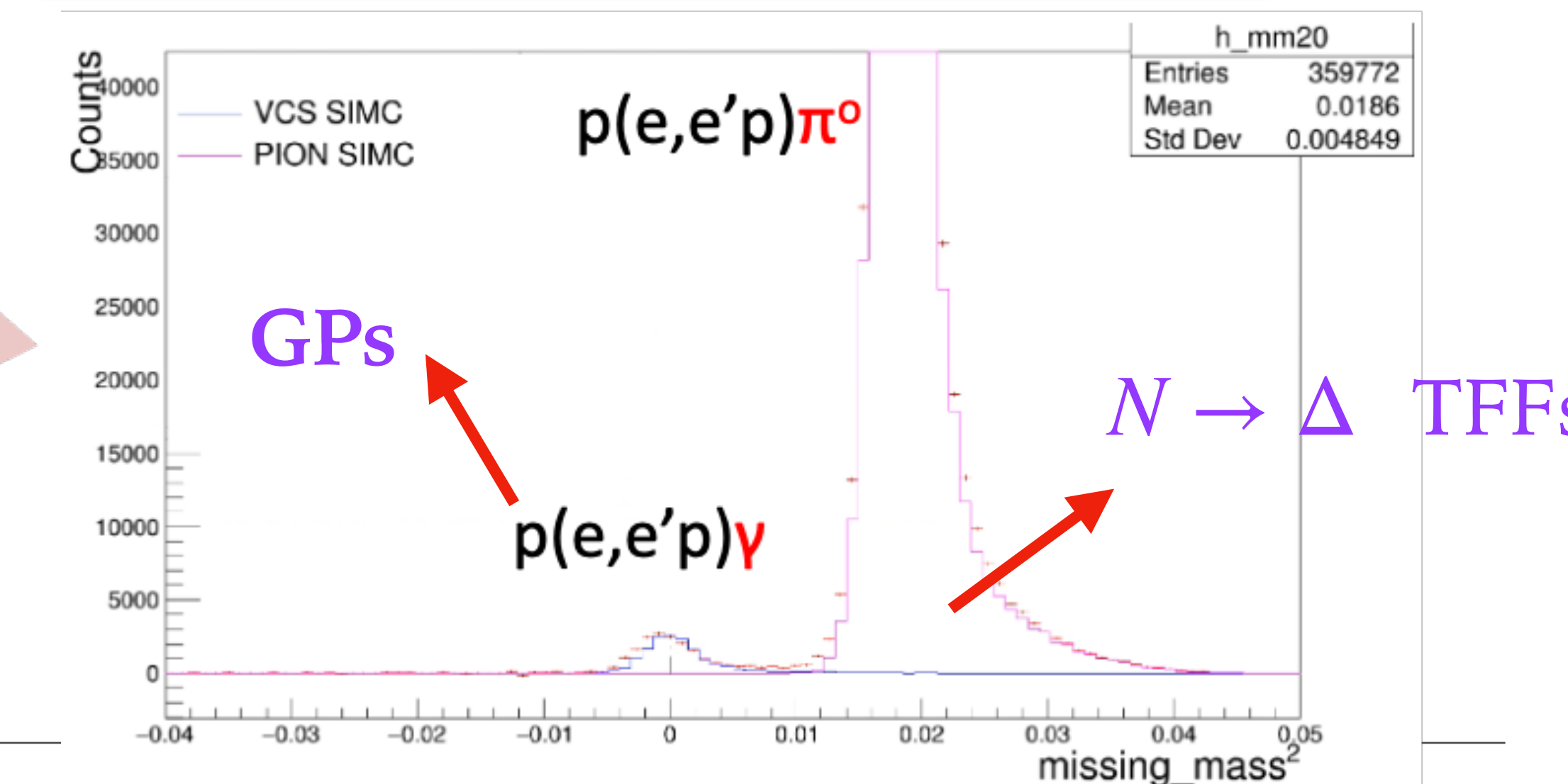


- Summer 2019: July 20 - August 5
- Beam $E = 4.56\text{GeV}$
- $Q^2 = 0.25 - 0.4 \text{ GeV}^2$, $W = 1.232 \text{ GeV}$

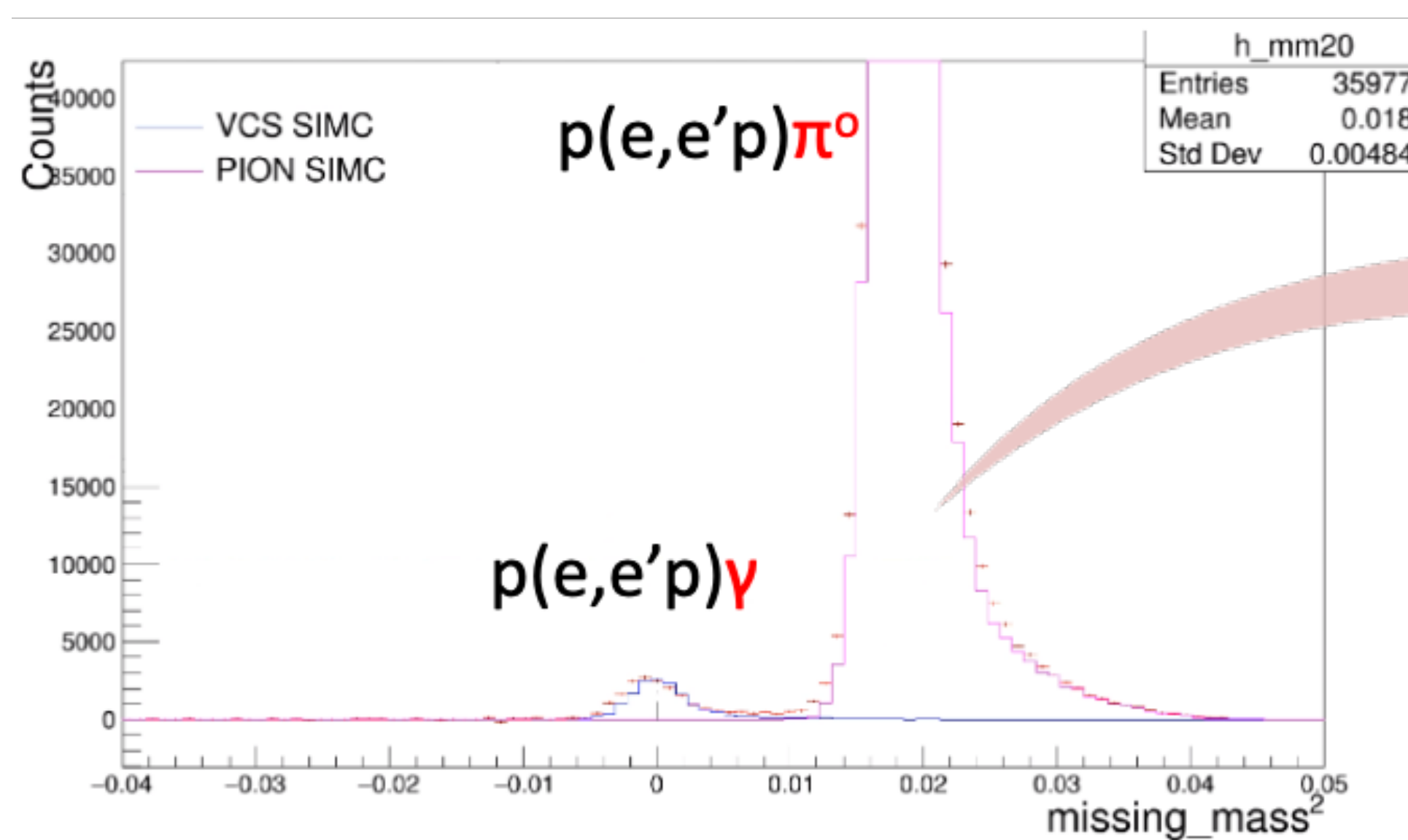
	Kinematical Setting	$\theta_{\gamma^*\gamma}^\circ$	θ_e°	$P'_e(\text{MeV}/c)$	θ_p°	$P'_p(\text{MeV}/c)$	S/N	beam time (days)
Part I	Kin Ia	155	7.97	3884.4	37.20	893.20	1.1	0.5
	Kin Ib	155	7.97	3884.4	51.26	893.20	2.7	0.5
	Kin IIa	140	7.97	3884.4	33.08	859.90	1	0.45
	Kin IIb	140	7.97	3884.4	55.38	859.90	3.7	0.55
	Kin IIIa	120	7.97	3884.4	27.85	794.68	0.9	0.45
	Kin IIIb	120	7.97	3884.4	60.61	794.68	6.2	0.55
	Kin IVa	165	9.39	3820.5	40.85	1010.40	1.3	0.5
	Kin IVb	165	9.39	3820.5	48.45	1010.40	2.4	0.5
	Kin Va	155	9.39	3820.5	38.34	995.20	1	0.5
	Kin Vb	155	9.39	3820.5	50.96	995.20	3.2	0.5
Part II	Kin VIa	128	9.39	3820.5	31.84	919.43	0.7	0.95
	Kin VIb	128	9.39	3820.5	57.46	919.43	7.8	0.55
	Kin VIIa	165	11.54	3708.6	40.81	1175.25	2.6	1.5
	Kin VIIb	165	11.54	3708.6	47.35	1175.25	5	2
	Kin VIIIa	160	11.54	3708.6	39.73	1167.72	2.2	1.5
	Kin VIIIb	160	11.54	3708.6	48.43	1167.72	6.3	2
Part II	Kin IXa	140	11.54	3708.6	35.52	1117.38	1.2	1.5
	Kin IXb	140	11.54	3708.6	52.64	1117.38	8	2

Part I

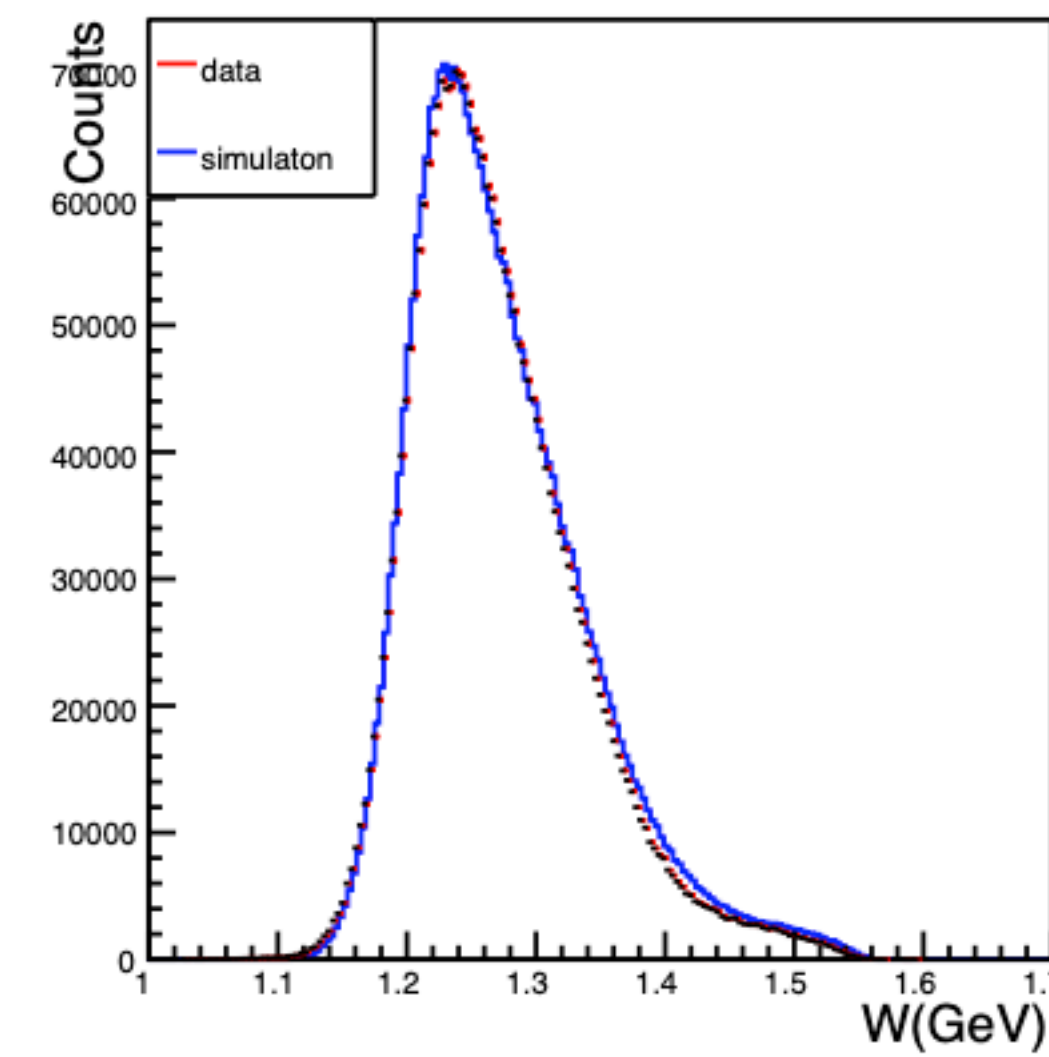
Part II



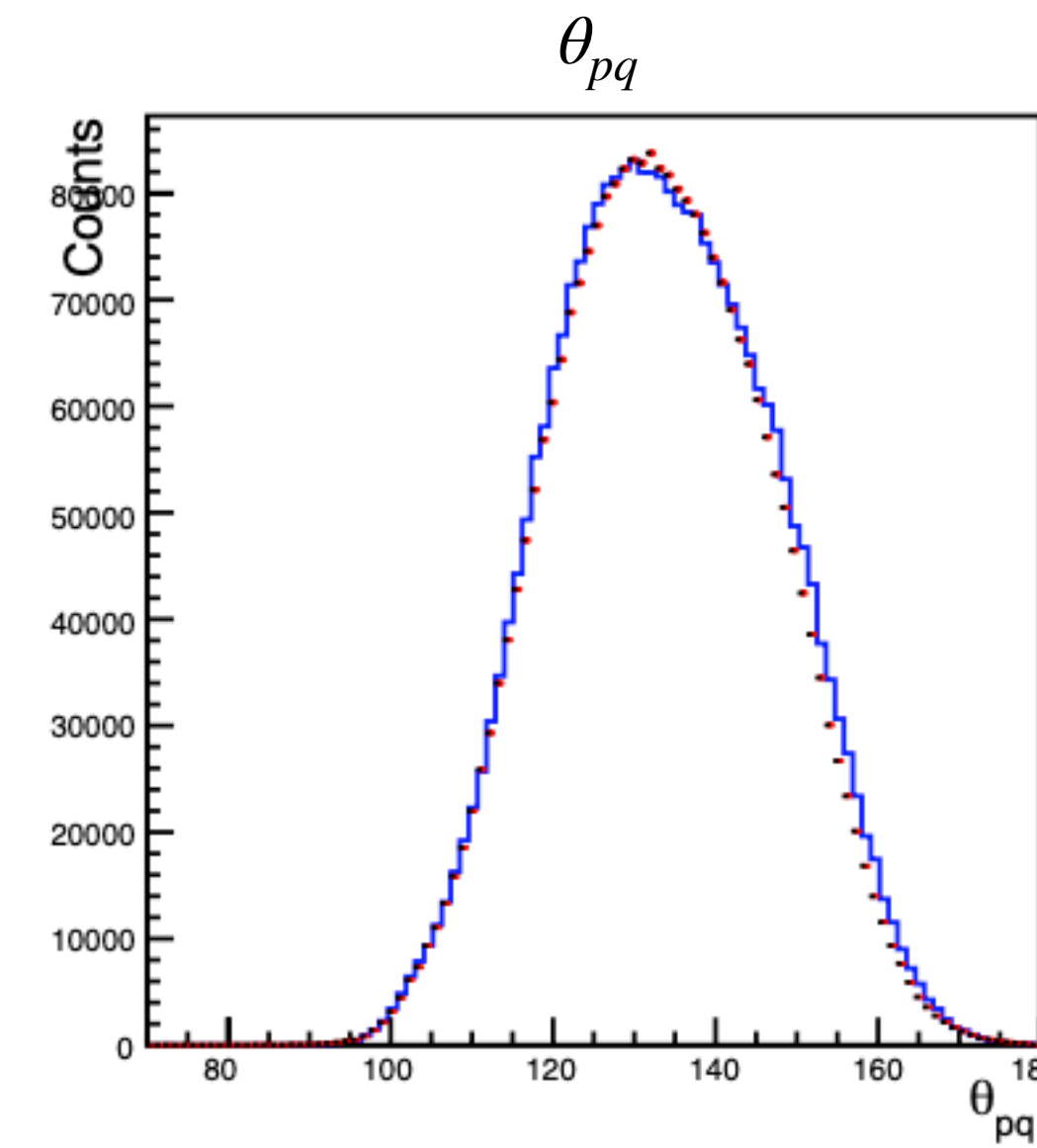
π^0 Analysis



W

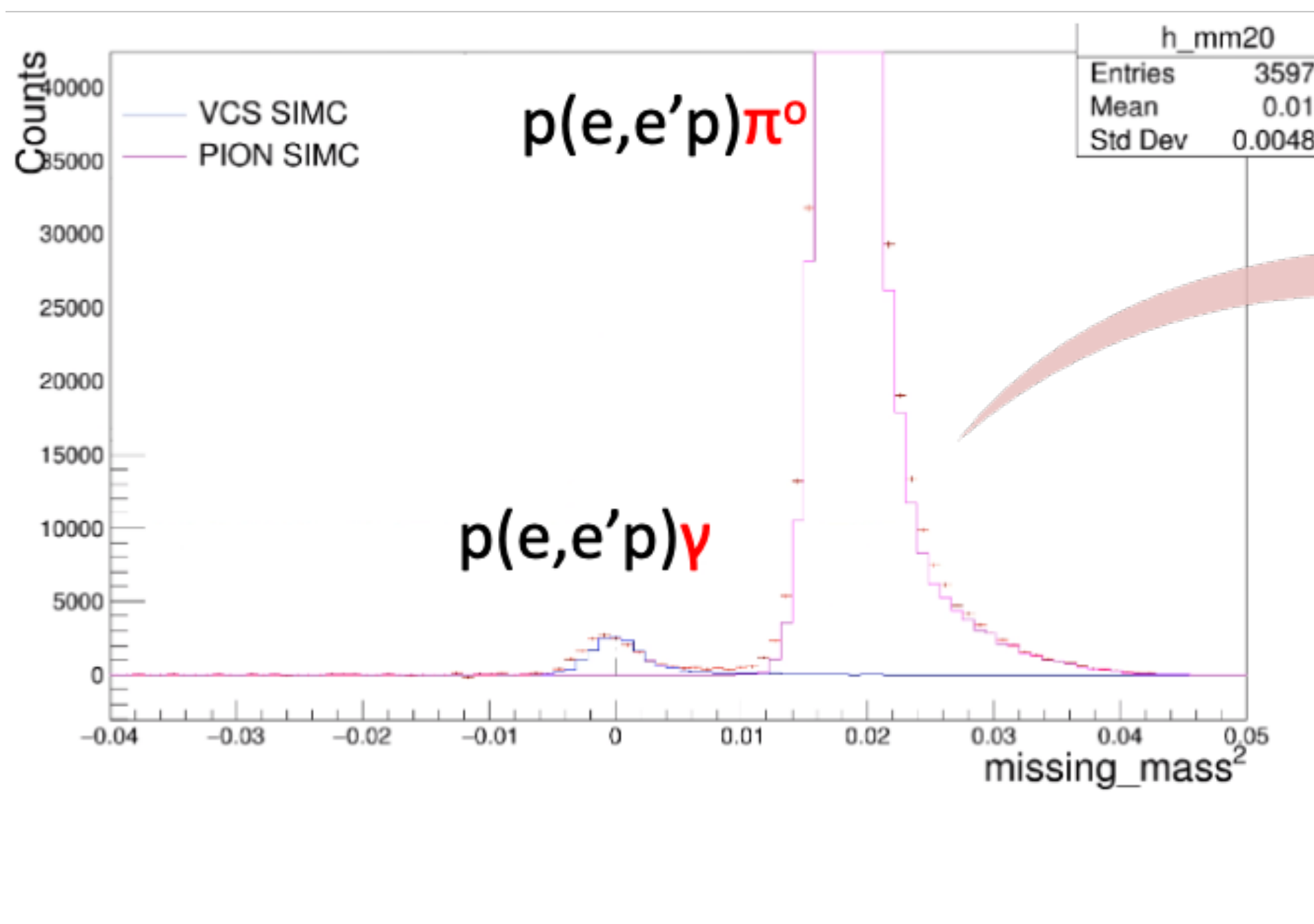


MAID
Data



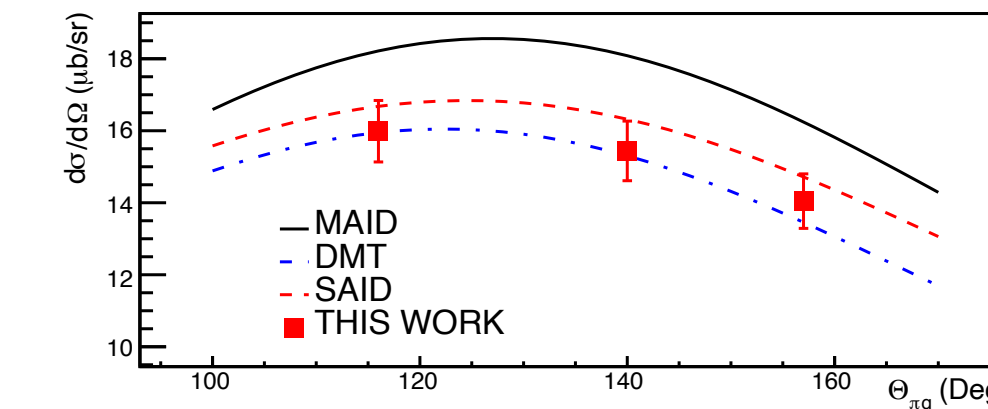
π^0 Cross Sections

Q²=0.36 (GeV/c)²

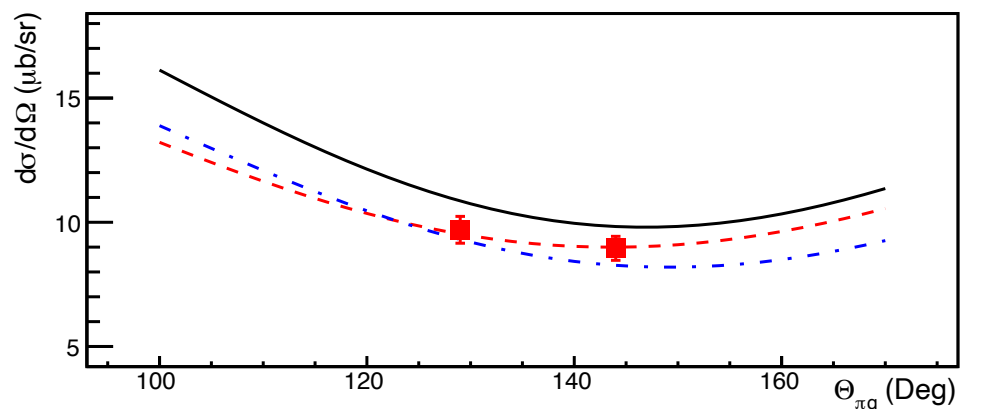


W=1212 MeV

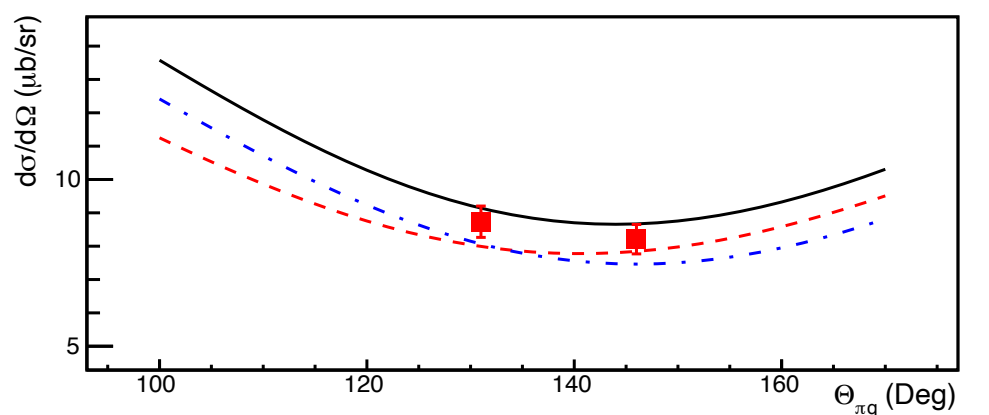
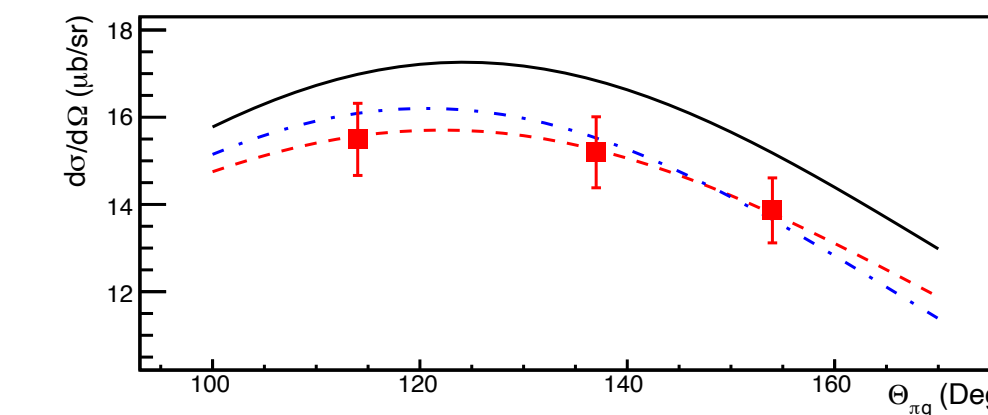
$\phi = 0$



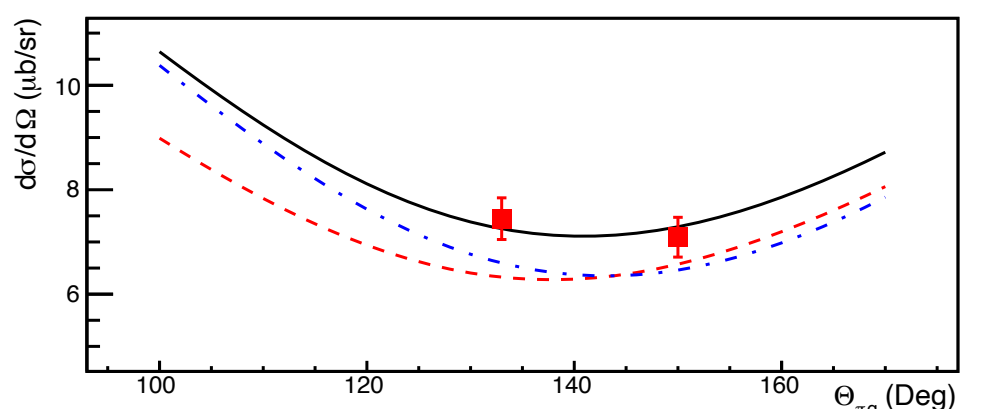
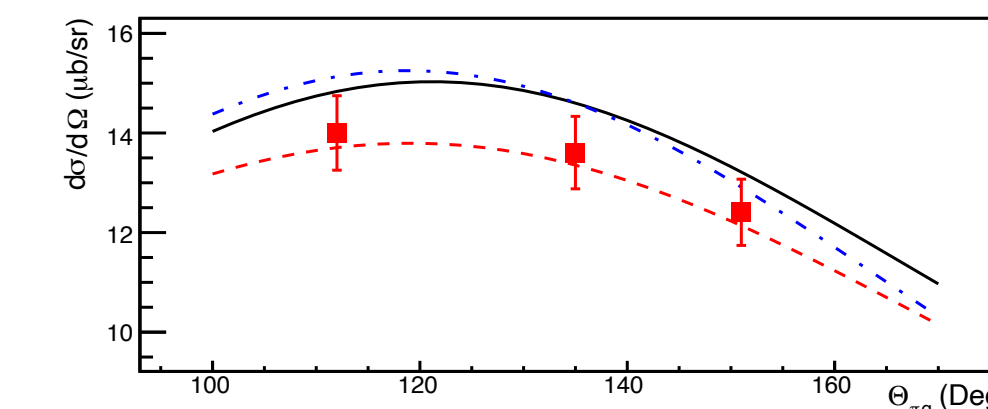
$\phi = 180$



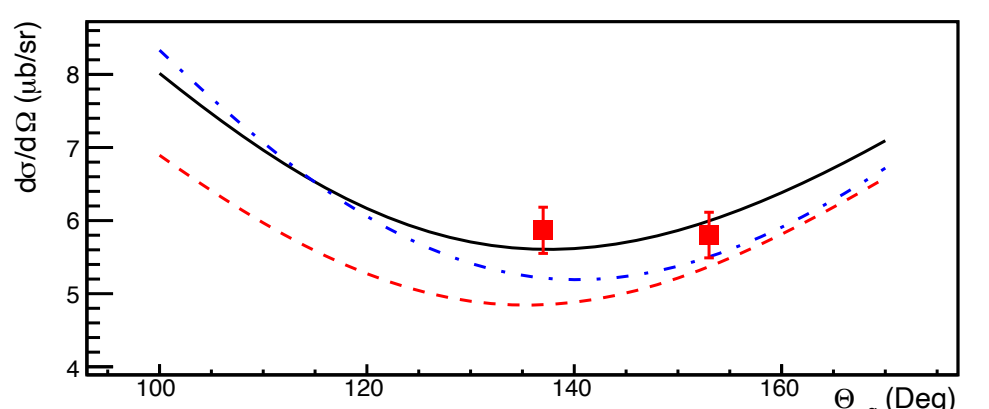
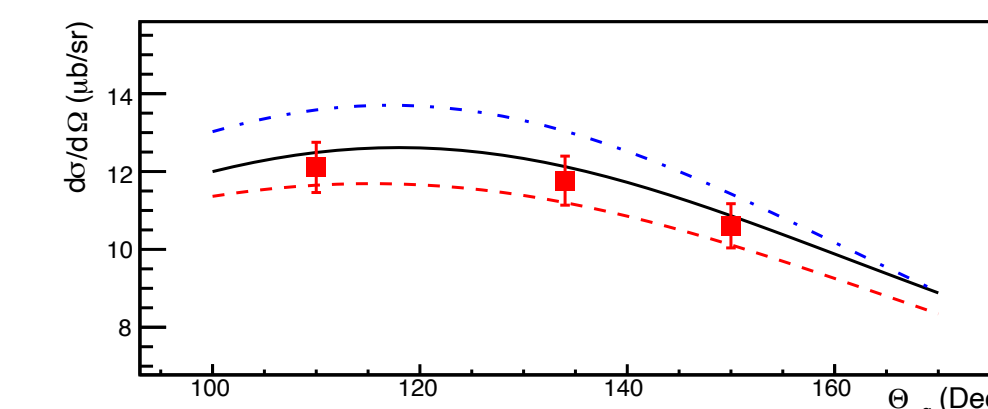
W=1222 MeV



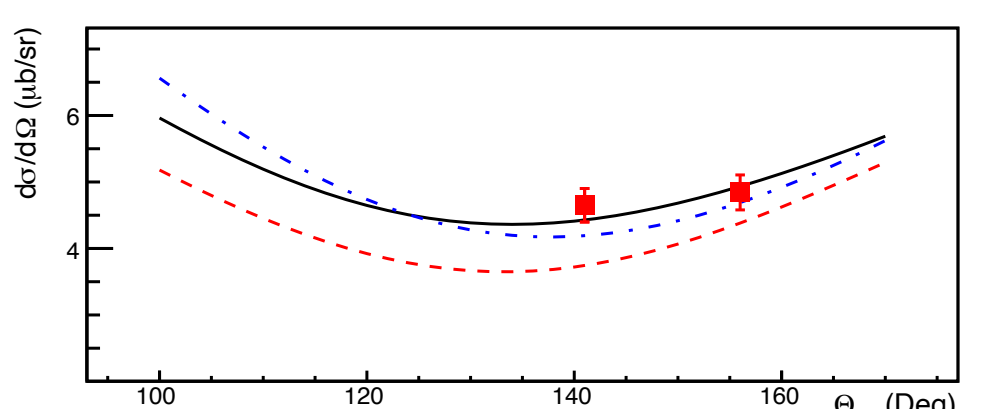
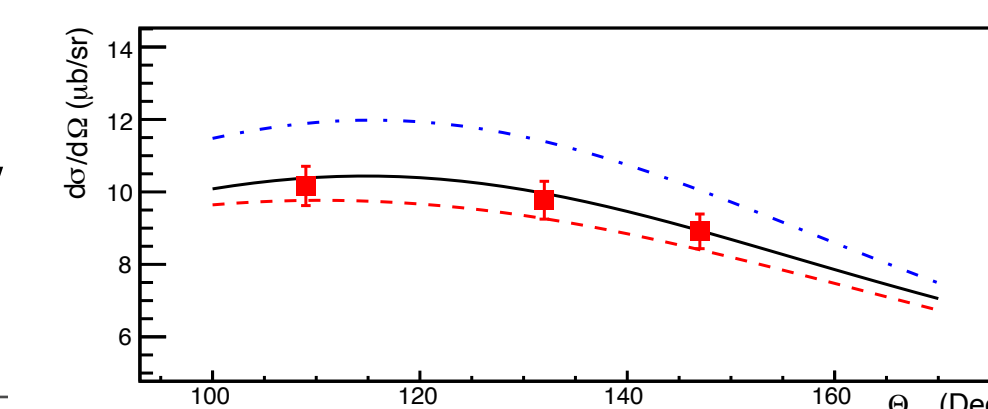
W=1232 MeV



W=1242 MeV



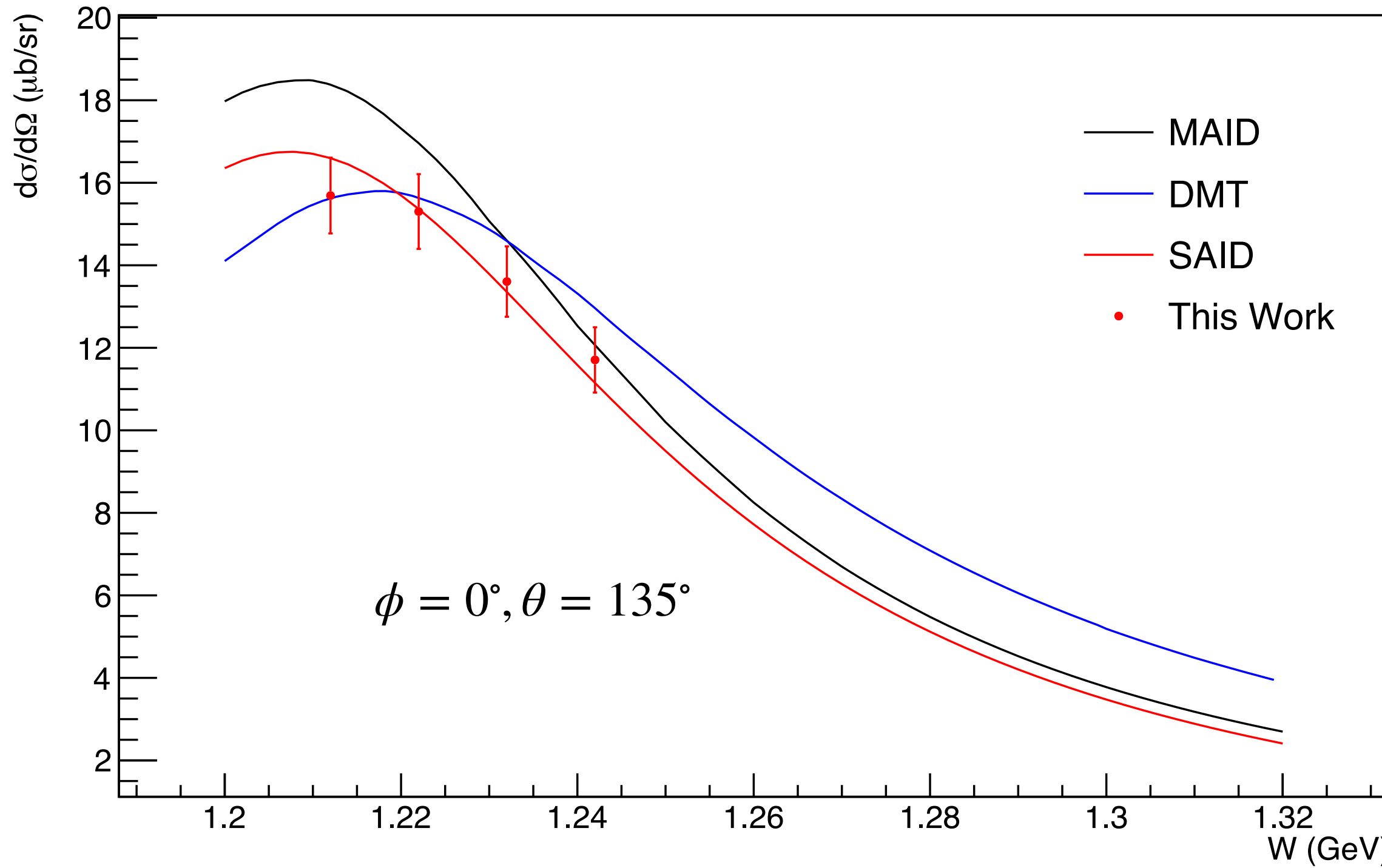
W=1252 MeV



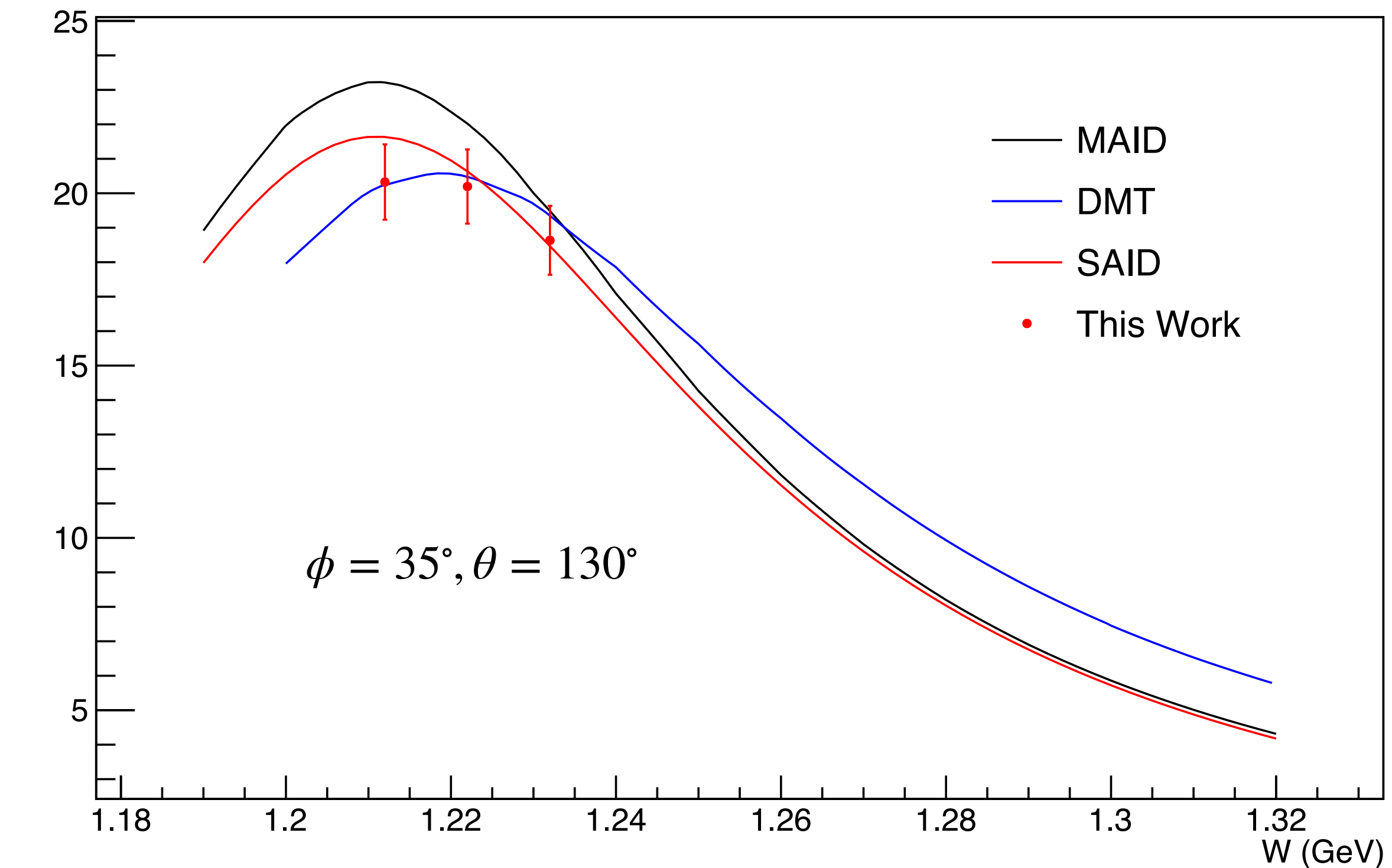
π^0 Cross Sections

○ $Q^2=0.36 \text{ (GeV/c)}^2$

In Plane



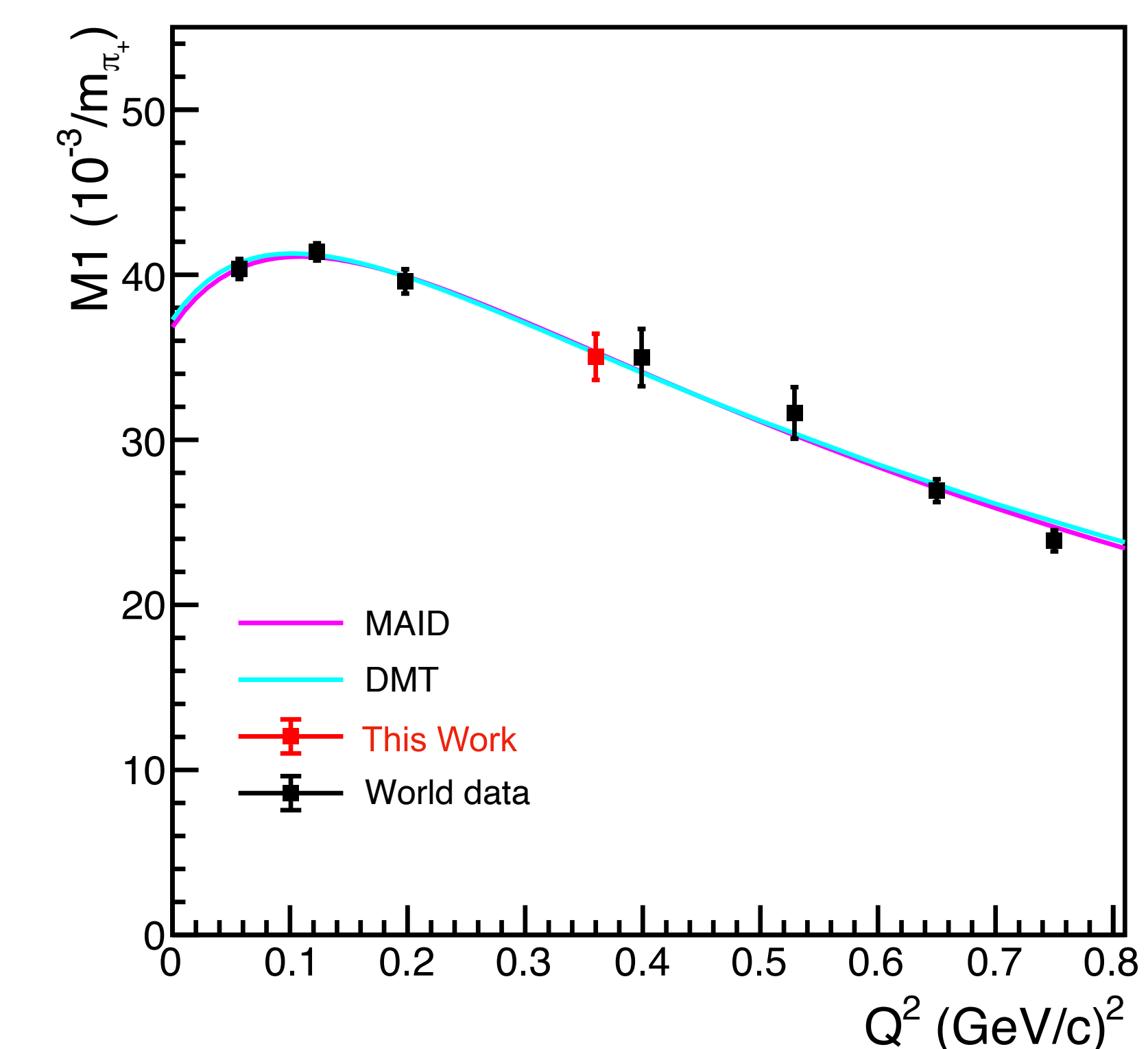
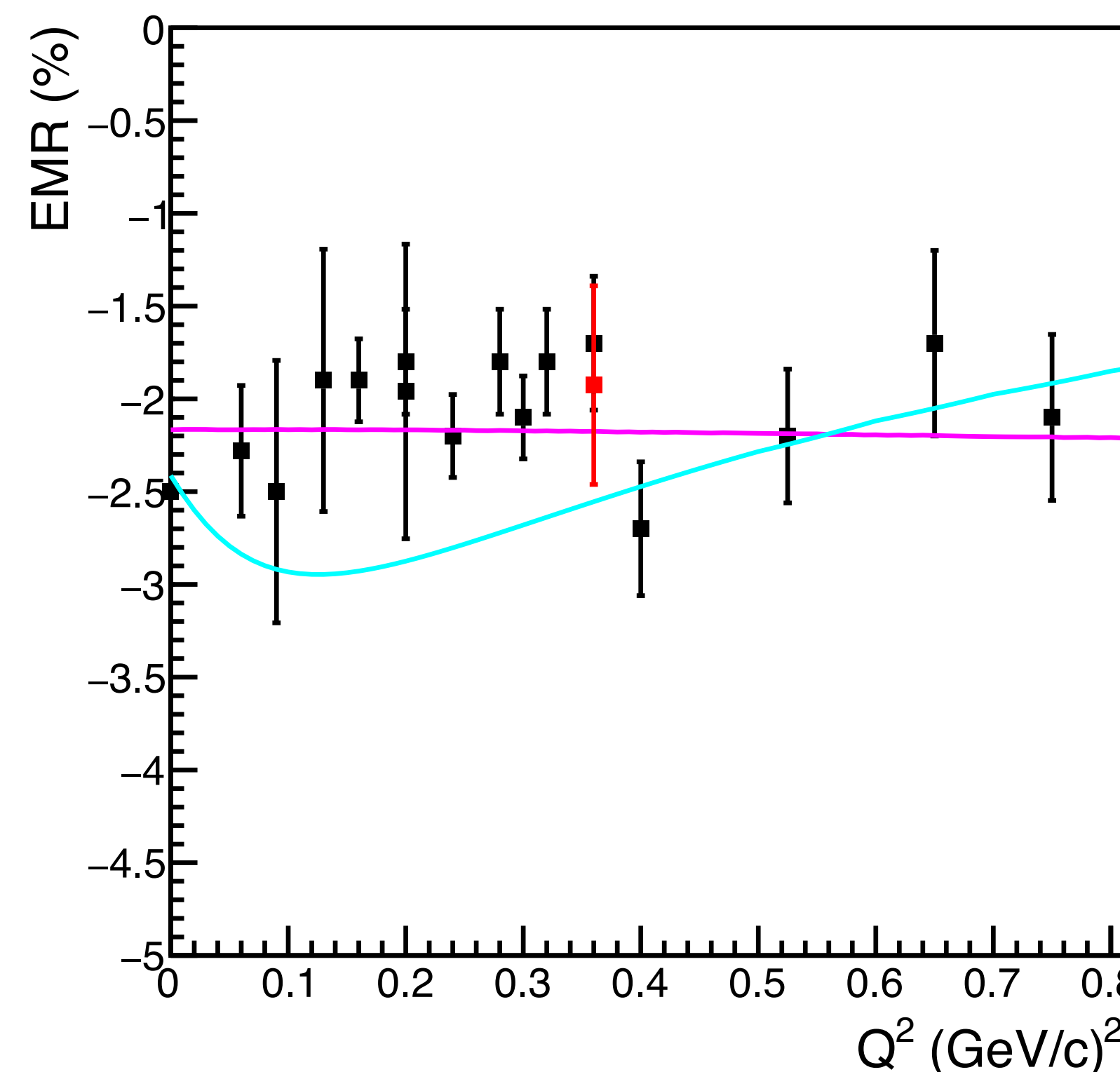
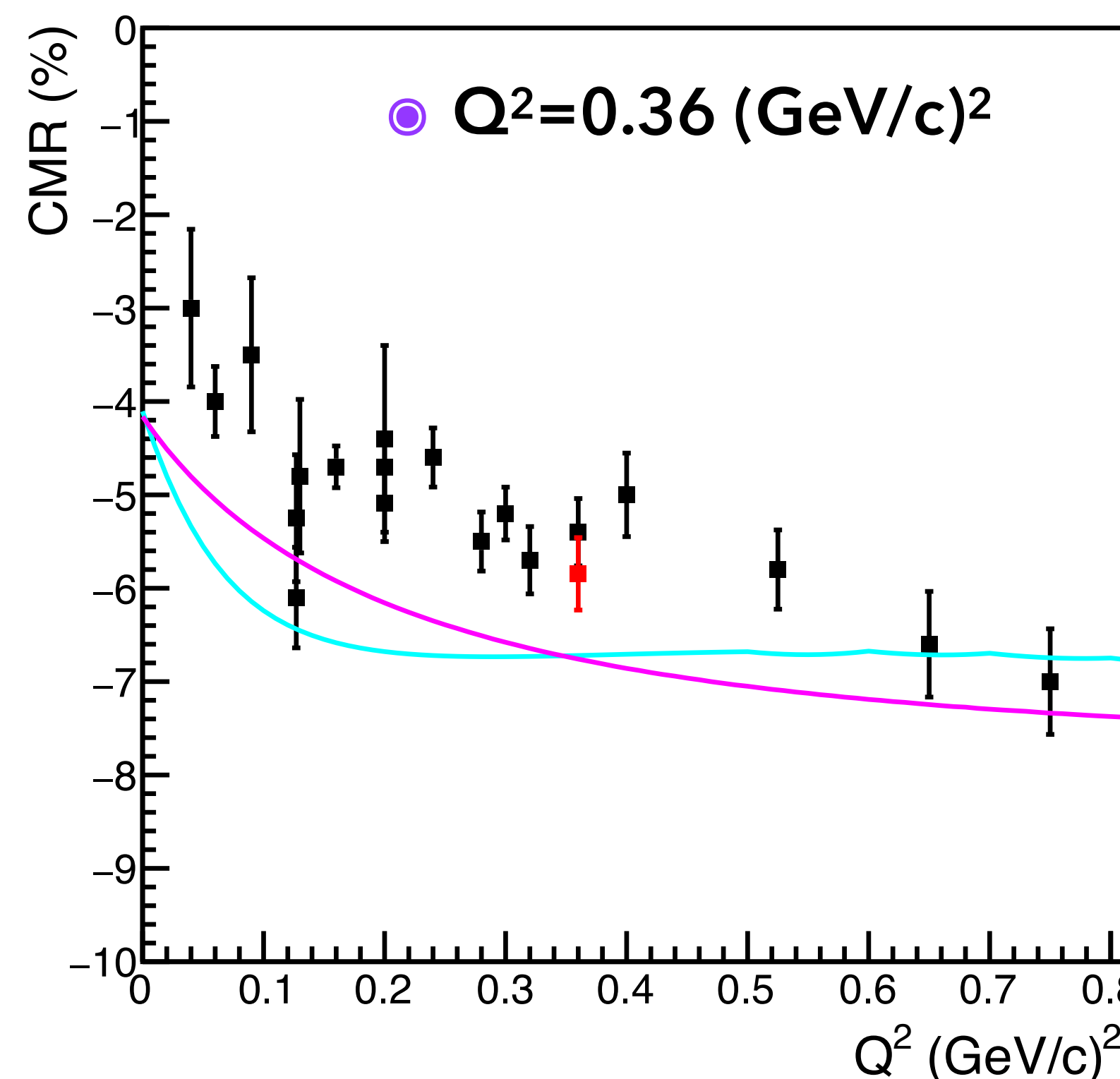
Out of Plane



$N \rightarrow \Delta$ Transition Form Factors

M1 - Magnetic dipole amplitude
C2 - Coulomb quadrupole amplitude
E2 - Electric quadrupole amplitude

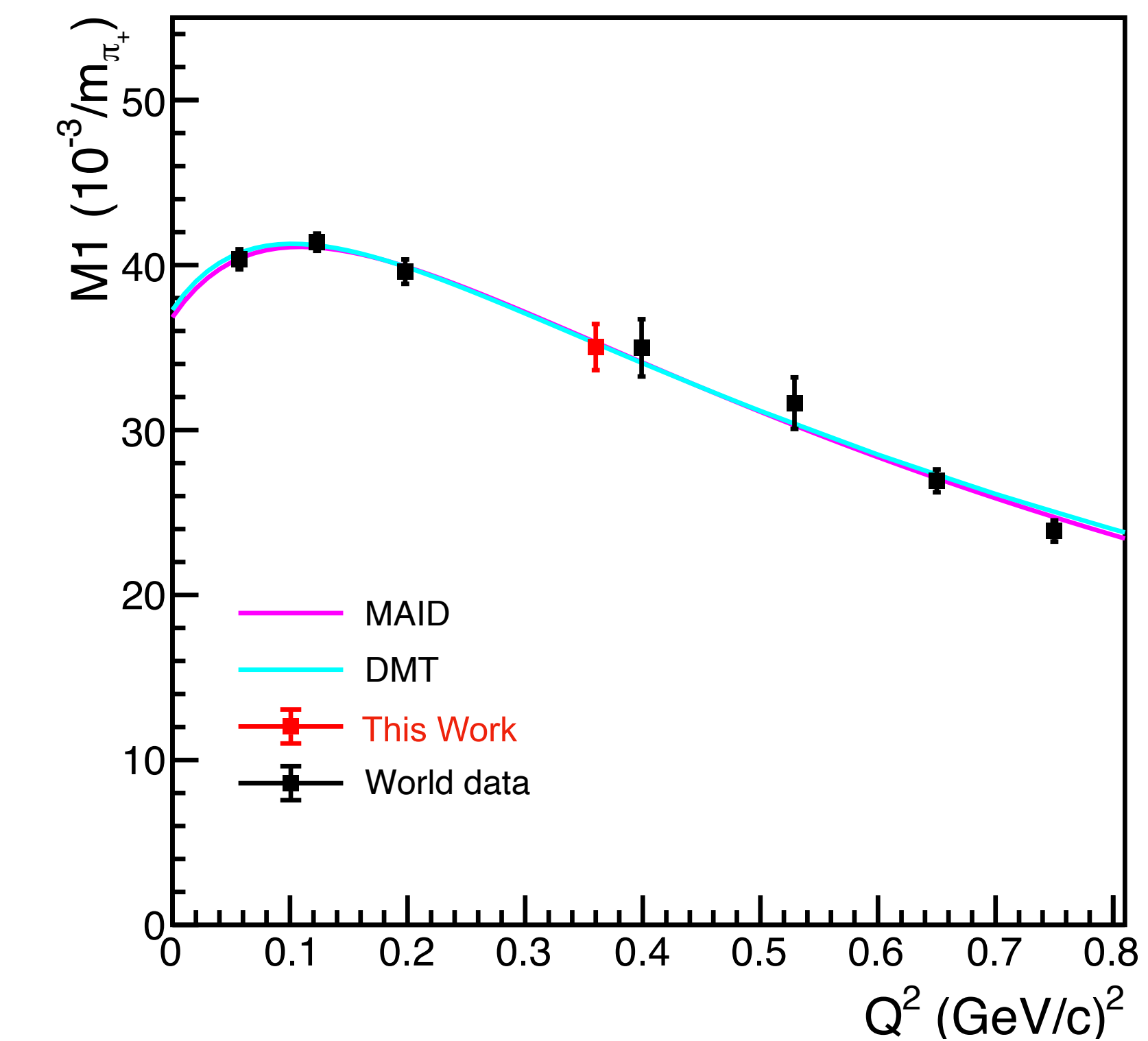
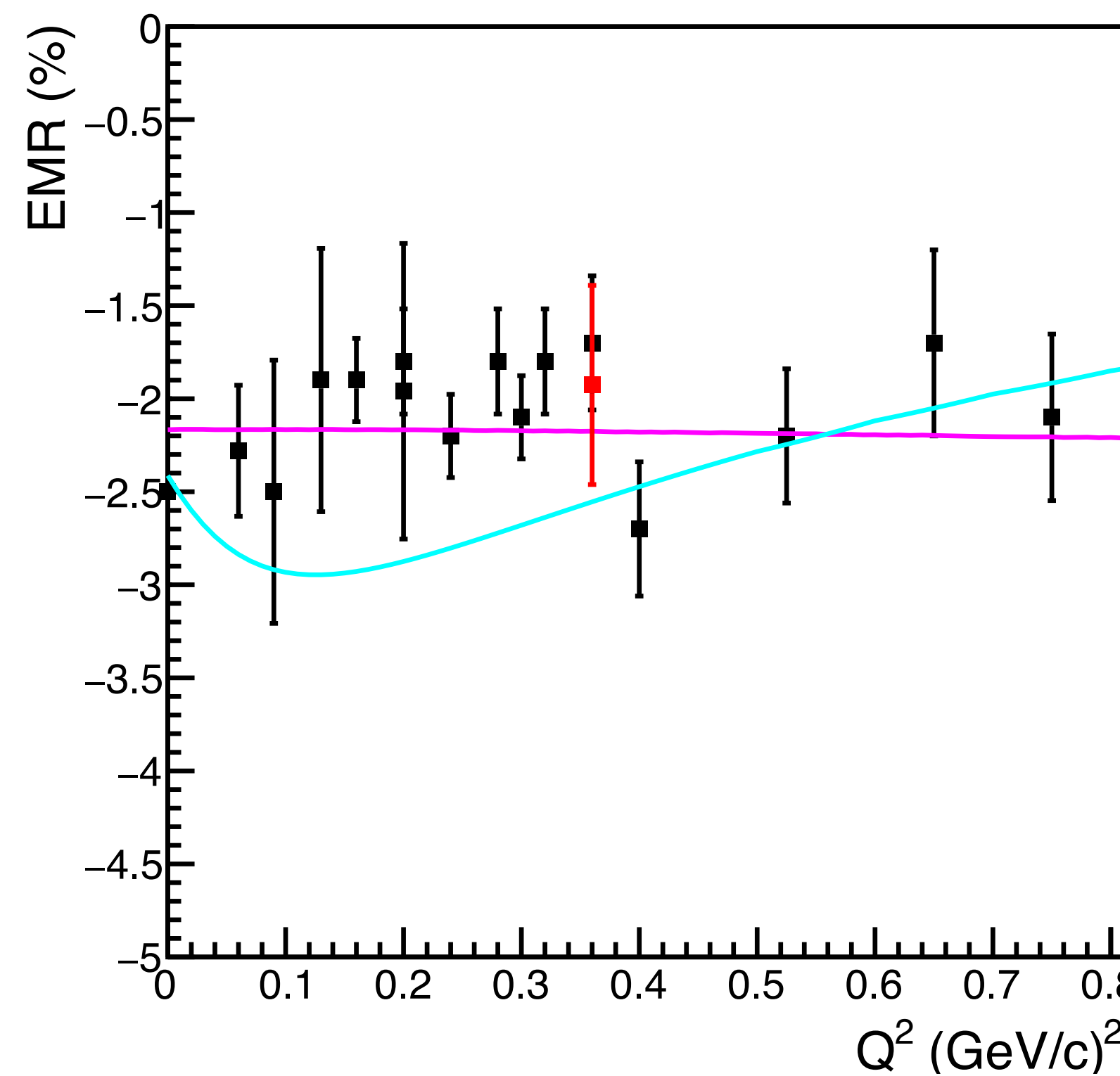
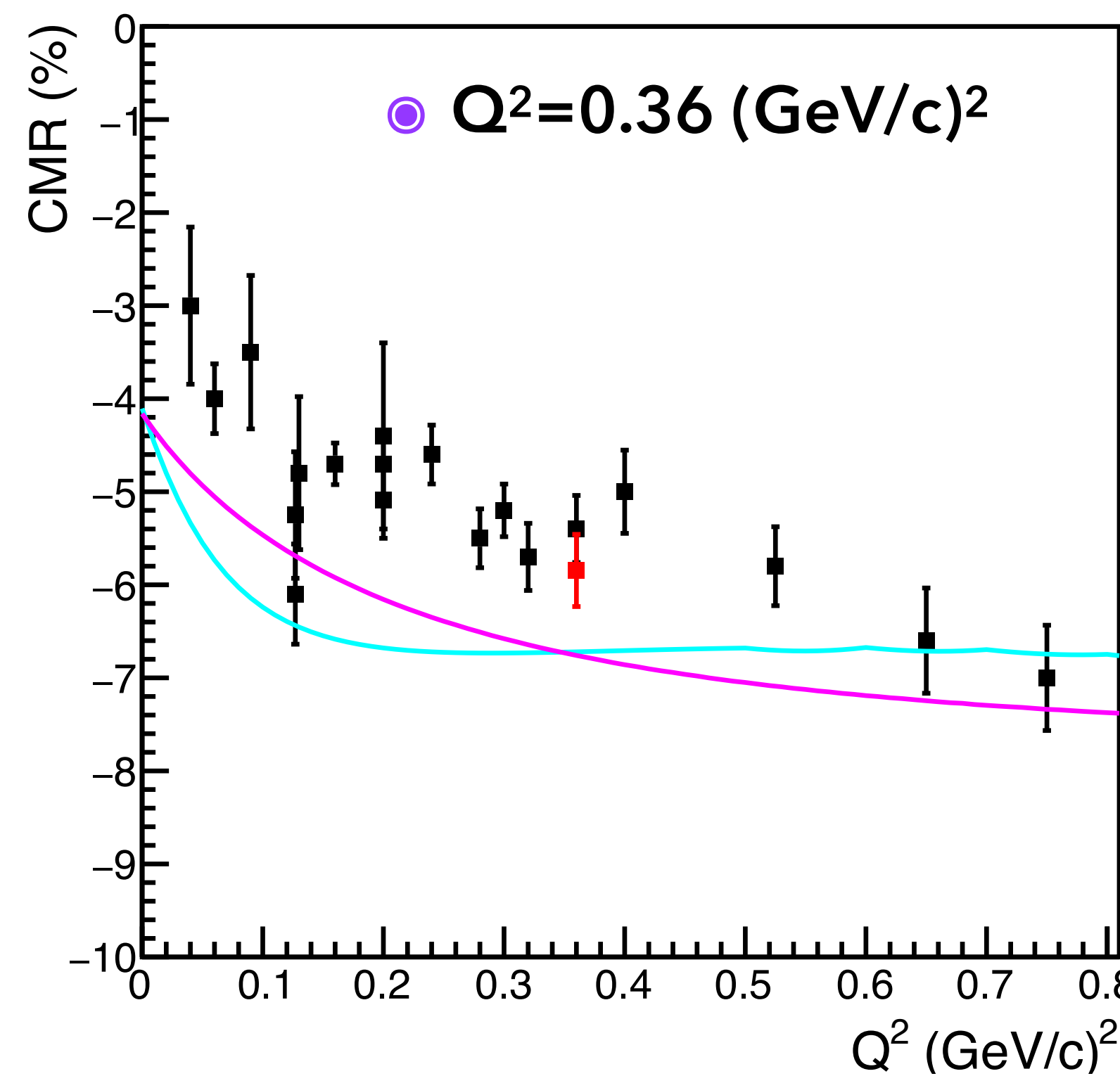
CMR = C2/M1
EMR = E2/M1



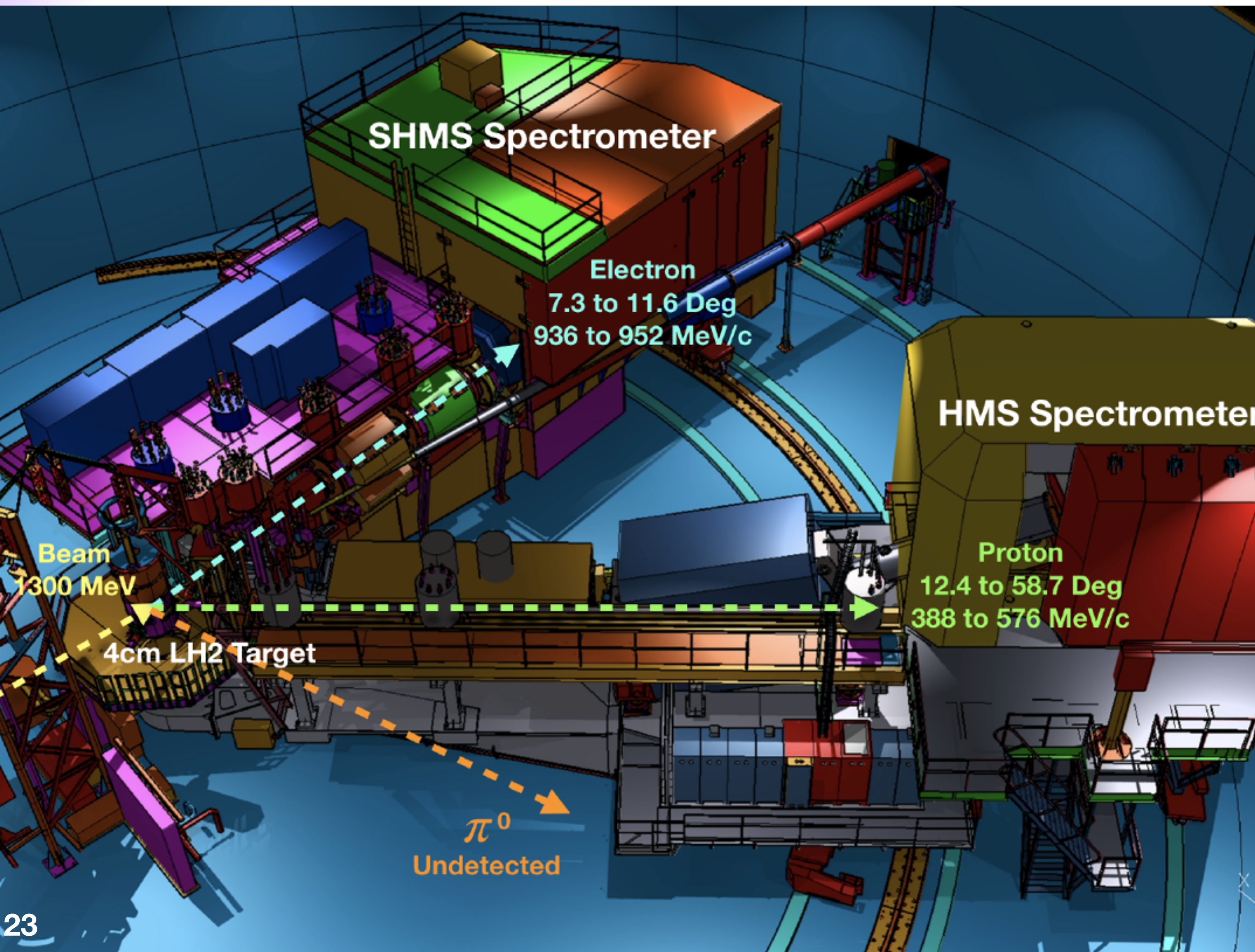
$N \rightarrow \Delta$ Transition Form Factors

M1 - Magnetic dipole amplitude
C2 - Coulomb quadrupole amplitude
E2 - Electric quadrupole amplitude

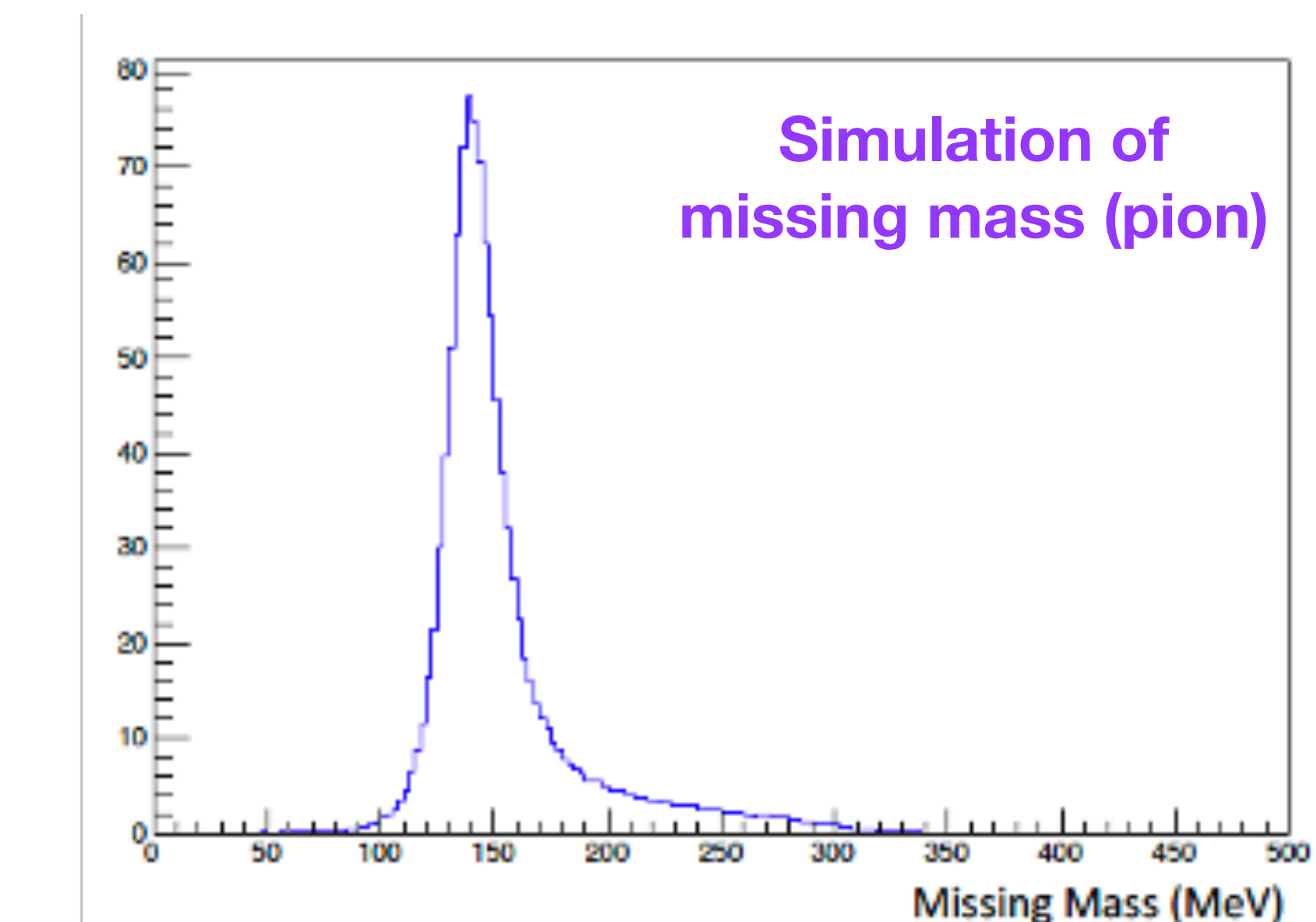
CMR = C2/M1
EMR = E2/M1



Proposed to PAC49 and PAC50: low- Q^2 TFF measurements in Hall-C



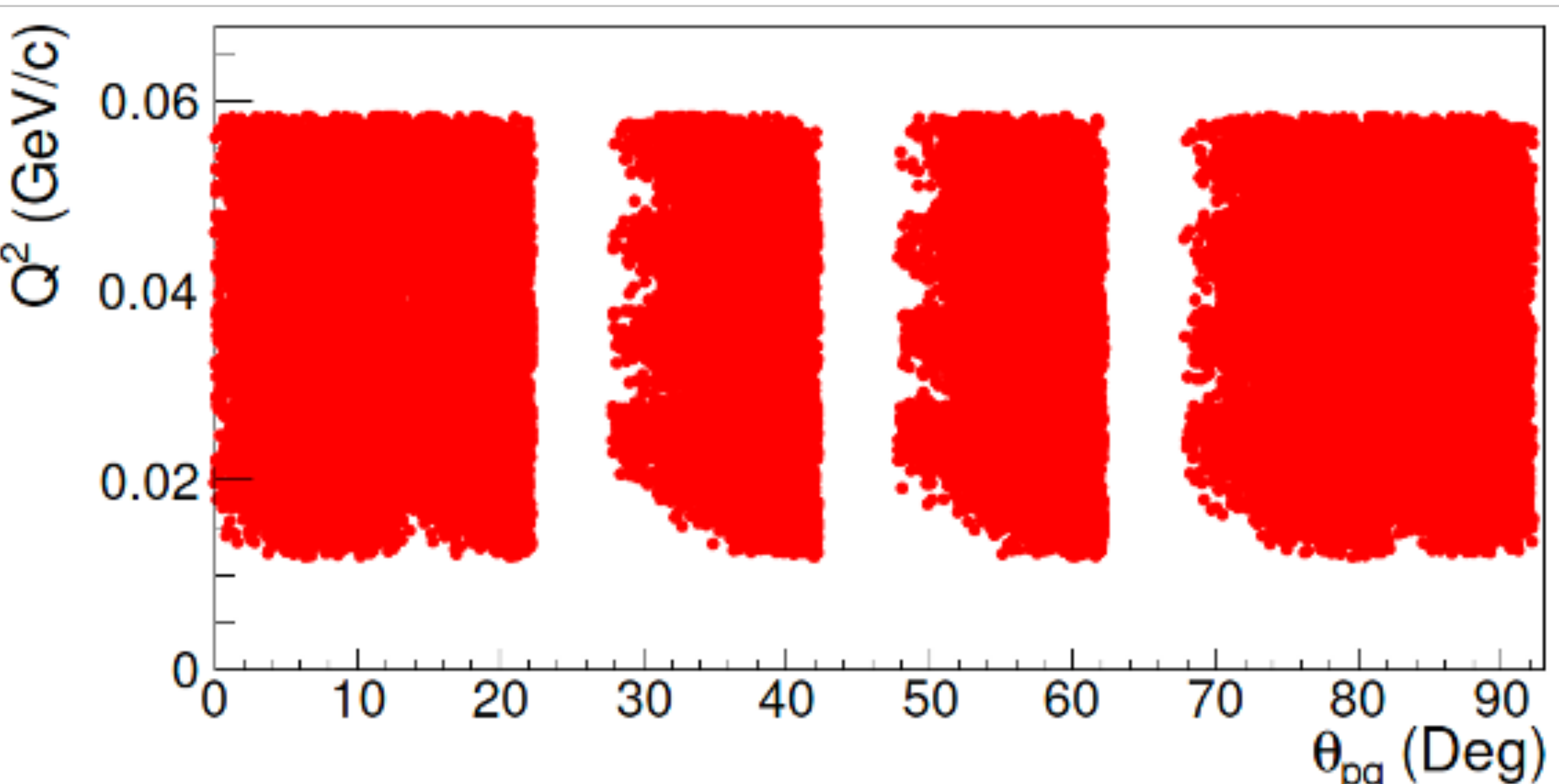
- Standard Hall-C equipment
 - 1300 MeV electron beam
 - Detect proton and electron in coincidence
 - Reconstruct pion from missing mass.



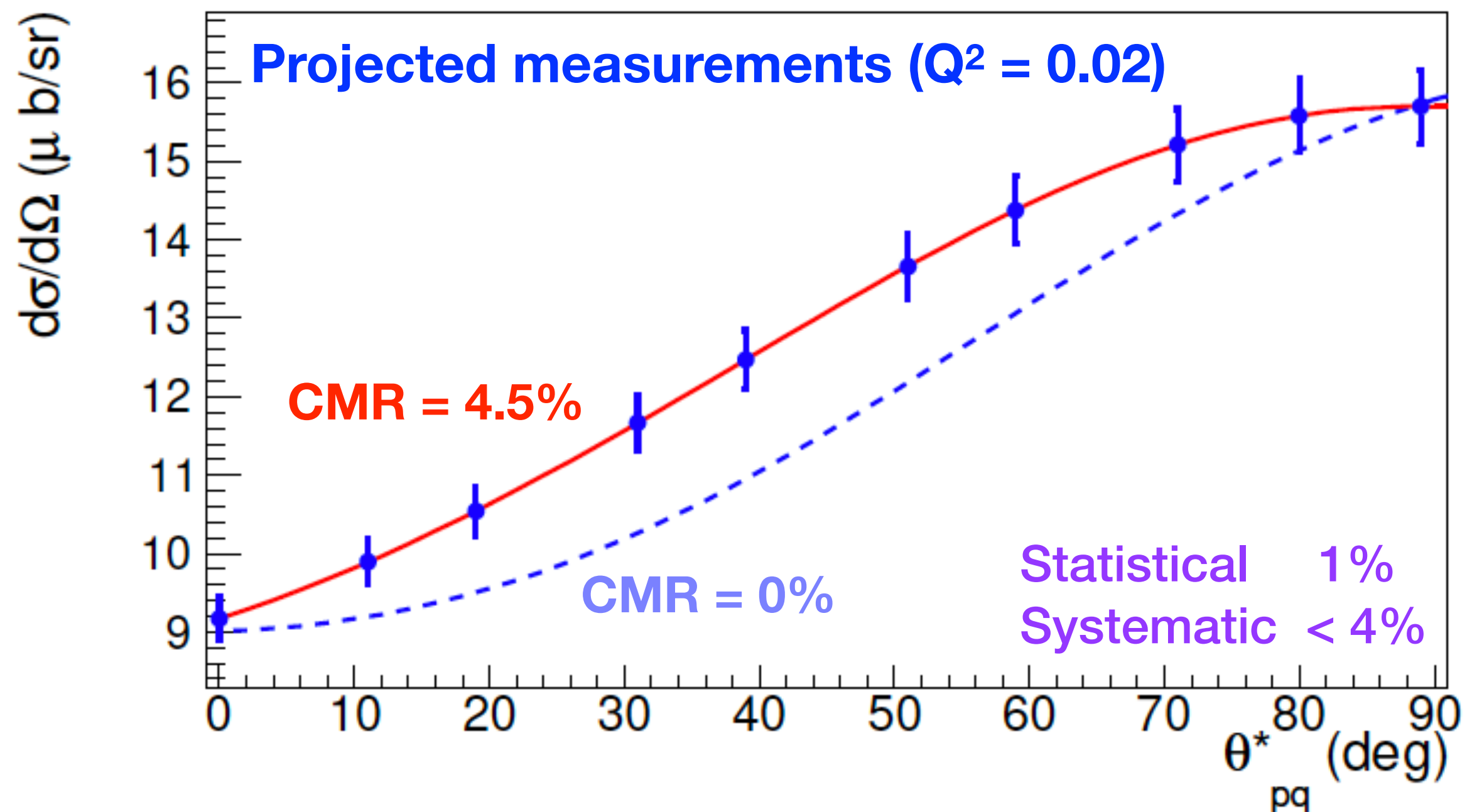
Measurement Settings

Setting	SHMS θ (deg)	SHMS P (MeV/c)	HMS θ (deg)	HMS P (MeV/c)	S/N	Time (hrs)
1a	7.29	952.26	18.77	532.53	2	7
2a			25.17	527.72	2	7
3a			33.7	506.61	3.2	6
4a			42.15	469.66	4.3	5
5a			50.44	418.56	4.9	5
6a			54.47	388.38	4.9	5
7a			12.37	527.72	2.7	6
1b	8.95	946.93	22.01	547.54	1.2	6
2b			28.24	542.61	1.4	6
3b			36.52	520.95	2.5	5
4b			44.64	483.08	3.4	4
5b			52.68	430.78	3.7	4
6b			56.53	399.92	3.5	4
7b			12.46	535.98	1.6	5
1c	10.37	941.61	24.40	562.00	1.5	9
2c			30.47	556.95	1.9	9
3c			38.52	534.79	3.5	6
4c			46.47	496.06	4.4	6
5c			54.17	442.64	4.8	6
6c			57.85	411.16	4.8	6
7c			12.69	543.24	2	6
1d	11.63	936.28	26.24	575.96	1.8	12
2d			32.16	570.80	2.5	11
3d			40.01	548.17	4.5	8
4d			47.73	508.64	5.5	8
5d			55.18	454.17	6.9	7
6d			58.71	422.13	6	8
7d			12.47	548.17	2.1	10

- Cover a Q^2 range of 0.015 to 0.055 (GeV/c) 2
- 28 arm configurations
- Coverage for 9 Q^2 bins.
- 8 days production
- 3 days other (dummy, calibration, etc..)

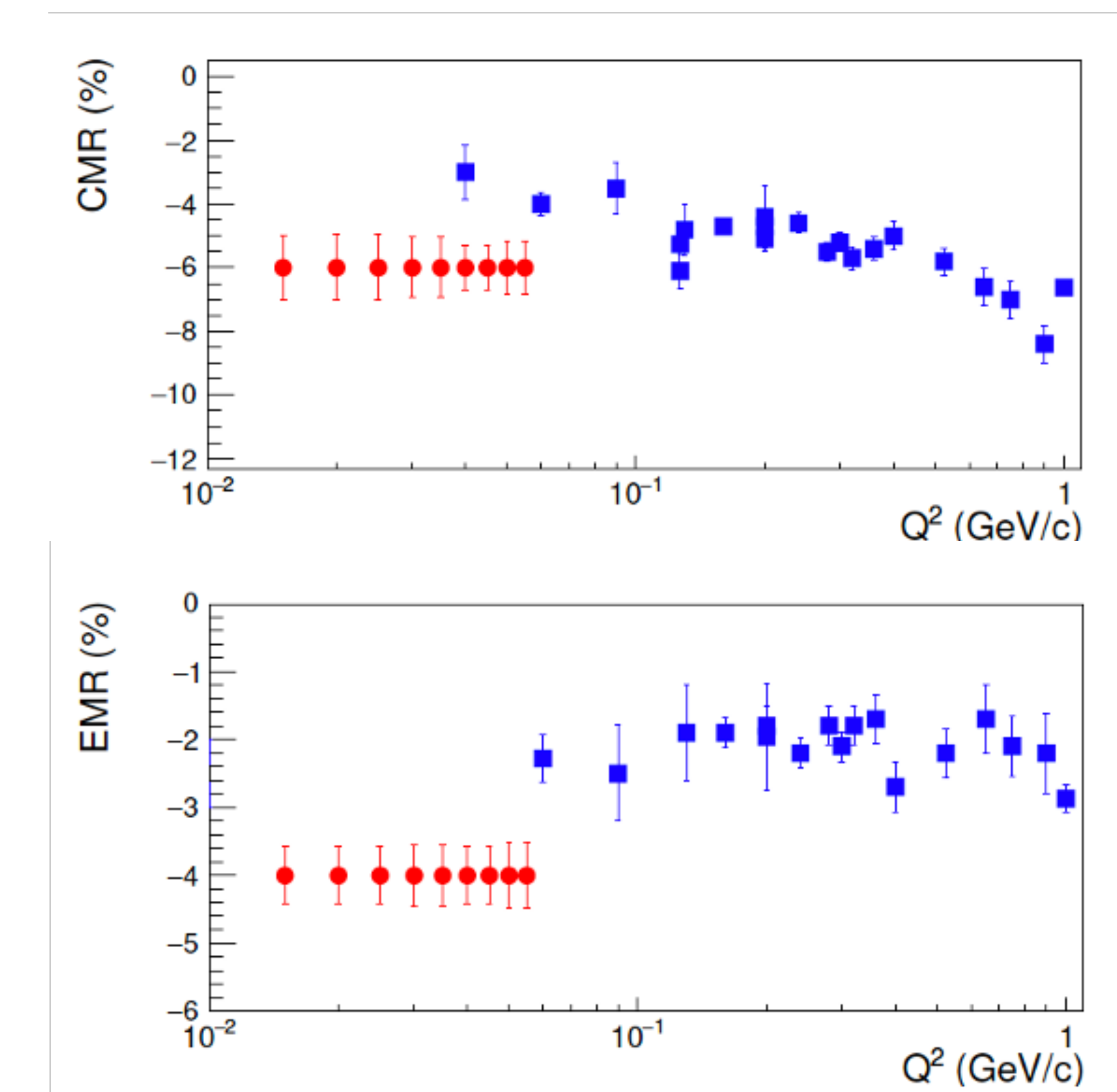


Projected CMR and EMR measurements

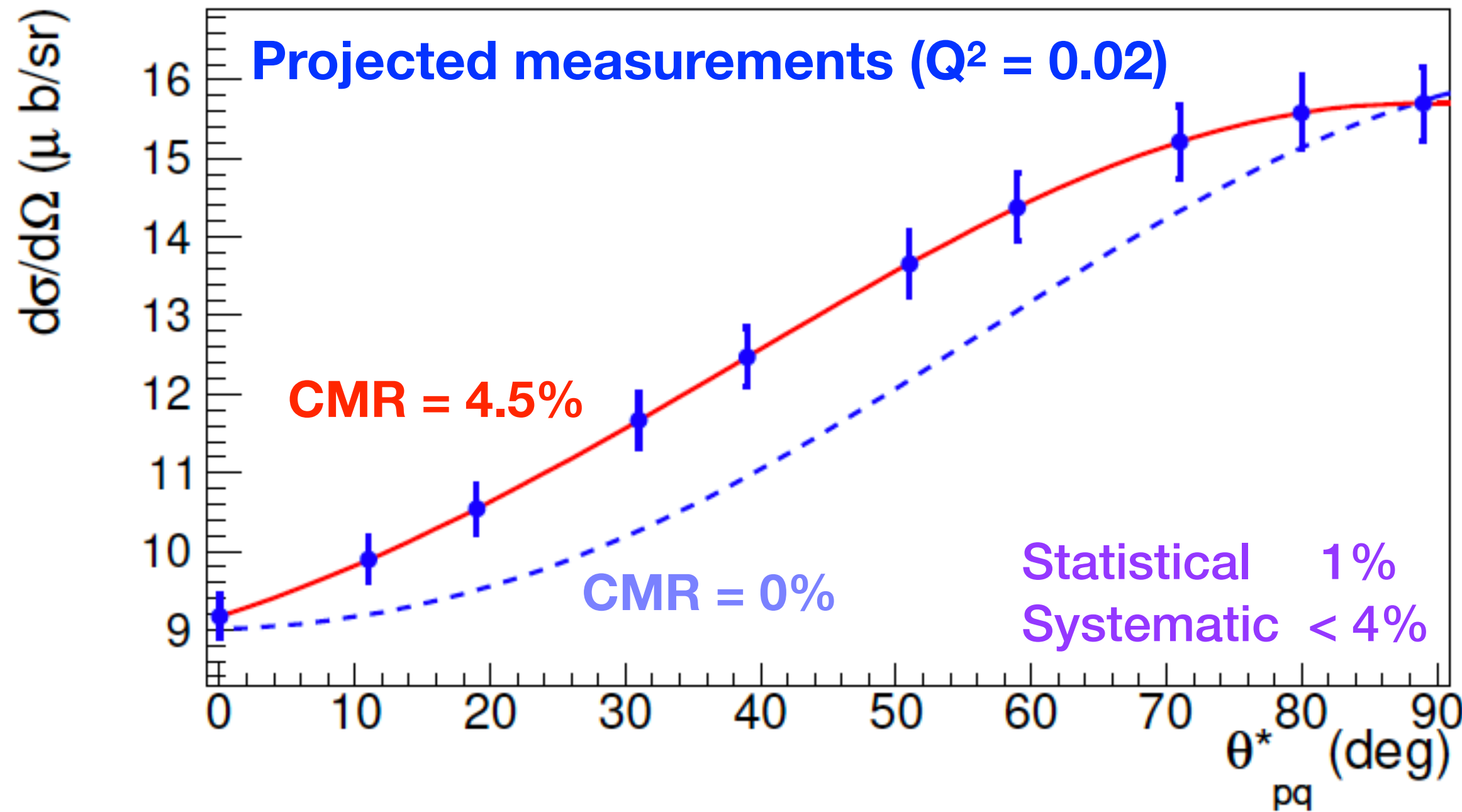


Resolution	2% - 3%
Acceptance	1%
Scattering angle	0.4% - 0.6%
Beam energy	0.7% - 1.2%
Beam charge	1%
Target density	0.5%
Detector efficiencies	0.5%
Target cell background	0.5%
Target length	0.5%
Dead-time corrections	0.5%
Total	2.8% - 3.8%

- High precision in very low Q^2 region that is sparsely populated
- Region where pion-cloud effects are expected to be prominent

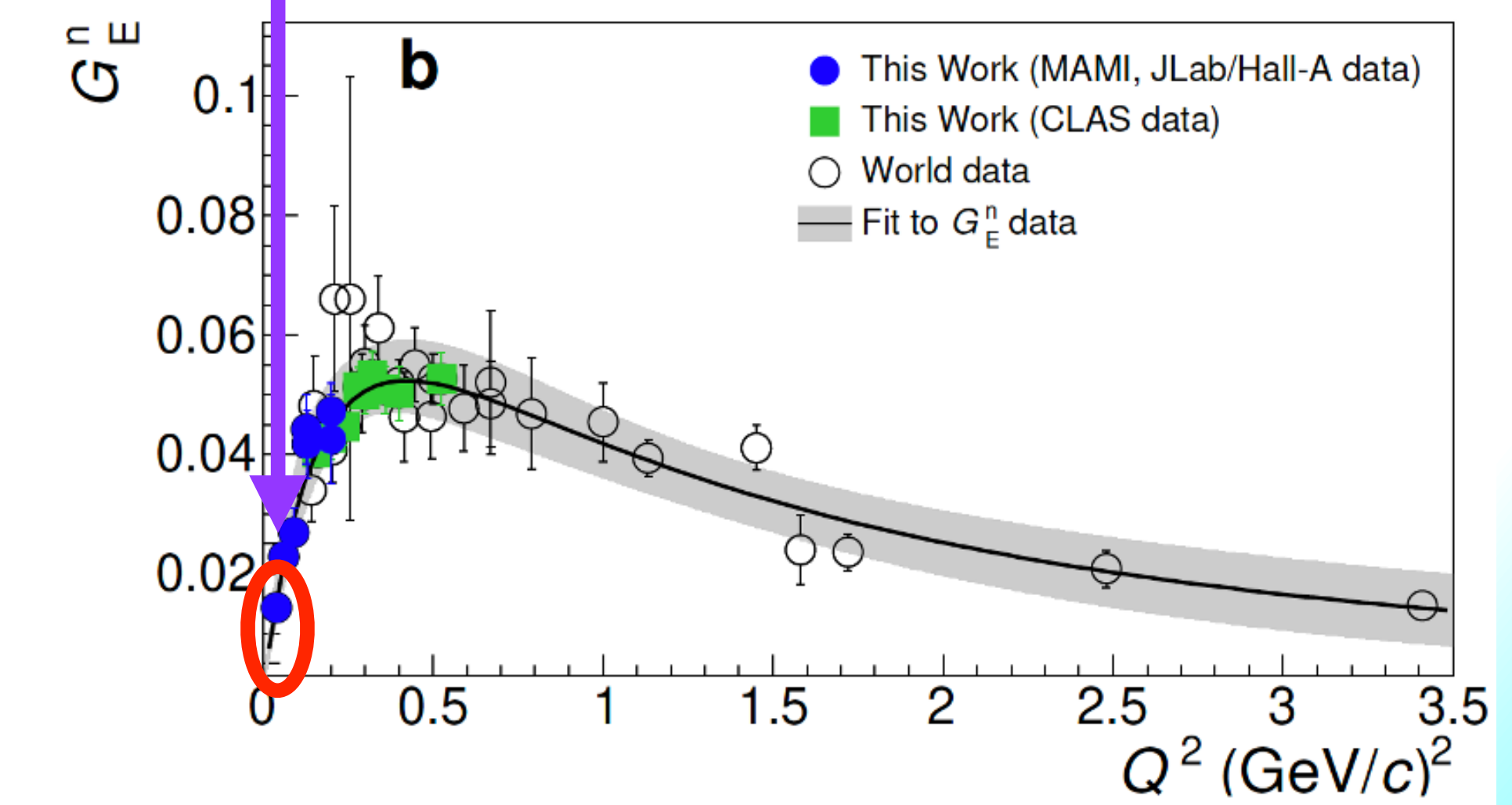
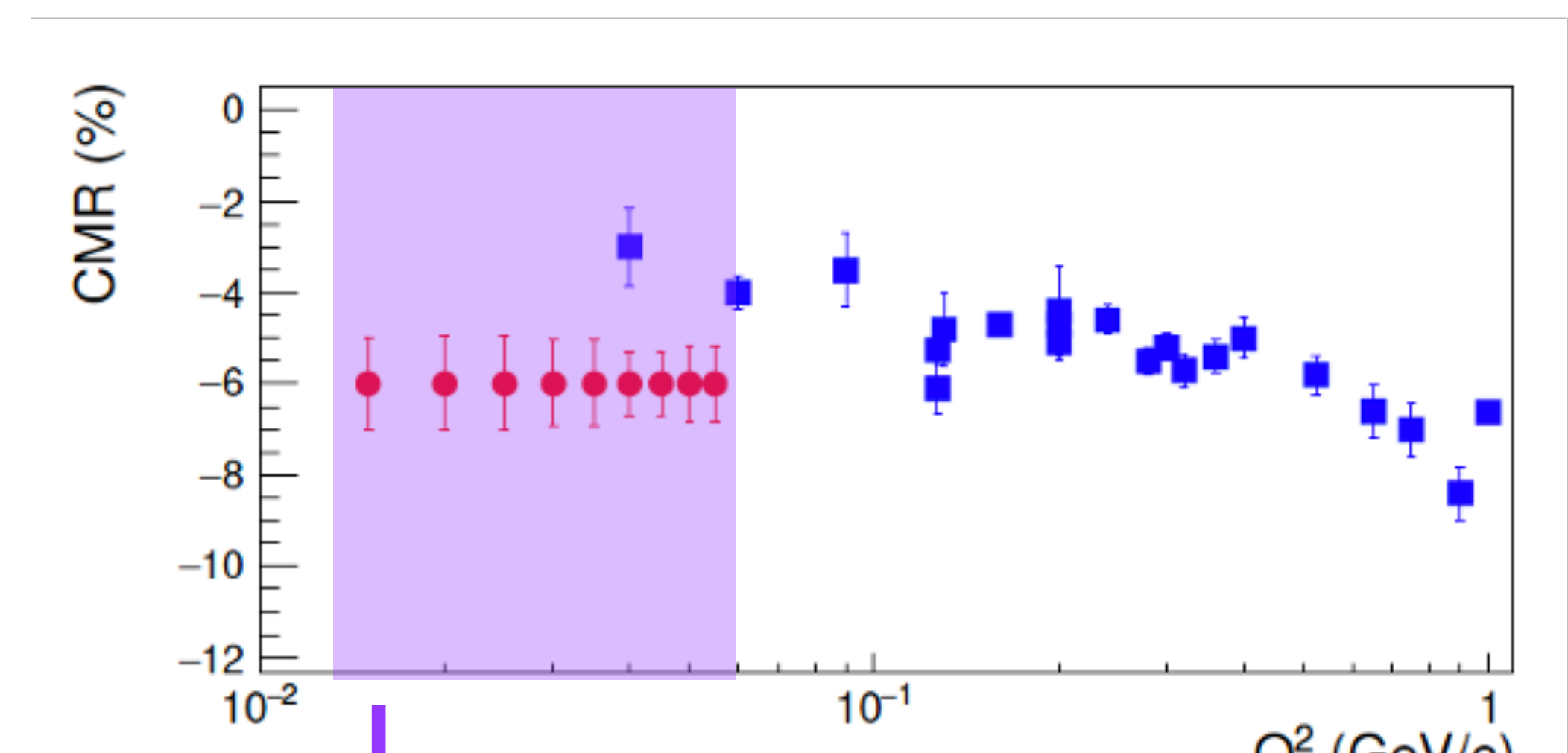


Projected CMR and EMR measurements

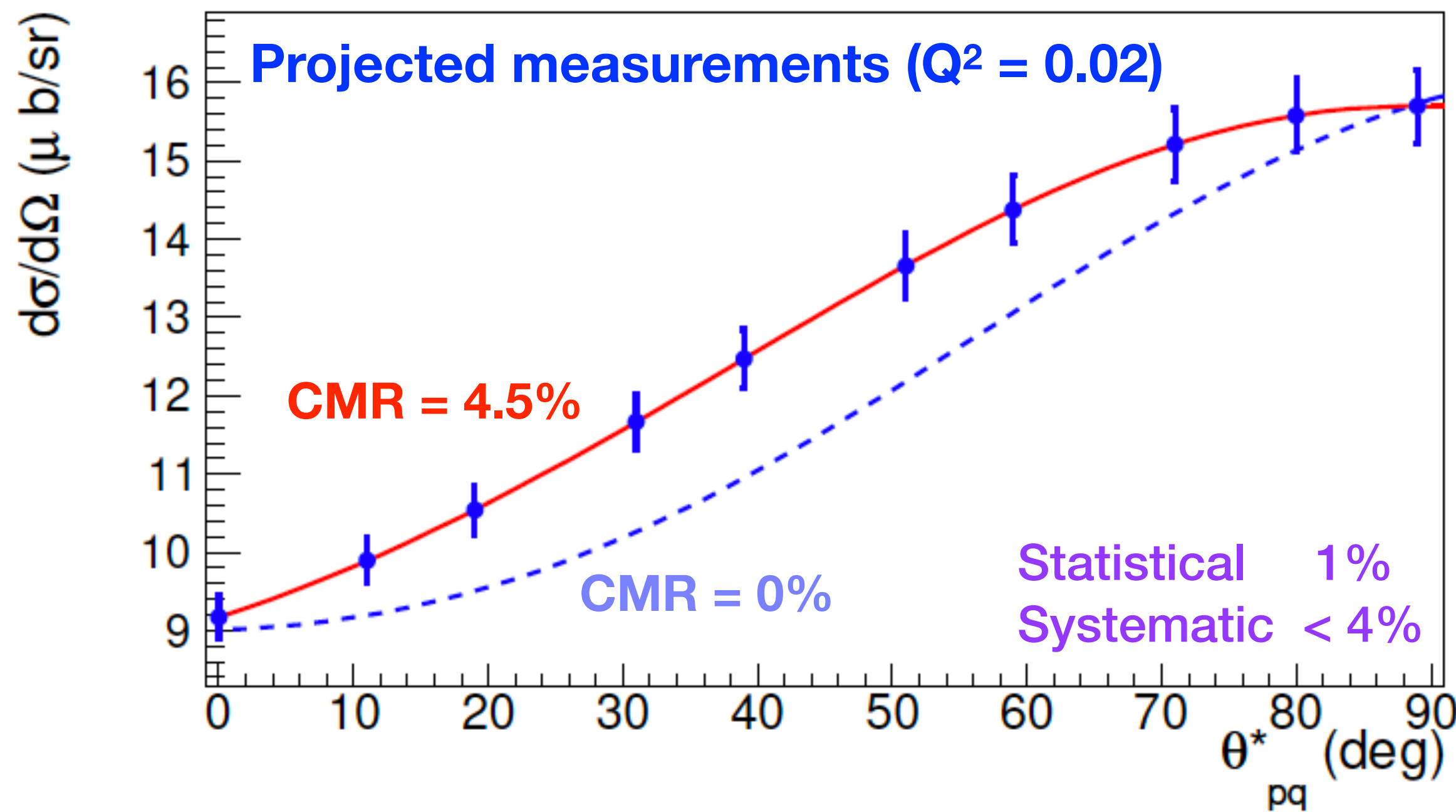


Resolution	2% - 3%
Acceptance	1%
Scattering angle	0.4% - 0.6%
Beam energy	0.7% - 1.2%
Beam charge	1%
Target density	0.5%
Detector efficiencies	0.5%
Target cell background	0.5%
Target length	0.5%
Dead-time corrections	0.5%
Total	2.8% - 3.8%

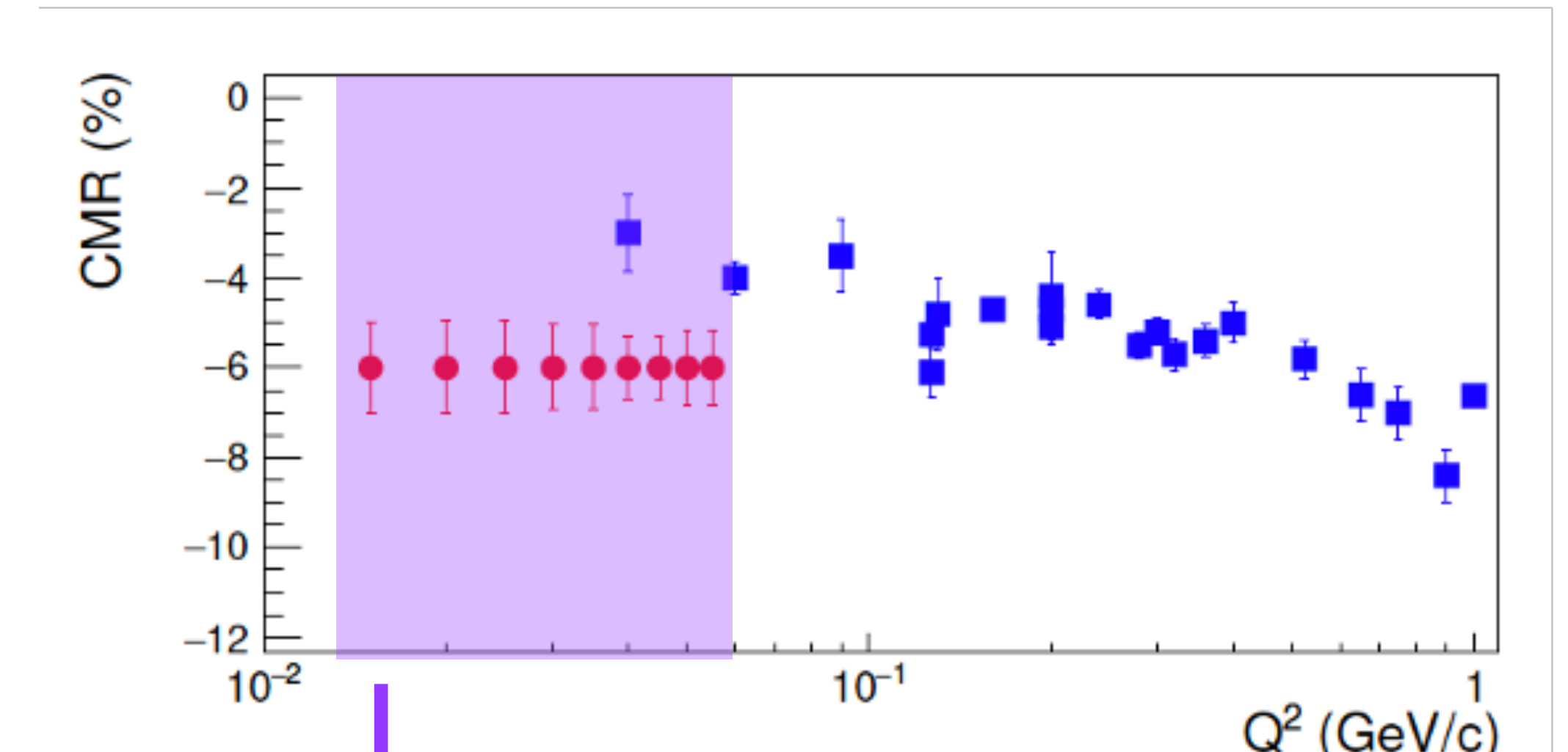
**Proposed to PAC49:
Extraction of Neutron
Charge Radius**



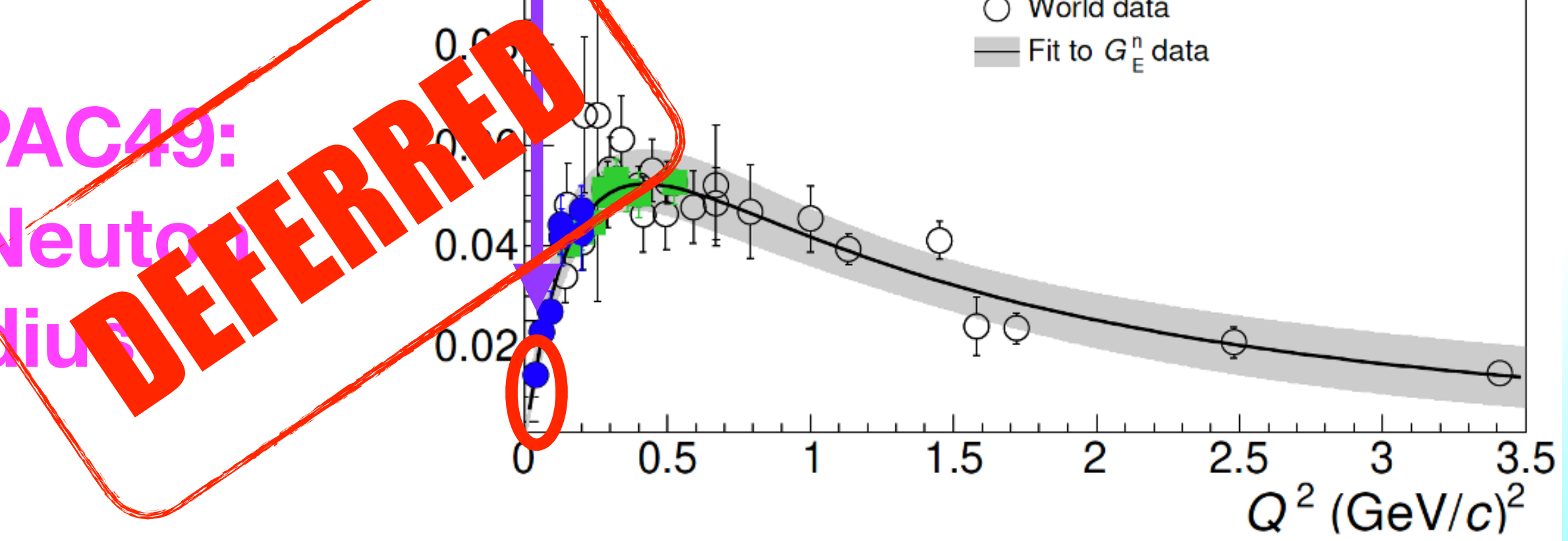
Projected CMR and EMR measurements



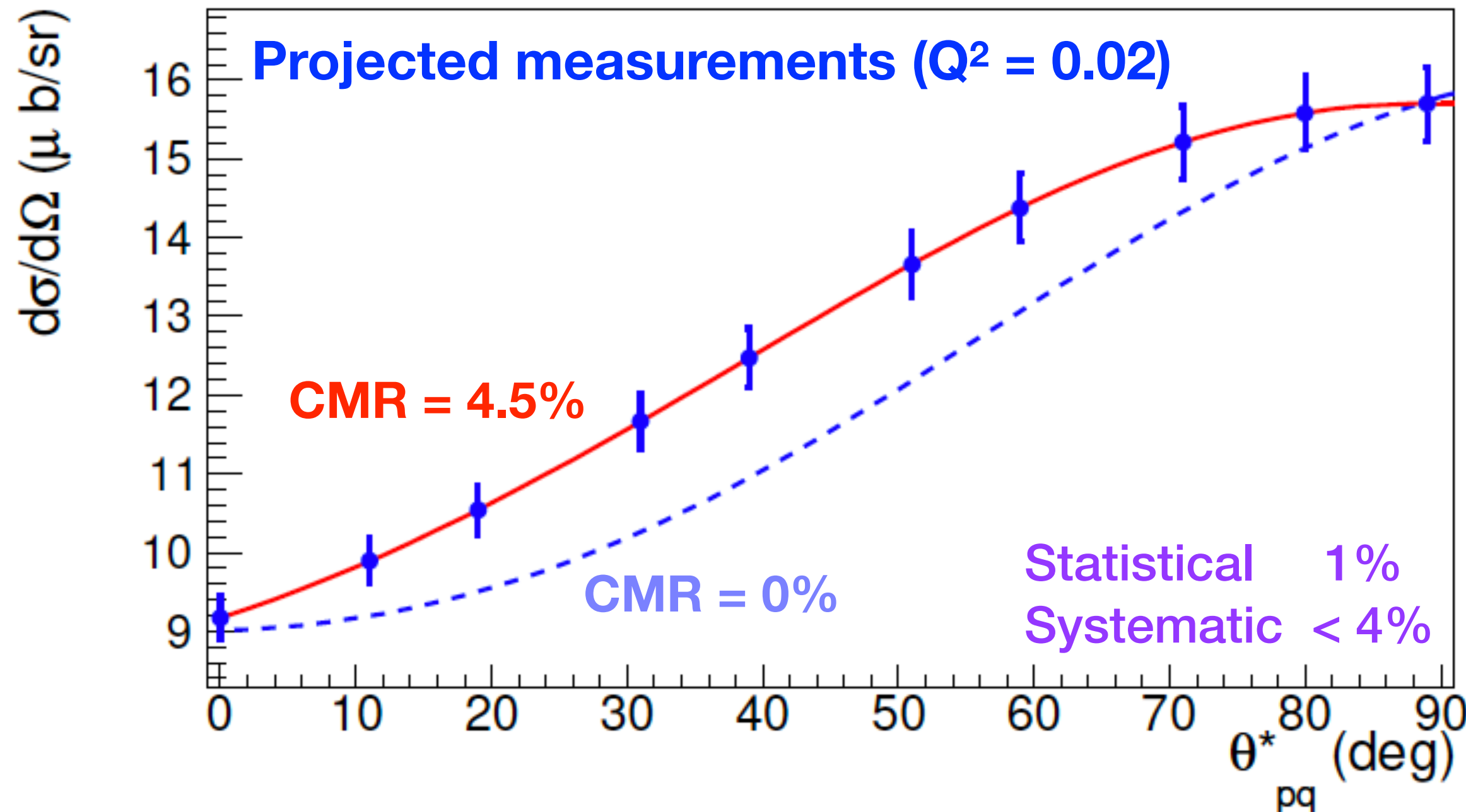
Resolution	2% - 3%
Acceptance	1%
Scattering angle	0.4% - 0.6%
Beam energy	0.7% - 1.2%
Beam charge	1%
Target density	0.5%
Detector efficiencies	0.5%
Target cell background	0.5%
Target length	0.5%
Dead-time corrections	0.5%
Total	2.8% - 3.8%



**Proposed to PAC49:
Extraction of Neutron
Charge Radius**

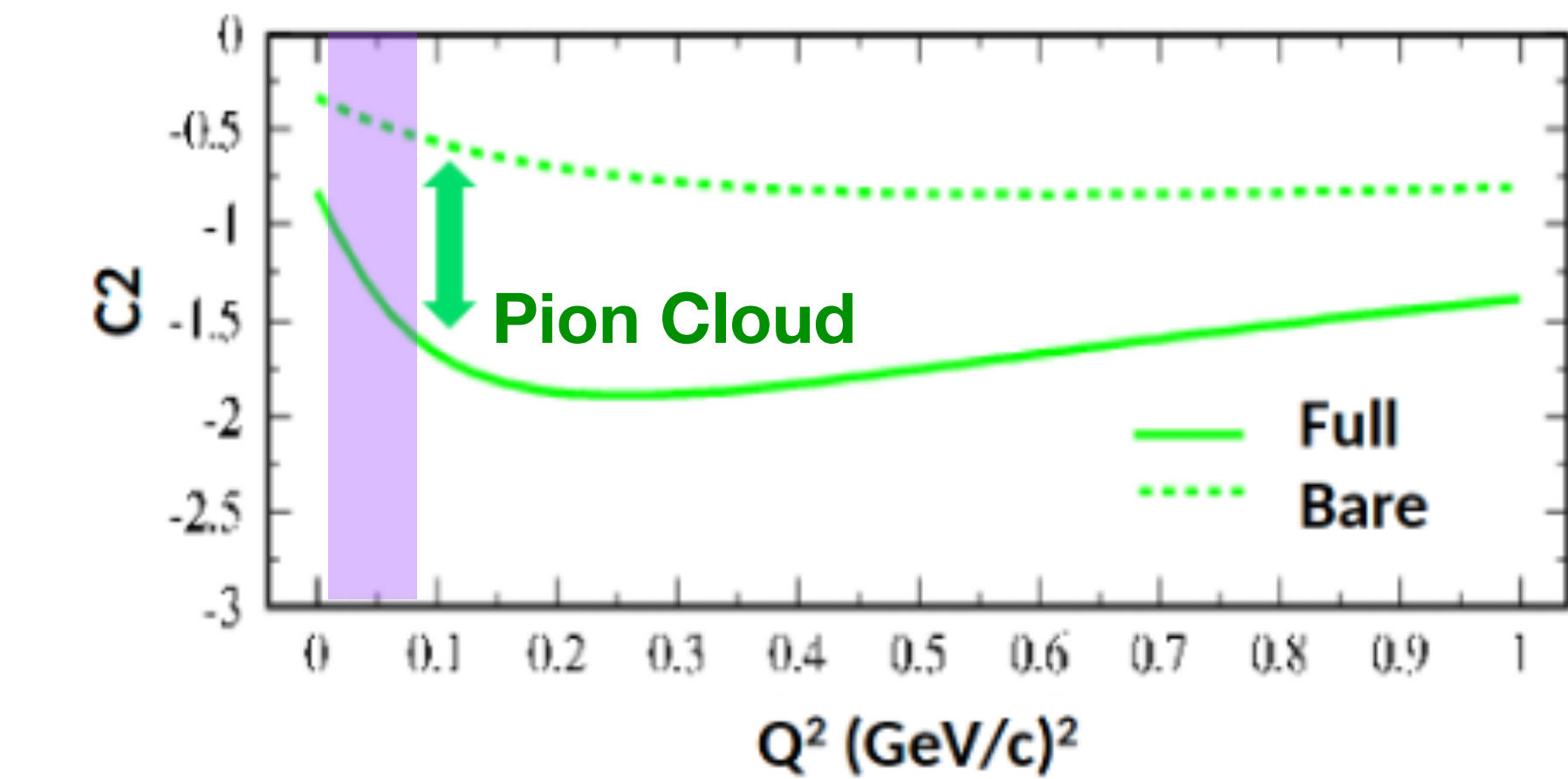
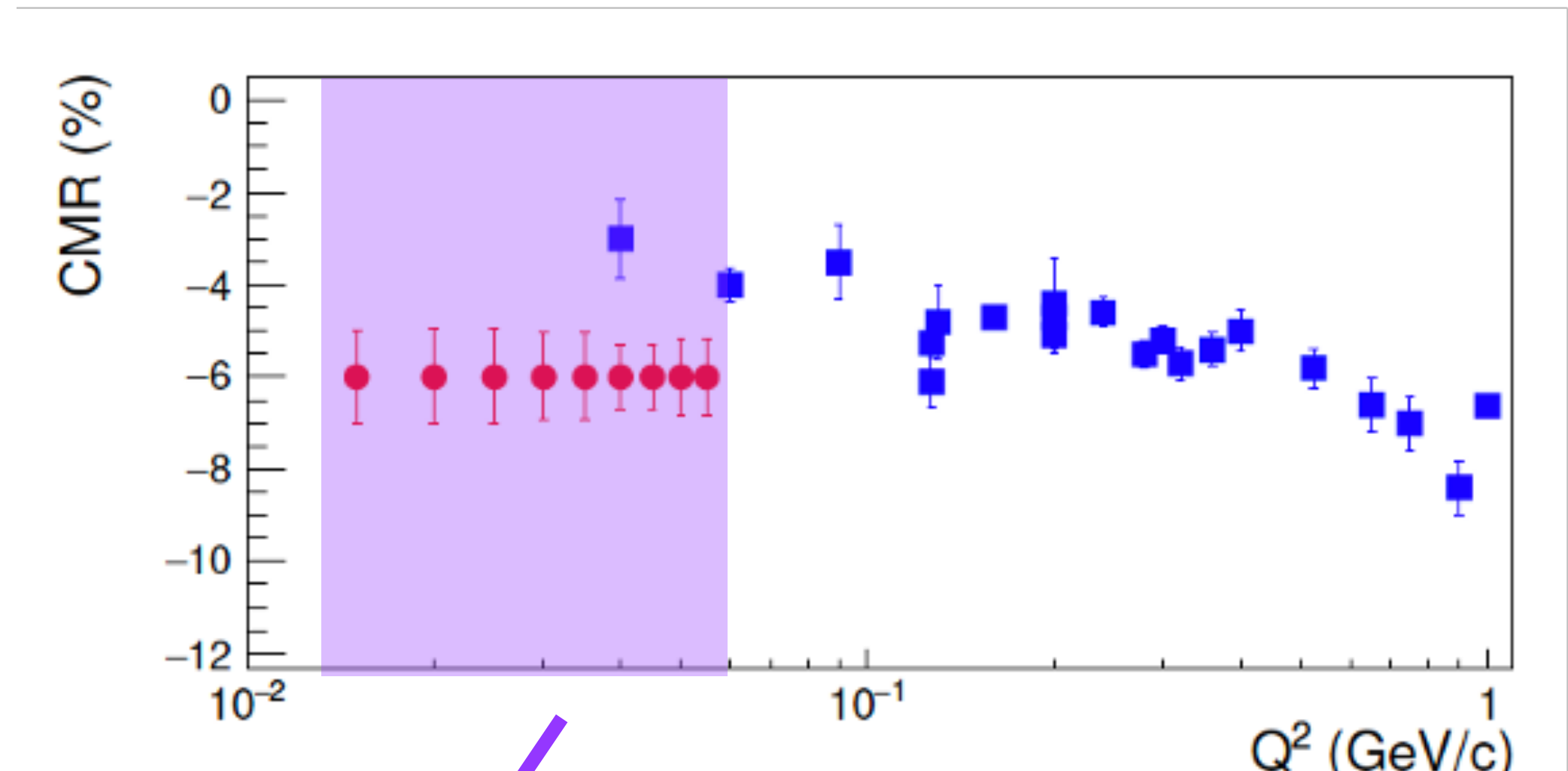


Projected CMR and EMR measurements

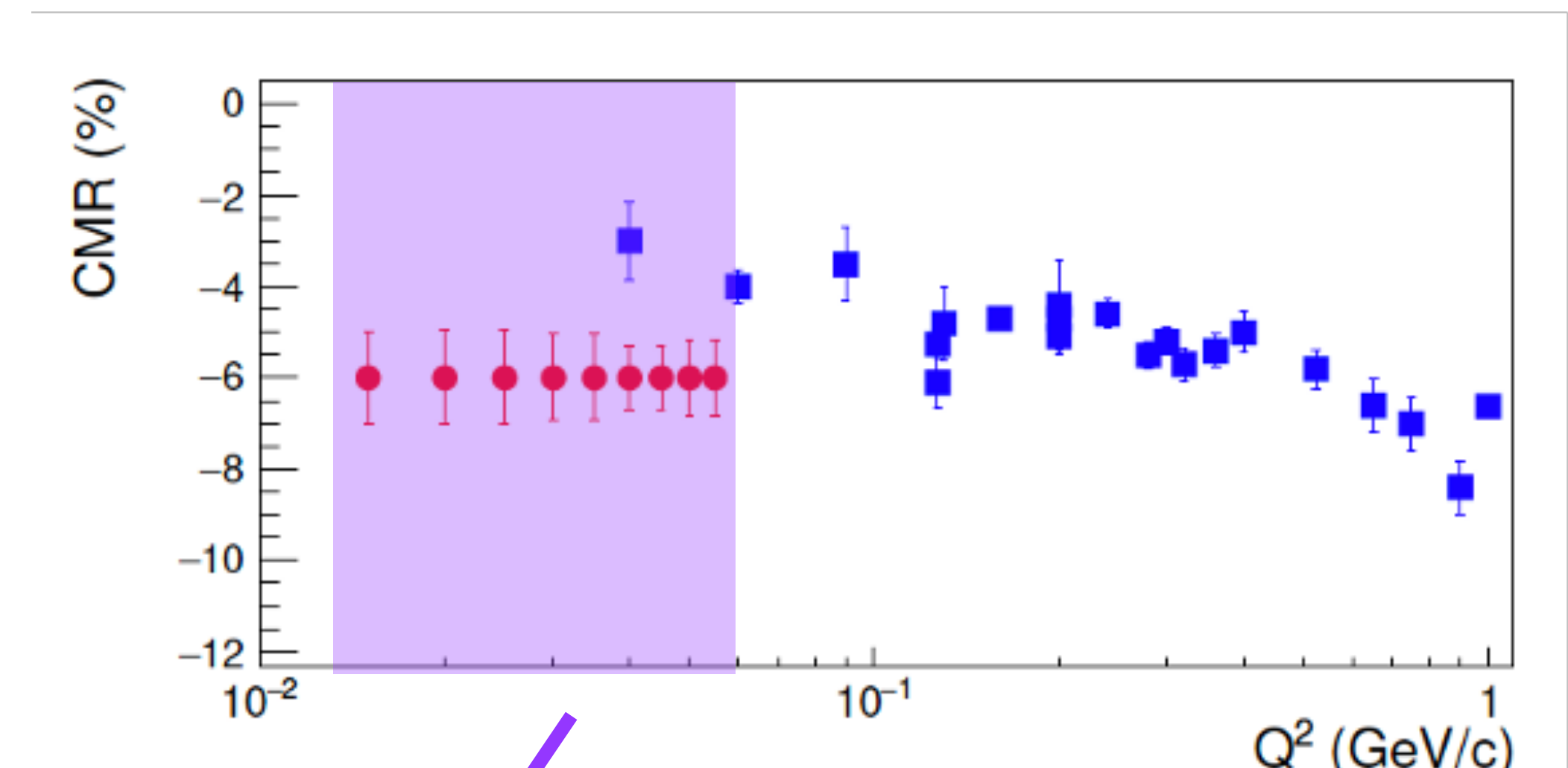
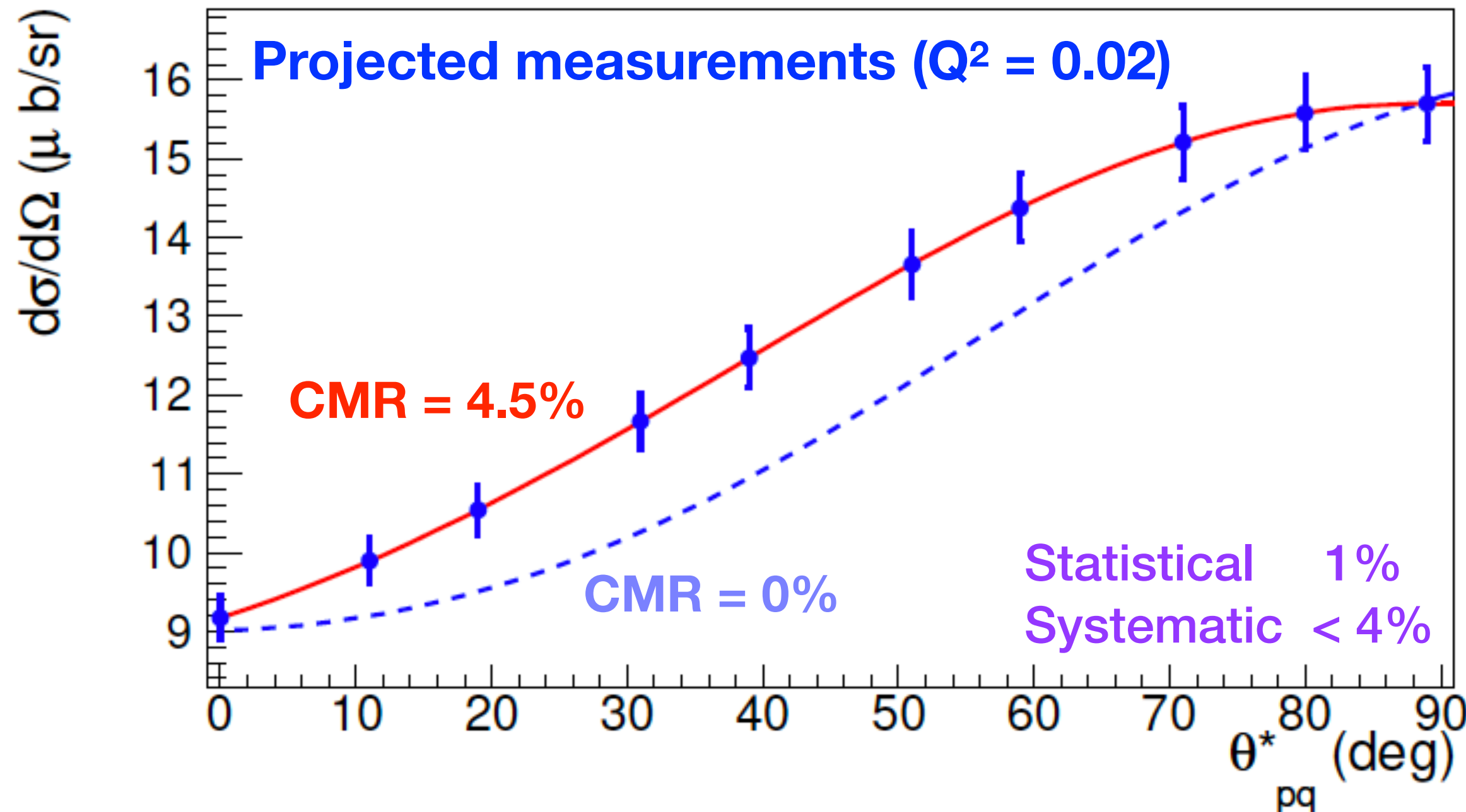


Resolution	2% - 3%
Acceptance	1%
Scattering angle	0.4% - 0.6%
Beam energy	0.7% - 1.2%
Beam charge	1%
Target density	0.5%
Detector efficiencies	0.5%
Target cell background	0.5%
Target length	0.5%
Dead-time corrections	0.5%
Total	2.8% - 3.8%

**Proposed to PAC50:
Extraction of TFFs at
low Q^2**



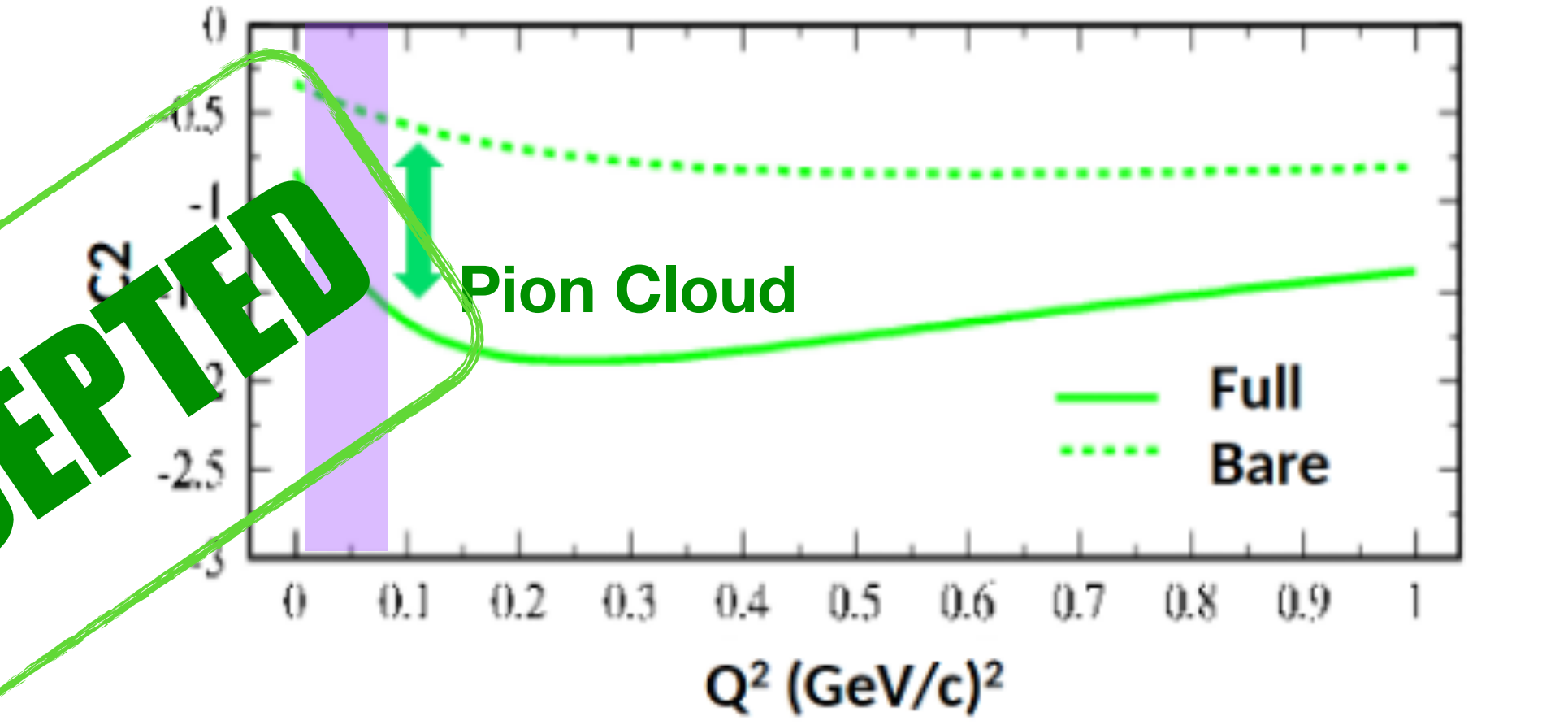
Projected CMR and EMR measurements



Resolution	2% - 3%
Acceptance	1%
Scattering angle	0.4% - 0.6%
Beam energy	0.7% - 1.2%
Beam charge	1%
Target density	0.5%
Detector efficiencies	0.5%
Target cell background	0.5%
Target length	0.5%
Dead-time corrections	0.5%
Total	2.8% - 3.8%

**Proposed to PAC50:
Extraction of TFFs at
low Q^2**

ACCEPTED

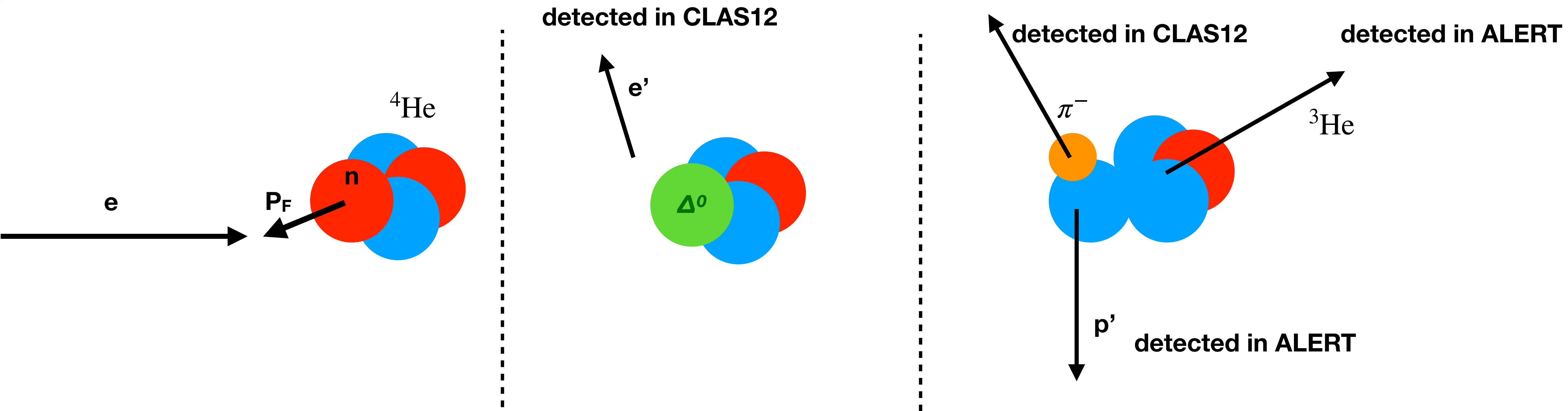


11 days, to run sometime in the near future.

Future Analyses at JLab

- CLAS12 has single-pion production coverage up to $Q^2 = 12 \text{ GeV}^2$ over a large range of W .
 - Program focused on large range Nucleon excitation resonances.
 - Specific sensitivity of expected data to EMR and CMR extraction is unclear.
 - How does low-luminosity affect rates at large Q^2 ?
 - ALERT phase space will allow:
 - $e + {}^4He \rightarrow e' + p + \pi^- + {}^3He$
 - $e + d \rightarrow e' + p + \pi^- + p_{\text{spec}}$
 - Fully exclusive $n \rightarrow \Delta^0$ production, bound tightly vs loosely
 - Q2 between 4 and 16 GeV^2 , haven't estimated rates yet.
- SoLID:
 - Can detect azimuthal 2π with high luminosity:
 - Limited somewhat by polar angle acceptance and resolution

Exclusive bound $n-\Delta^0$ TFFs in ${}^4\text{He}$



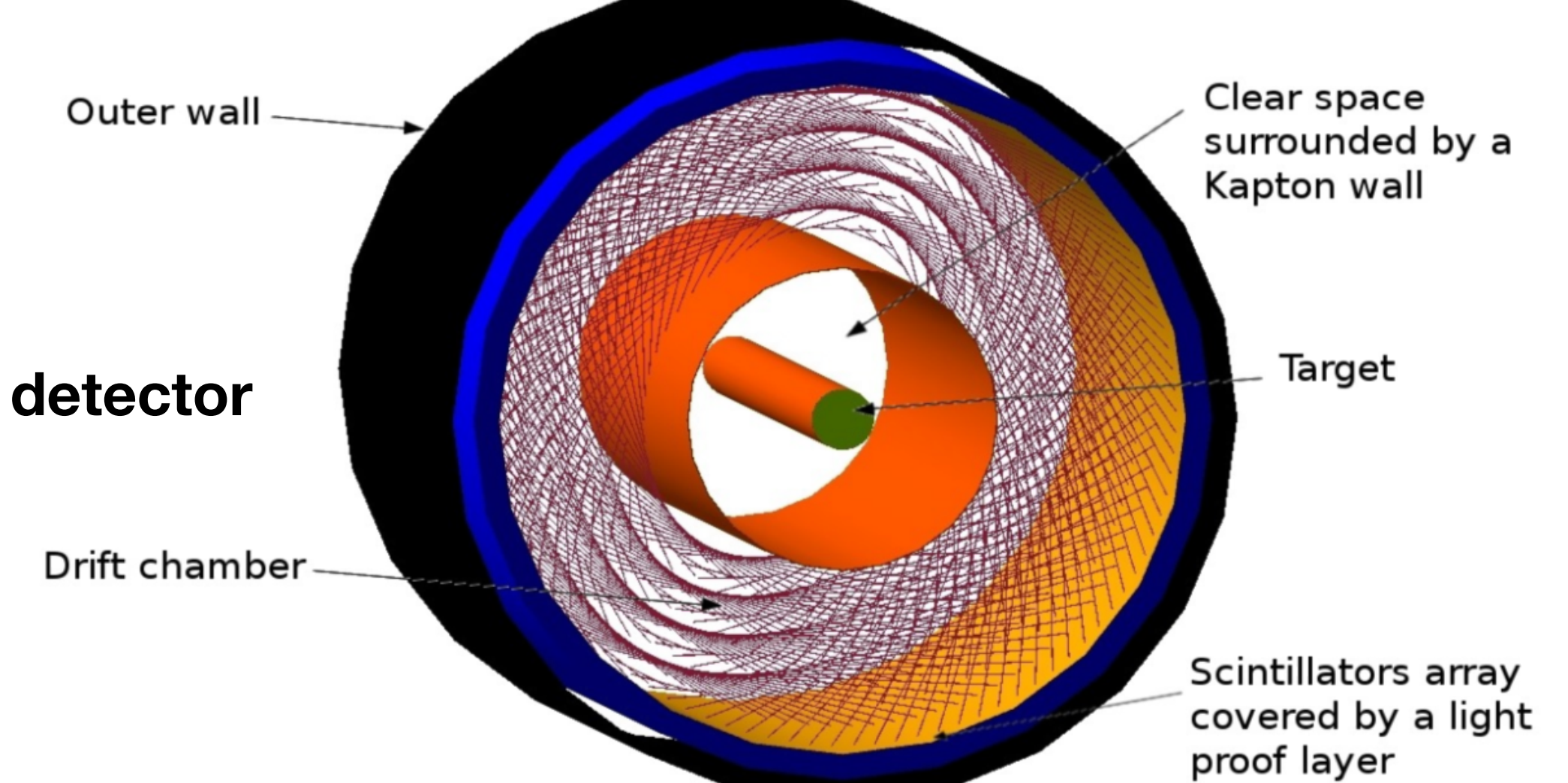
CLAS12 RG-L

11 GeV Beam
65 cm ${}^4\text{He}$ target, d target

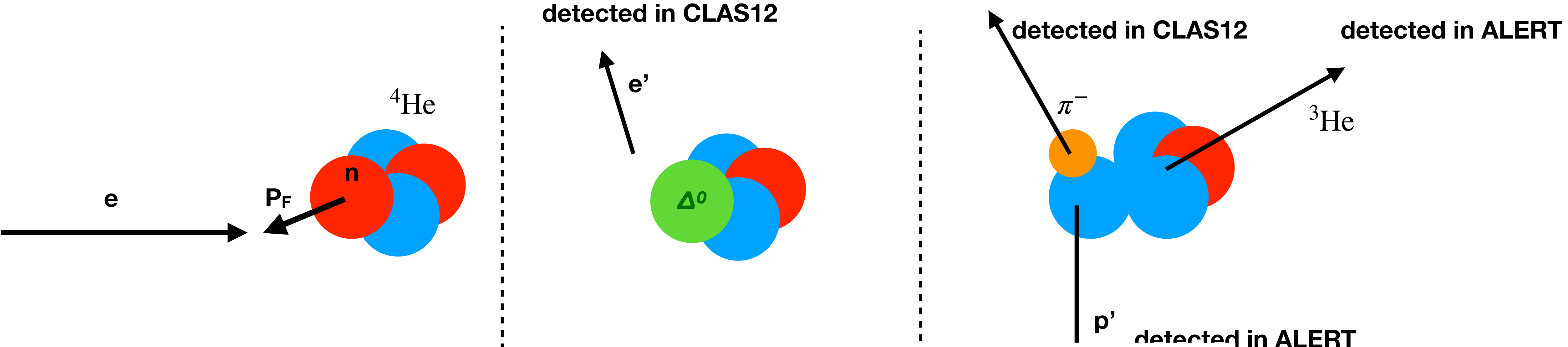
CLAS12 Forward detector (standard)
ALERT recoil detector

Running Early 2025

The ALERT detector



Exclusive bound $n-\Delta^0$ TFFs in ${}^4\text{He}$

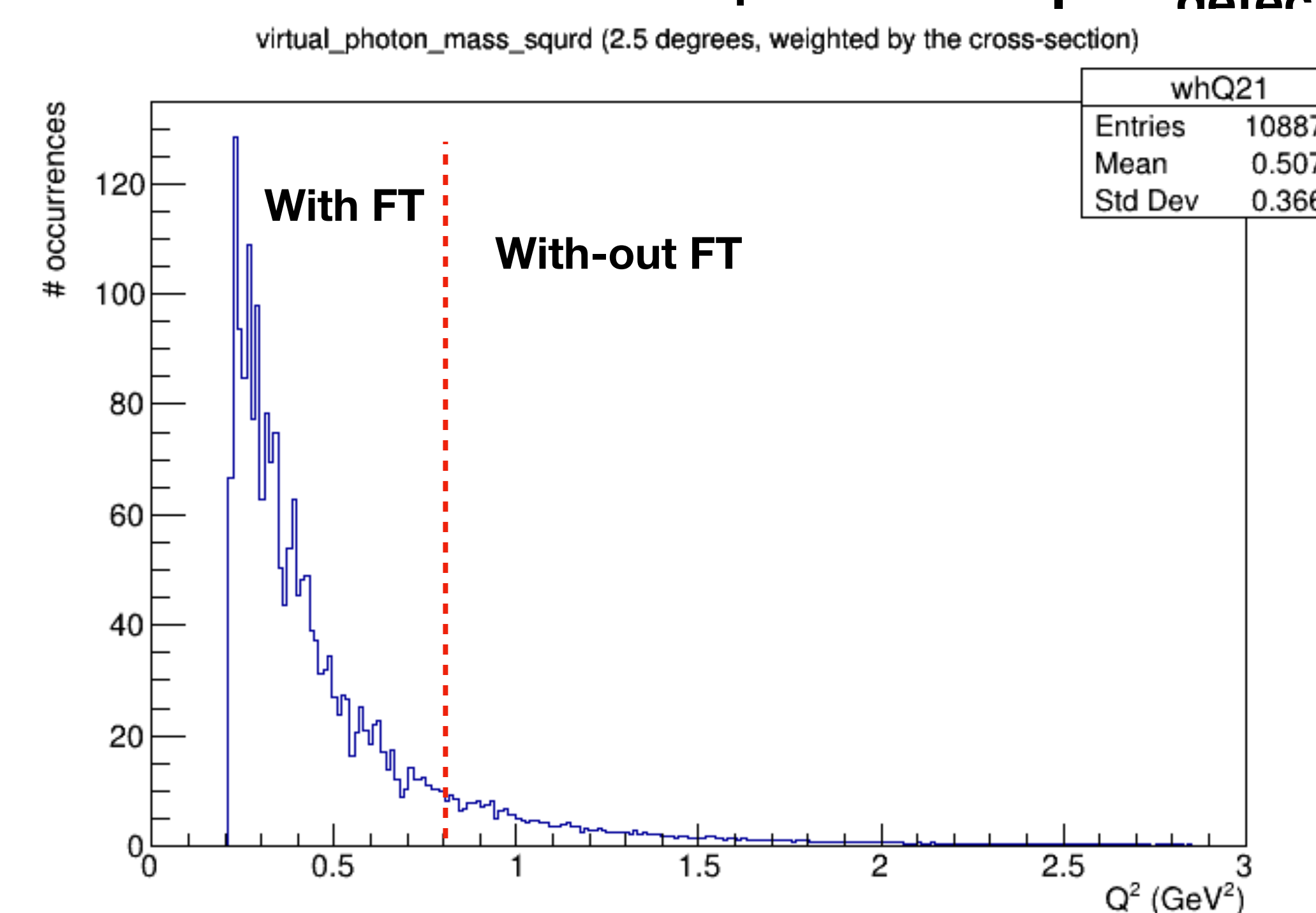


CLAS12 RG-L

11 GeV Beam
65 cm ${}^4\text{He}$ target, d target

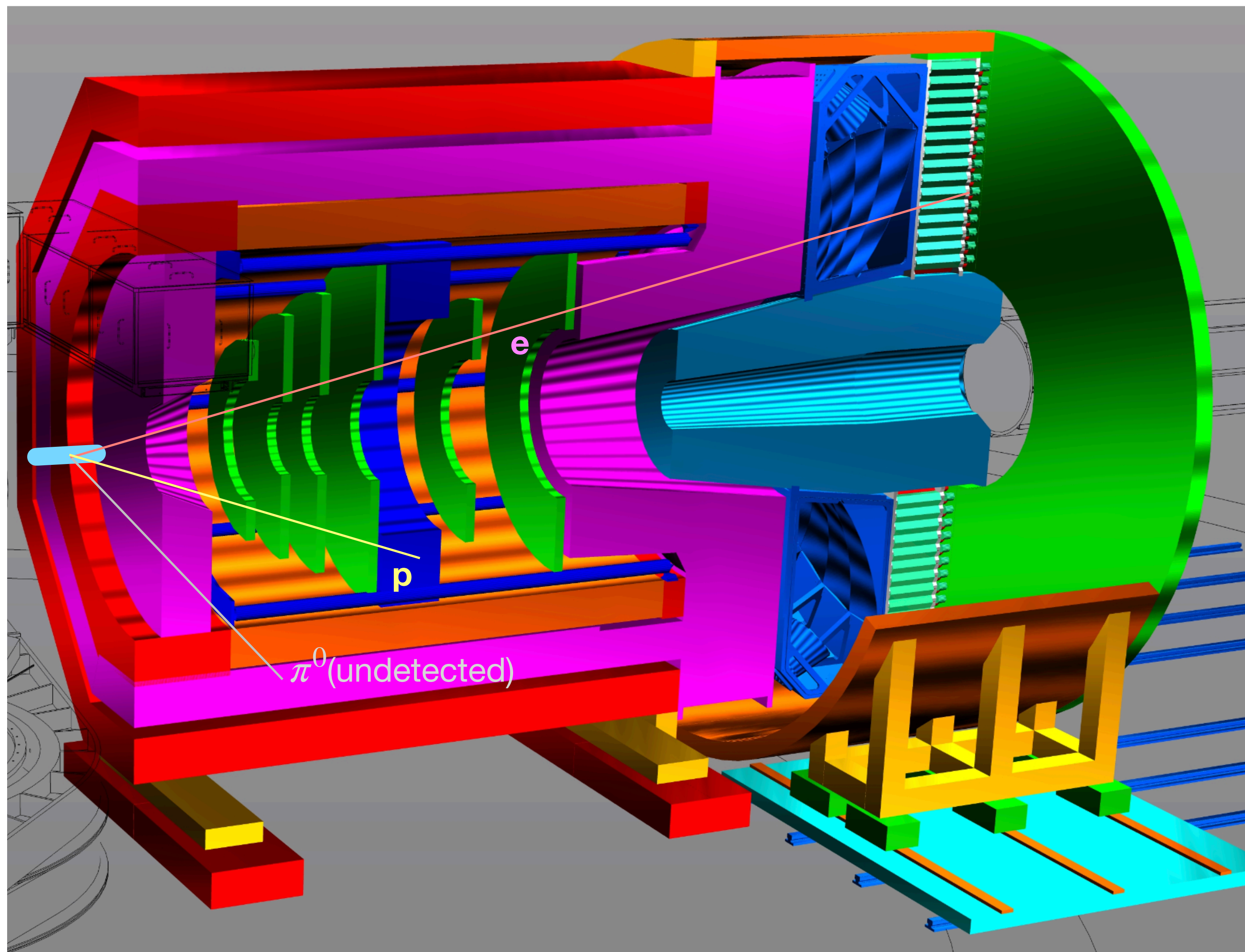
CLAS12 Forward detector (standard)
ALERT recoil detector

Running Early 2025



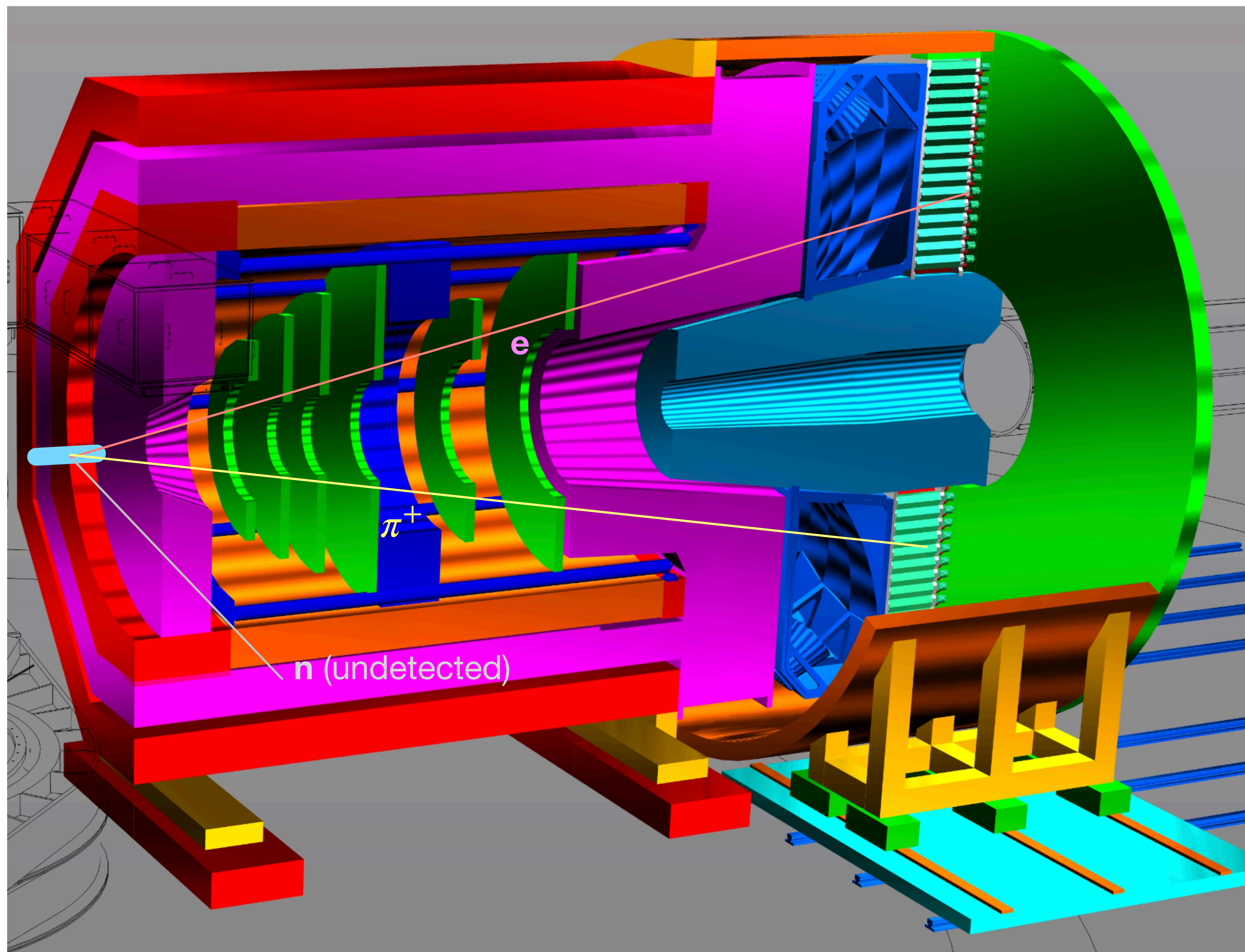
TFFs with SoLID at JLab (J/psi Set-up)

- 15 cm LH2 target
- 11.0 GeV beam Energy
- Luminosity = $10^{37} \text{ N cm}^{-2} \text{ s}^{-1}$
- 4 possible kinematics:
 - $p - \pi^0$
 - Electron detected w small angle
 - Electron detected w large angle
 - $n - \pi^+$
 - Electron detected w small angle
 - Electron detected w large angle



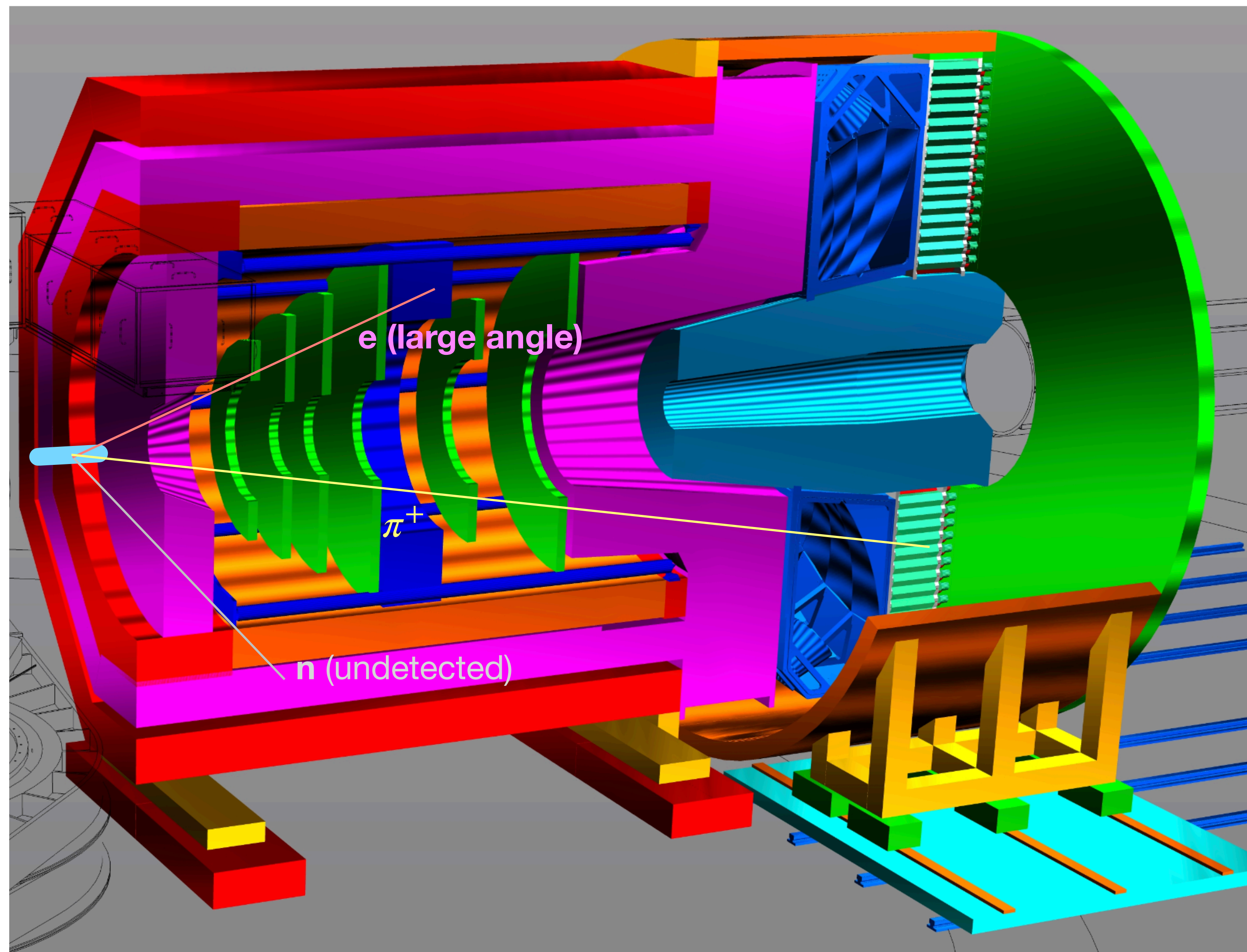
TFFs with SoLID at JLab (J/psi Set-up)

- 15 cm LH2 target
- 11.0 GeV beam Energy
- Luminosity = $10^{37} \text{ N cm}^{-2} \text{ s}^{-1}$
- 4 possible kinematics:
 - $p - \pi^0$
 - Electron detected w small angle
 - Electron detected w large angle
 - $n - \pi^+$
 - Electron detected w small angle
 - Electron detected w large angle



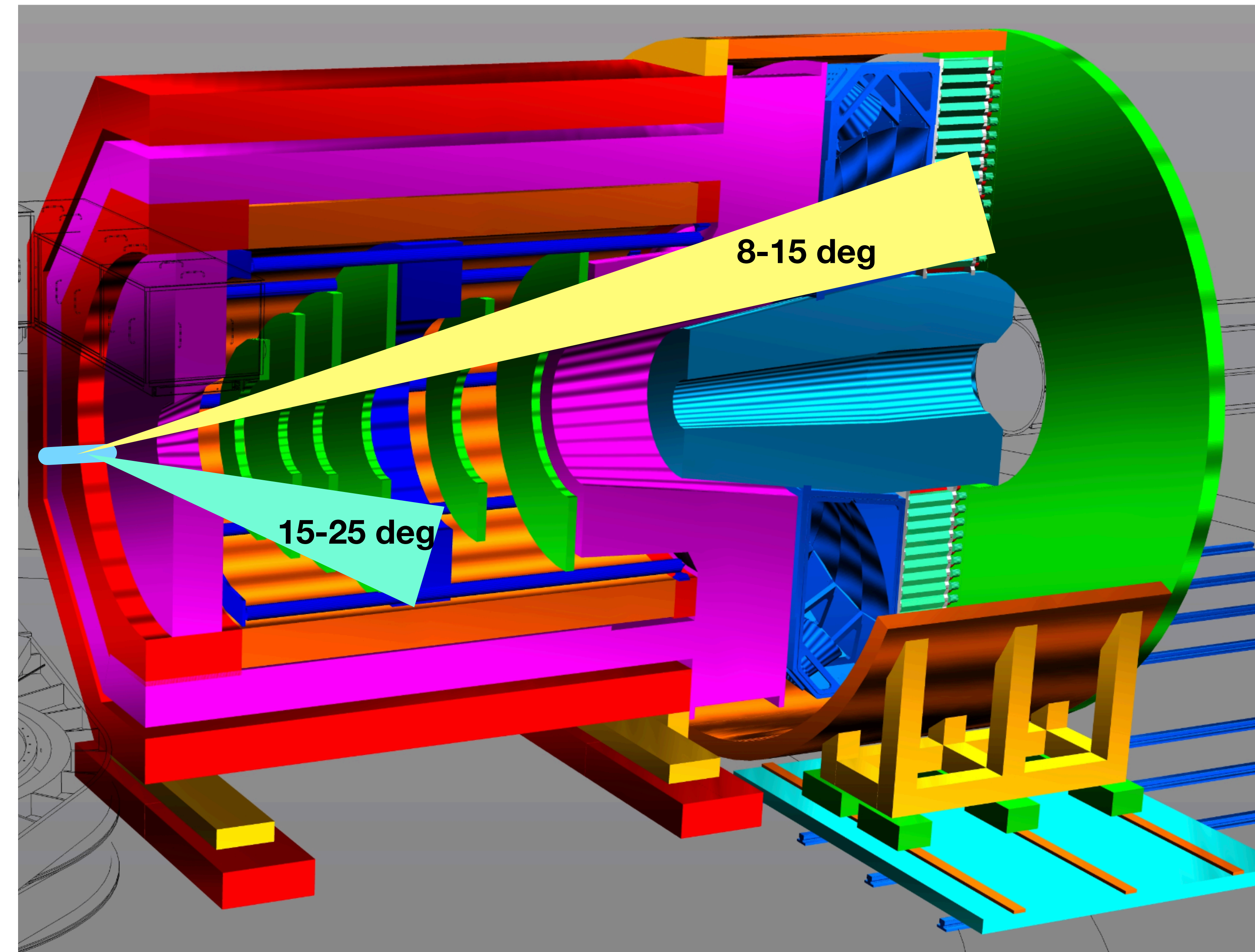
TFFs with SoLID at JLab (J/psi Set-up)

- 15 cm LH2 target
- 11.0 GeV beam Energy
- Luminosity = $10^{37} \text{ N cm}^{-2} \text{ s}^{-1}$
- 4 possible kinematics:
 - $p - \pi^0$
 - Electron detected w small angle
 - Electron detected w large angle
 - $n - \pi^+$
 - Electron detected w small angle
 - Electron detected w large angle



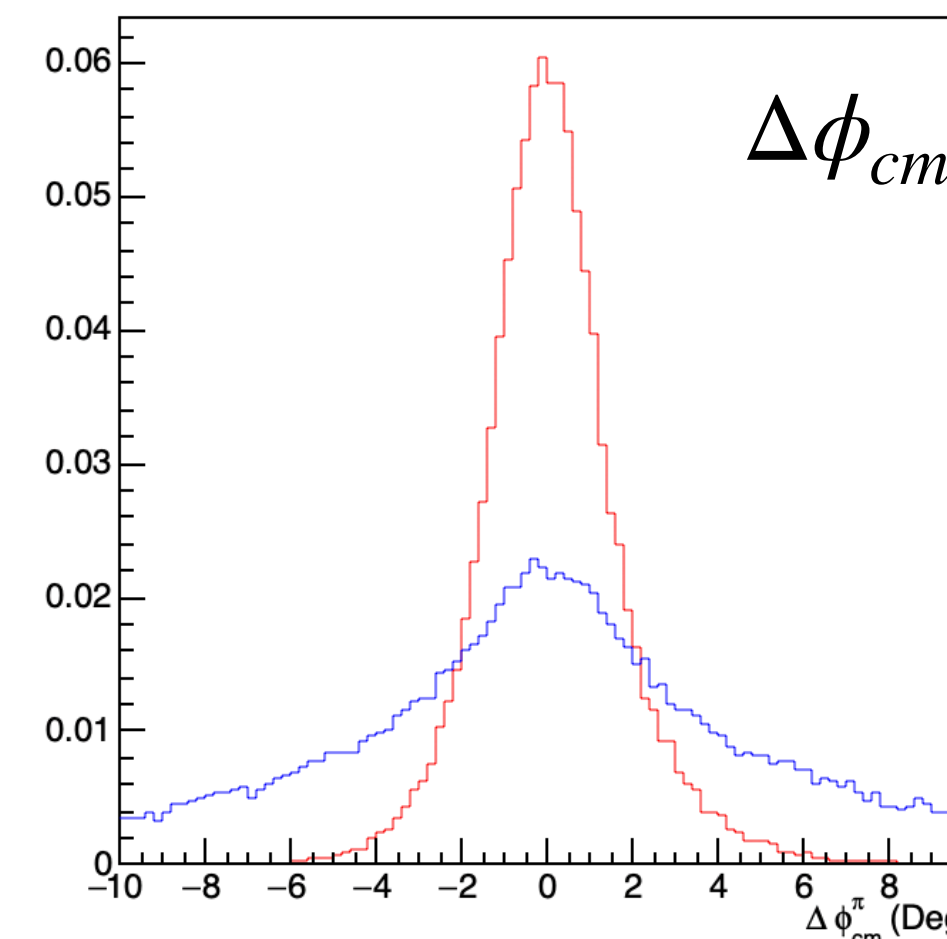
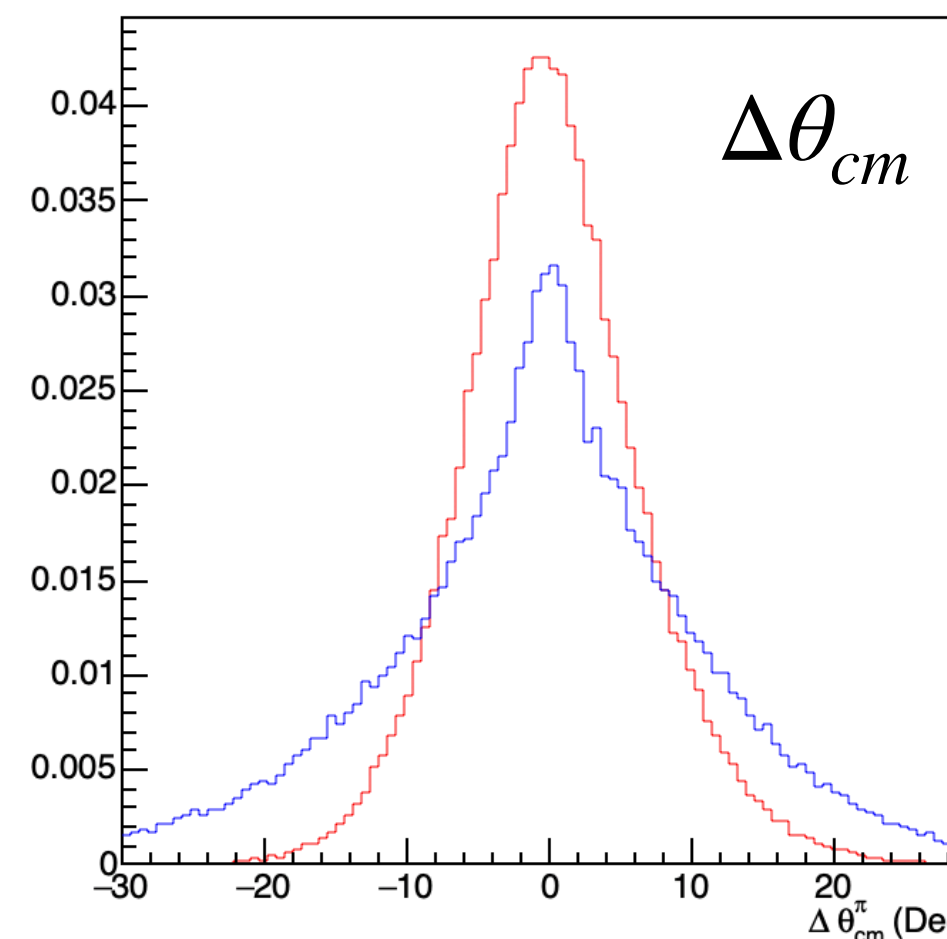
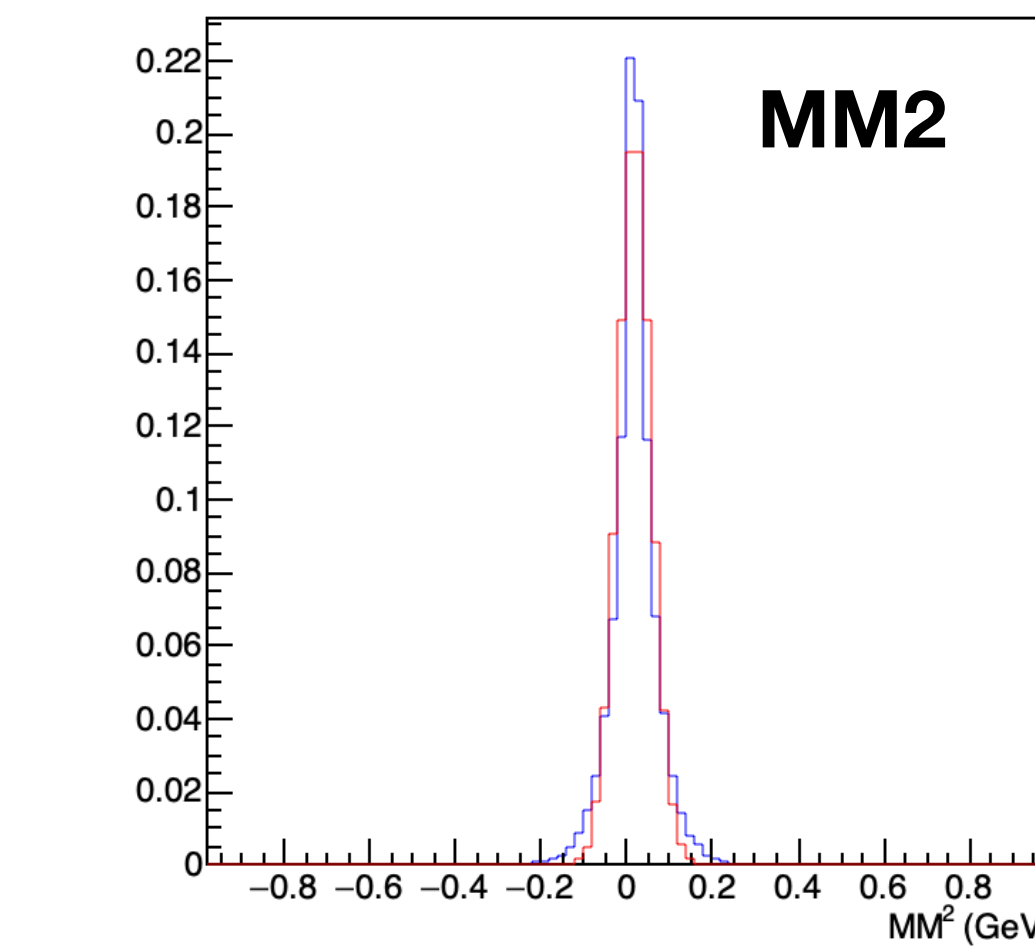
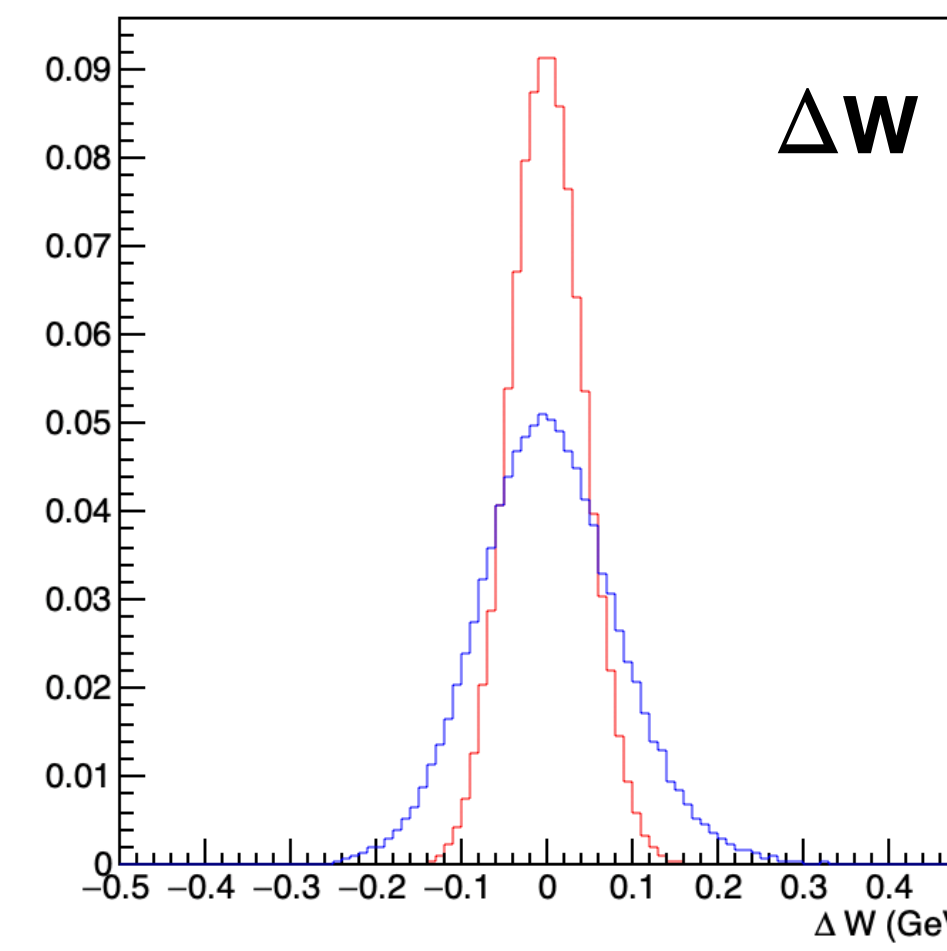
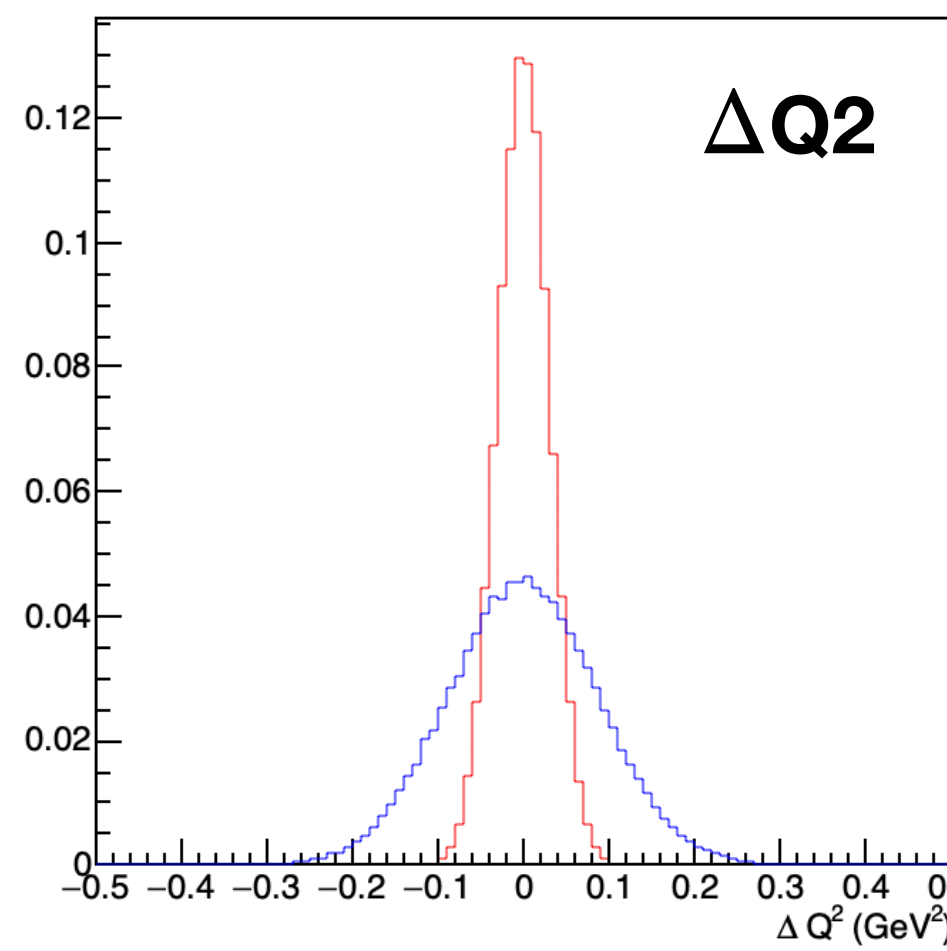
TFFs with SoLID at JLab (J/psi Set-up)

- Small angle electrons vs large angle electrons:
 - Advantages for small angle:
 - Better resolutions
 - LGC for PID
 - Standard Trigger Setup
 - Better systematics
 - Advantages for large angle:
 - Higher Q₂ reach
 - Better θ_{cm} and ϕ_{cm} coverage



TFFs with SoLID at JLab (J/psi Set-up)

- Resolutions of large angle vs small angle electron detection (Tracking only)

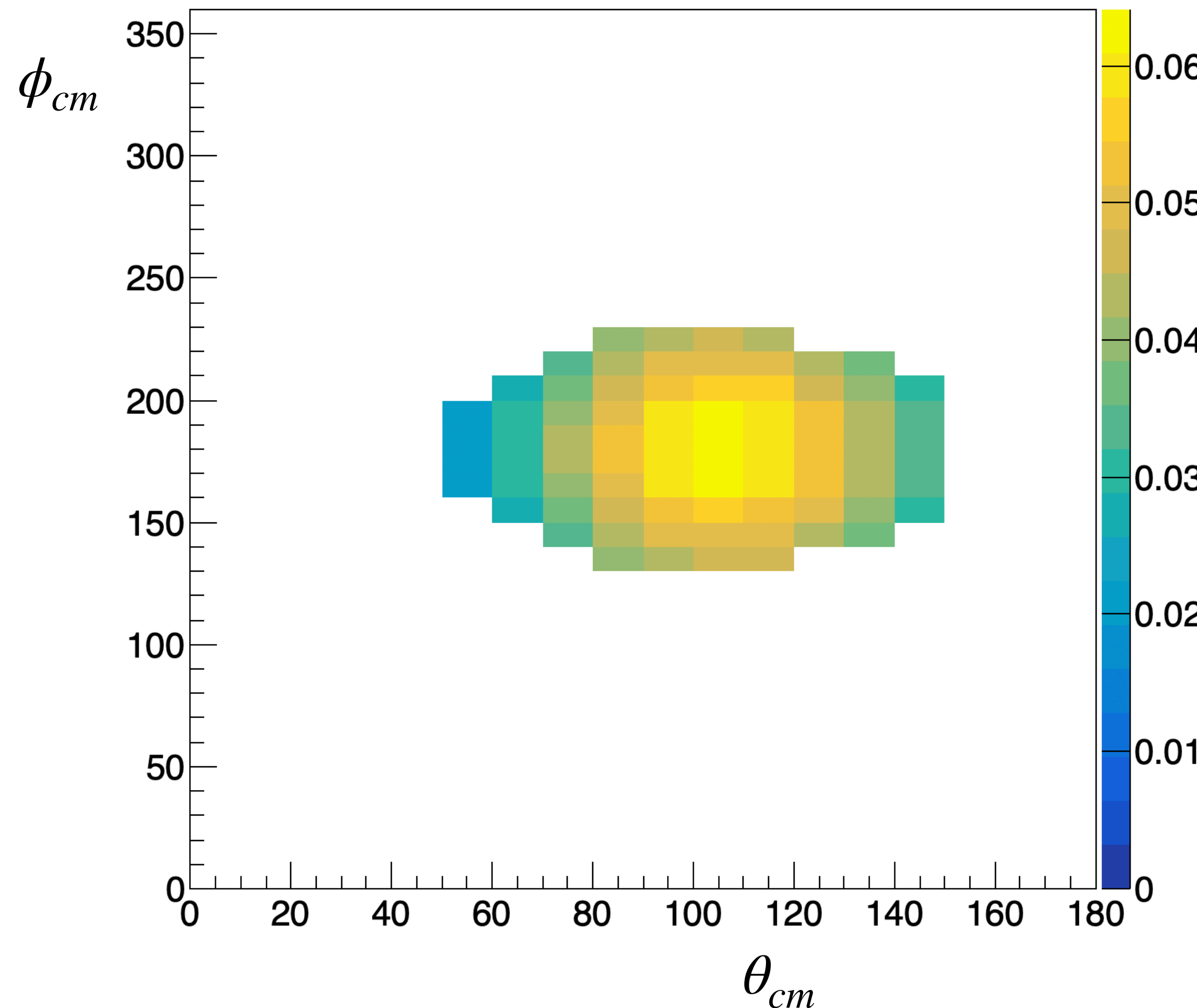


Small angle
Large Angle

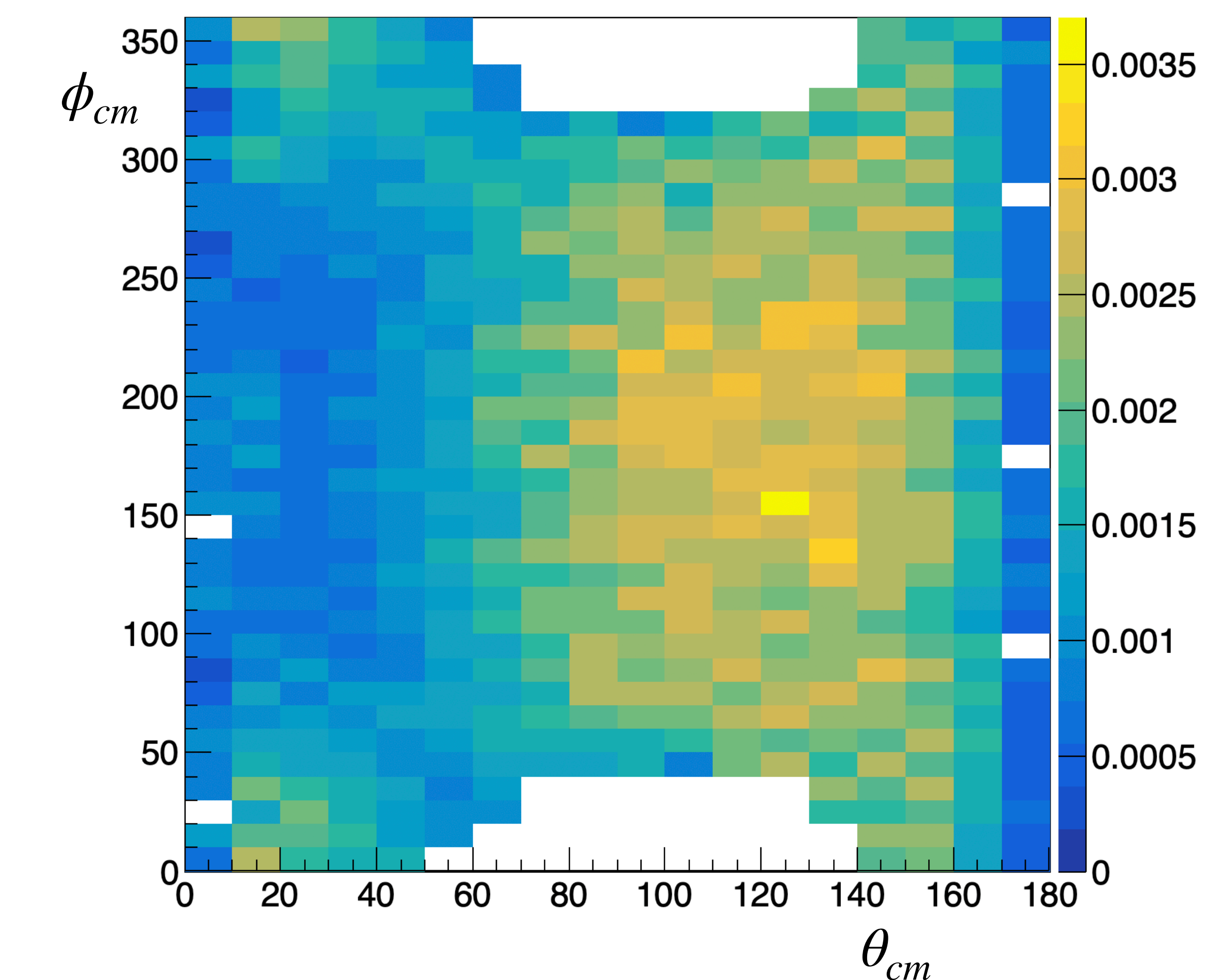
TFFs with SoLID at JLab (J/psi Set-up)

- θ_{cm} and ϕ_{cm} coverage

Small angle electrons: Q2 = 5.7 GeV

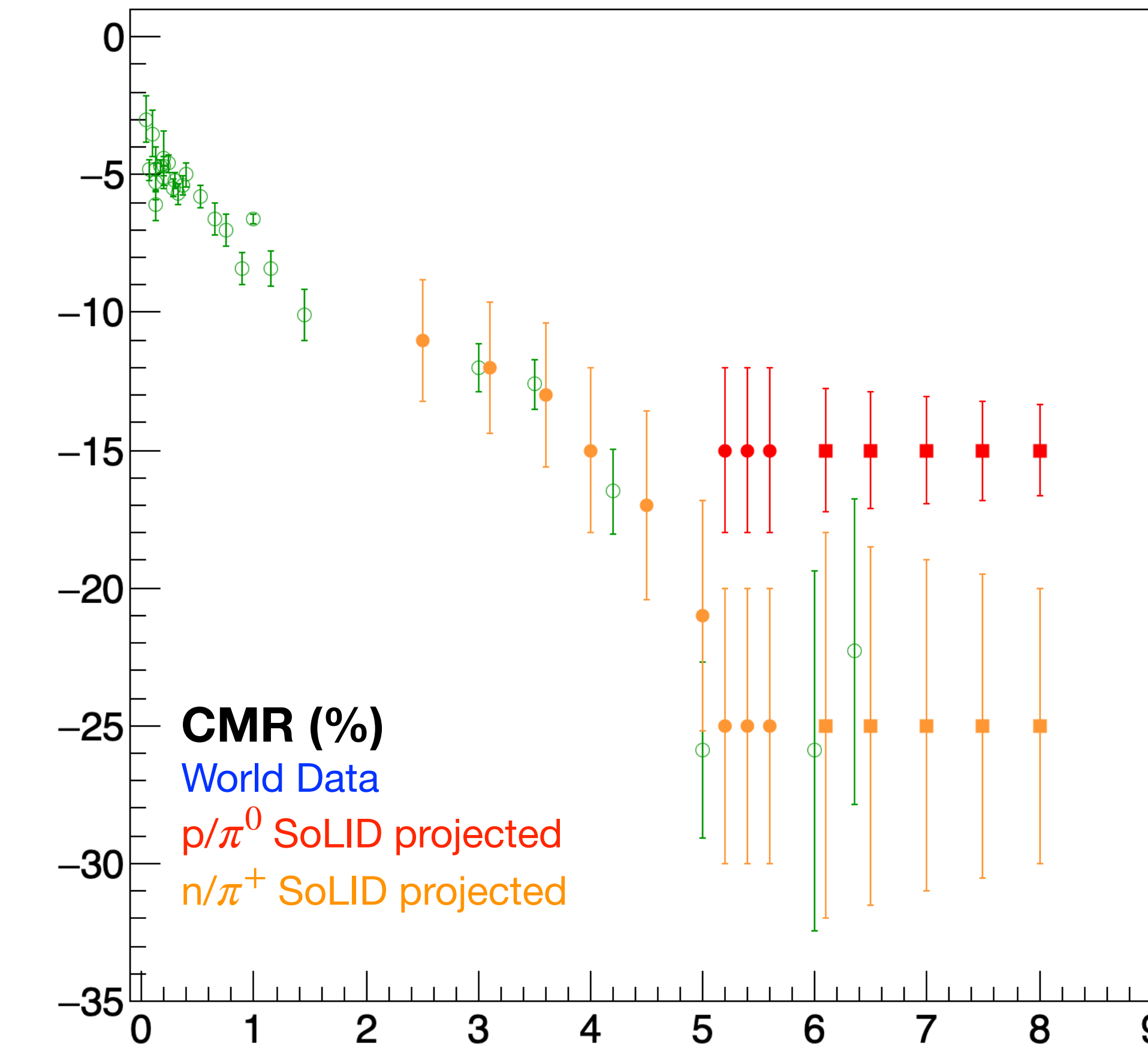
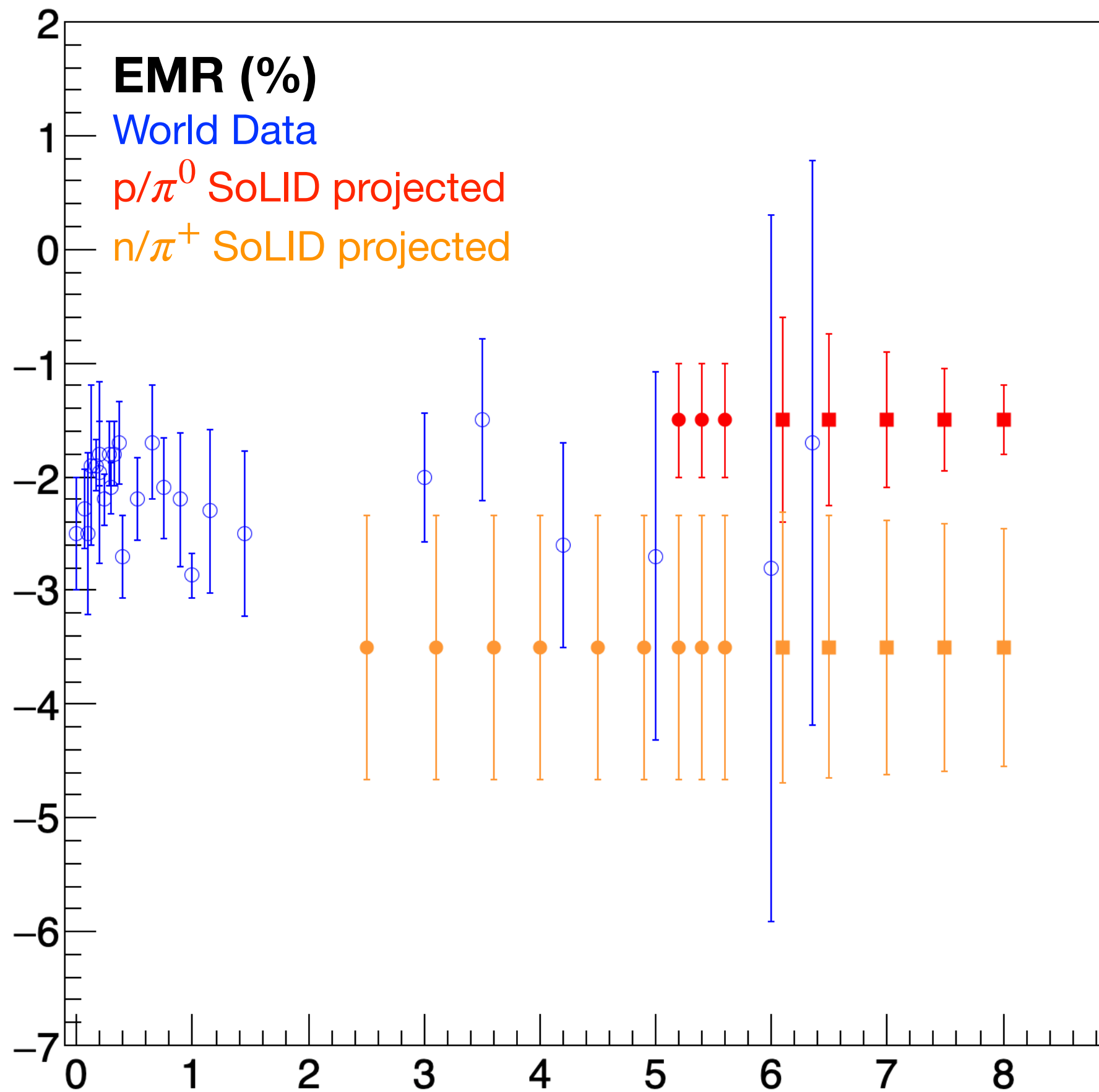


Large angle electrons: Q2 = 8.0 GeV



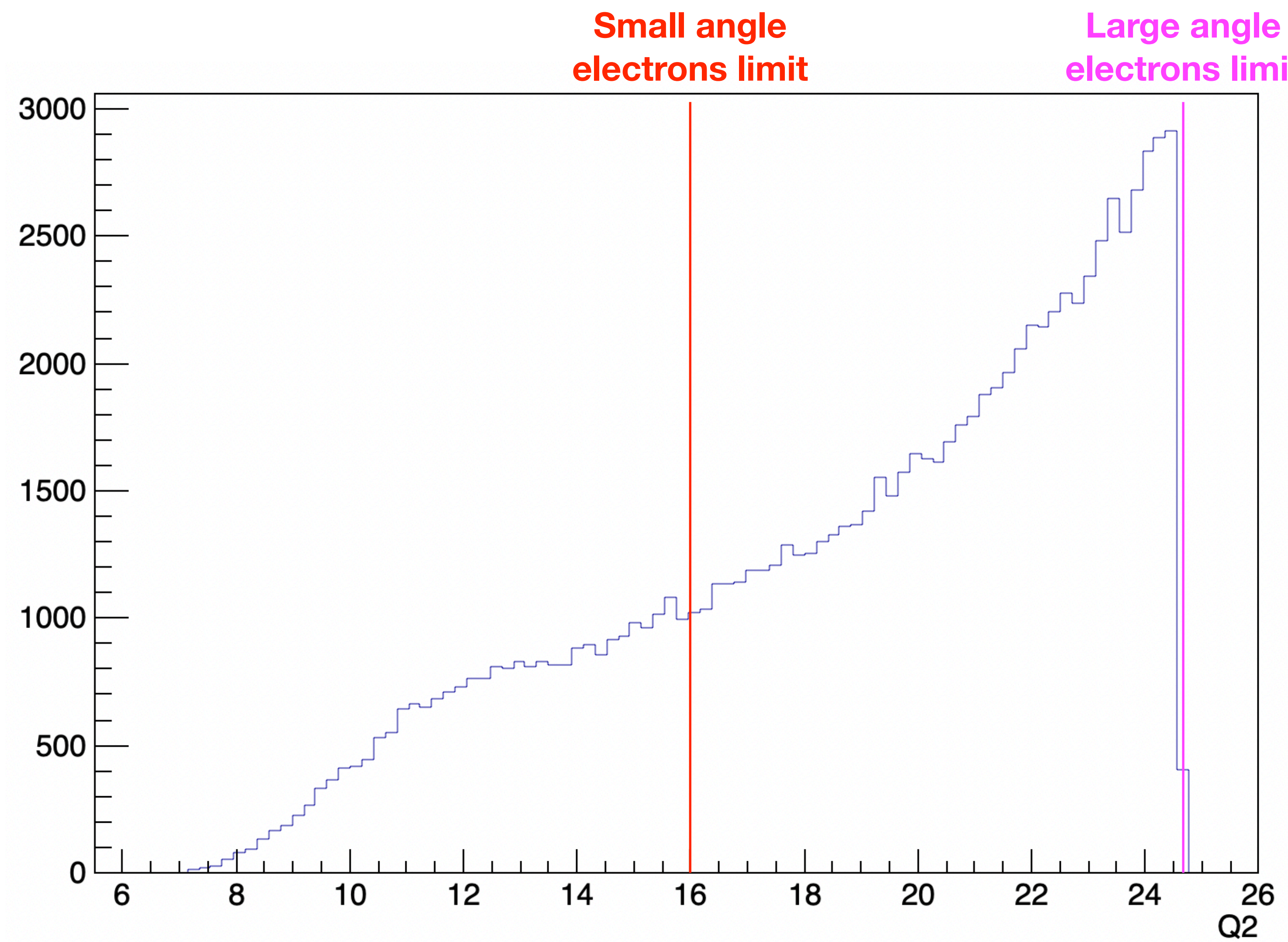
TFFs with SoLID at JLab (J/psi Set-up)

○ Projections



TFFs with SoLID at JLab @ 20 GeV

○ Q2 reach



Summary

- The $N \rightarrow \Delta$ TFFs represent a central element of the nucleon dynamics & has been an important part of Jefferson Lab's experimental program (Halls A, B & C)
 - Approved experiment will extend these measurements in the low Q^2 region:
 - Test bed for ChEFT calculations
 - High precision benchmark data for the Lattice QCD calculations
 - Insight to the mesonic-cloud dynamics within a region where they are dominant and rapidly changing
 - Insight to the origin of non-spherical components in the nucleon wave-function
 - Will test if the QCD prediction that CMR & EMR converge as $Q^2 \rightarrow 0$
- $N \rightarrow \Delta$ TFFs enter as an input in scientific problems that extend from hadronic to neutrino physics, and will advance our understanding of the baryon structure & beyond
- With CLAS12/ALERT
 - In-medium influence to TFF?
- With SoLID:
 - We can extend world data for high Q^2 and test pQCD predictions while running parasitic with J/psi

